



**MAGNETICALLY RECYCLABLE ACTIVATED
CARBON PREPARED FROM BREWER'S SPENT GRAIN FOR
HEXAVALENT CHROMIUM REMEDIATION**

By

BELAY GETYE ZAFU

A Thesis Submitted as a Partial Fulfillment for the Degree of Master of Science in
Industrial Chemistry
to

Department of Industrial Chemistry

Addis Ababa Science and Technology University

DECEMBER, 2020

DECLARATION

I hereby declare that this thesis entitled "Synthesis of Magnetically Recyclable Activated Carbon from Brewer's Spent Grain for Hexavalent Chromium Remediation" was prepared by me, with the guidance of my advisors. The work contained herein is my own except where explicitly stated otherwise in the text, and that this work has not been submitted in whole or in part, for any other degree or professional qualification.

Author:

Signature, Date:

Belay Getye Lafu

[Signature] 28/11/2020

Witnessed by:

Name of student advisor:

Signature, Date:

Dr. Getachew Adam

[Signature] 28/11/2020

Name of student Co-advisor:

Signature, Date:

Dr. Gebrehiwot Gebreselassie

[Signature] 28/11/2020

CERTIFICATE

This is to certify that the thesis prepared by **Mr. Belay Getye Zafu** entitled "**Synthesis of Magnetically Recyclable Activated Carbon from Brewer's Spent Grain for Hexavalent Chromium Remediation**" submitted in a partial fulfillment for the Degree of Master of Science complies with the regulations of the University, and meets the accepted standards with respect to originality, content and quality.

Signed by Examining Board:

External Examiner

Dr. Seay Tadesse, Assoc. prof.

Signature, Date:

[Signature] 28/11/2020

Internal Examiner

Dr. Taye Sam

Signature, Date:

[Signature] 28/11/2020

Chairperson

Dr. Henshe L.

Signature, Date:

[Signature] 28/11/2020

DOC Chairperson

Dr. Henshe L.

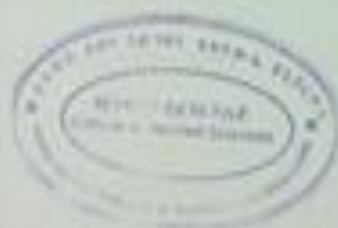
Signature, Date:

[Signature] 28/11/2020

College Dean/Associate Dean ~~Faculty~~ *College* Master Endorse (PhD)
Dean, College of Applied Sciences

Signature, Date:

[Signature] Dec. 22/2020



ABSTRACT

This study is focused on the removal of hexavalent Cr (VI) heavy metal ion from wastewater using an adsorbent prepared from a brewer's spent grain. Activated carbon is synthesized from spent grain and then magnetized for better recycling. The crystal structure, molecular constituent, morphology and surface area of the as-prepared AC and MAC were characterized using XRD, FTIR, SEM and BET characterization techniques. The removal efficiency of MAC for Cr (VI) from synthetic wastewater and real wastewater from Awash tannery effluent was examined. The BOD and COD of real wastewater were characterized before and after adsorption experiment. Factors such as change in pH of solution, adsorbent dose, initial concentration and contact time were optimized for the best Cr (VI) removal efficiency of the adsorbent. It was found that solution pH 2, initial concentration of 40 mg/l, a dosage of 5 g/l and a contact time of 30 min are optimum condition for the most efficient removal of chromium (VI). Almost 97.5% removal of Cr (VI) was achieved under the optimized conditions. The adsorption phenomena are consistent with pseudo-second order kinetics model, and the corresponding rate constant was found to be $11.47 \times 10^{-2} \text{ g mg}^{-1} \text{ min}^{-1}$ with a high regression coefficient ($R^2 = 0.9954$). The adsorption isotherm of Cr (VI) best fits with Temkin isotherm compared to other isotherm models. At the optimum conditions, adsorption process with MAC as an adsorbent showed a removal of $317.833 \pm 14 \text{ mg/l COD}$ and $41.3 \pm 7.8 \text{ mg/l BOD}$ from Awash tannery effluent. Recycling study using the optimized parameters showed promising recovery with only a slight fluctuation for the five consecutive cycles.

Key word: Brewery spent grain, Hexavalent chromium, Magnetic Activated Carbon, Wastewater

ACKNOWLEDGEMENT

First of all, I want to thank the Almighty GOD for giving me all things, the time and the chance to do this work. Secondly, I would like to acknowledge my advisors Dr. Getachew Adam and Dr. Gebrehiwot Gebreslasie for their unlimited support, proper guidance and prompt feedback with constant encouragement throughout my thesis work. My appreciation is unlimited to whom that supported me during my experimental work including Mr. Abraham Getahun central lab assistant, Mr. Abate Ayele, Department of Ecobiology, Dr. Menbere Leul and Mr. Yakob Godebo, Department of Industrial Chemistry. I have also many thanks to Mr. Tsegaye Sisay and Estifanos Kassahun Department of Chemical Engineering for their unlimited support during my experiment.

TABLE OF CONTENTS

DECLARATION.....	Error! Bookmark not defined.
CERTIFICATE	Error! Bookmark not defined.
ABSTRACT	iii
ACKNOWLEDGEMENT	iv
TABLE OF CONTENTS.....	v
LIST OF ABBREVIATIONS	ix
LIST OF TABLES	x
LIST OF FIGURES.....	xi
CHAPTER 1 INTRODUCTION.....	1
1.1 Background of the Study.....	1
1.2 Statement of the Problem	3
1.3 Objectives	4
1.3.1 General Objective	4
1.3.2 Specific Objectives.....	4
1.4 Significance of the Study	4
CHAPTER 2 LITERATURE REVIEW	5
2.1 Water Contaminant	5
2.2 Wastewater from Tannery Industries	5
2.3 Environmental Impact of Tannary Industry Wastewater	6
2.4 Heavy Metals.....	6
2.5 Source of Heavy Metals	7
2.6 Toxicity of Heavy Metals.....	8
2.7 Importance of Heavy Metals	10
2.8 Guide Line of Heavy Metal Discharge to the Environment.....	11
2.9 Common Wastewater Remediations.....	12
2.9.1 Adsorption Methods.....	13
2.9.2 Adsorption Mechanism	14
2.9.3 Adsorption Mechanism of Cr (VI).....	15
2.10 Adsorbent Materials	16
2.10.1 Agricultural Wastes.....	16
2.10.2 Industrial Byproducts/Wastes	17
2.10.2.1 Brewer’s Spent Grain	17

2.11 Metal Adsorption by Magnetic Activated Carbon.....	18
2.11.1 Activated Carbon	18
2.11.2 Magnetic Activated Carbon.....	19
2.12 Synthesis Methods of Activated Carbon and Magnetic Activated Carbon.....	20
2.12.1 Activation of Activated Carbon	20
2.12.2 Preparation Methods of Magnetic Activated Carbon.....	21
2.13 Factors Affecting Adsorption	21
2.14 Adsorption Isotherms	22
2.15 Adsorption Kinetics	24
2.16 Spectrophotometric Method of Cr (VI) Analysis	25
CHAPTER 3 MATERIALS AND METHODS.....	26
3.1 Apparatus and Instruments	26
3.2 Chemicals and Reagents.....	26
3.3 Sampling and Sample Preparations	26
3.3.1 Spent Grain Sample Collection.....	26
3.3.2 Preparation of Activated Carbon	27
3.3.3 Preparation of Magnetic Activated Carbon	29
3.4 Characterization Methods of Adsorbent	29
3.4.1 Proximate Analysis of Activated Carbon and Magnetic Activated Carbon.....	29
3.4.1.1 Moisture Content Determination.....	29
3.4.1.2 Ash Content Determination	30
3.4.1.3 Volatile Matter Content Determination	30
3.4.1.4 Fixed Carbon Determination.....	31
3.4.2 Scanning Electron Microscope (SEM).....	31
3.4.3 BET (Brunauer Emmett Teller) Analysis	31
3.4.4 FT-IR (Fourier Transform Infrared) Analysis	31
3.4.5 XRD (X-ray Diffraction) analysis.....	31
3.4.6 Point Zero Charge Determination	32
3.4.7 UV-Vis Spectrophotometry	32
3.4.7.1 Preparation of Diphenyl Carbazide	32
3.4.7.2 Preparation of Cr (VI) Stock Solution.....	32
3.5 Batch Adsorption Experiment	33
3.6 Effect of Adsorbent Parameters.....	33
3.6.1 Effect of Adsorbent Dose	33

3.6.2 Effect of pH	34
3.6.3 Effect of Contact Time	34
3.6.4 Effect of Initial Concentration of Metal ions	34
3.7 Experimental Design.....	34
3.8 Description of Study Area	35
3.8.1 Sampling Techniques	36
3.8.2 Characterization and Analysis of Wastewater	37
3.8.3 Awash Tannery Industry Wastewater Sample Digestion	38
3.9 Determination of Adsorption Isotherms and Kinetics	38
3.9.1 Isotherms Study	38
3.9.2 Kinetics Study	39
3.10 Recyclability Study of Magnetic Activated Carbon	39
CHAPTER 4 RESULTS AND DISCUSSIONS	40
4.1 Physio-Chemical Characterization of AC and MAC	40
4.2 Fourier Transformation Infrared Spectroscopy (FTIR) Analysis	40
4.3 BET Analysis.....	42
4.4 Scanning Electron Microscope	42
4.5 XRD Analysis.....	43
4.6 Point Zero Charge Analysis	44
4.7 Comparison of Percentage Removal of Cr (VI) by Different Ratio of Phosphoric Acid to AC	44
4.8 Optimization of Adsorption Parameters.....	45
4.8.1 Effect of Contact Time	45
4.8.2 Effect of pH	46
4.8.3 Effect of Initial Cr (VI) Concentration.....	47
4.8.4 Effect of Adsorbent Dose	48
4.9 Modelling and optimization	49
4.9.1 Effect of Individual Variables on Adsorption of Cr (VI).....	49
4.9.2 Development of Adsorption Percentage Model Prediction	51
4.10 Combined Effect of the Factors.....	53
4.10.1 Combined Effect of Adsorbent Dosage and Contact Time	54
4.10.2 Combined Effect of Dosage and pH	54
4.10.3 Combined Effect of Dosage and Initial Concentration	55
4.10.4 Combined Effect of Contact Time and pH	56

4.10.5 Combined Effect of pH and Initial Concentration	57
4.10.6 Combined Effect of Initial Concentration and Contact Time	58
4.11 Process Optimization and Evaluation	59
4.12 Study of Adsorption Isotherm Models	60
4.13 Study of Adsorption Kinetics	63
4.14 Real Sample Analysis	64
4.14.1 Physicochemical Characterization of Awash Tannery Effluent	64
4.14.2 Cr (VI) Analysis in Awash Tannery Effluent.....	65
4.15 Recycling of Magnetic Activated Carbon Adsorbent	66
CHAPTER 5 CONCLUSION AND RECOMMENDATIONS	68
5.1 CONCLUSION.....	68
5.2 RECOMMENDATIONS	69
REFERENCES	70
APPENDICES.....	83

LIST OF ABBREVIATIONS

AC.....	Activated Carbon
ANOVA.....	Analysis of Variance
APHA.....	American Public Health Association
ASTM.....	American Standard Test Method
BET.....	Brunauer Emmett Teller
BOD.....	Biological Oxygen Demand
CCD.....	Central Composite Design
COD.....	Chemical Oxygen demand
CERCLA.....	Comprehensive Environmental Response, Compensation, and Liability Act
EEPA.....	Ethiopian Environmental Protection Agency
FEPA.....	Federal Environmental Protection Agency
FT-IR.....	Fourier Transform Infrared
XRD.....	X-ray Diffraction
MAC.....	Magnetic Activated Carbon
MCCAC.....	Magnetic Corn Cob Activated Carbon
MC.....	Moisture Content
NAFDAC.....	National Agency for Food and Drugs Administration and Control
PZC.....	Point of Zero Charge
SEM.....	Scanning Electron Microscopy
WHO.....	World Health Organization

LIST OF TABLES

Table 2.1 Source and impact of heavy metal with their WHO limit in ppm	10
Table 2.2 Guideline in drinking water by the WHO and national agency for food and drugs administration and control (NAFDAC) for heavy metals [49].....	11
Table 2.3 Permissible limits of various toxic heavy metals in different country standards [77]	12
Table 3.1 Factors and corresponding levels for CCD experiments	35
Table 4.1 Physico-chemical characteristic of AC and MAC	40
Table 4.2 Characteristic IR adsorption frequencies of MAC functional groups	41
Table 4.3 The surface area of AC and MAC.....	42
Table 4.4 R ² squared value for the model	52
Table 4.5 Optimum condition for Cr (VI) removal by MAC adsorbents from the model	60
Table 4.6 Parameters for Langmuir, Freundlich and Temkin isotherms for the adsorption of Cr (VI) by MAC.....	61
Table 4.7 Kinetic parameters for 1 st and 2 nd order	63
Table 4.8 Physicochemical Characterization of untreated and treated effluent	65
Table 4.9 Optimum condition for Cr (VI) removal by MAC adsorbents	65
Table 4.10 Optimum condition for Cr (VI) removal by MAC adsorbents.	66

LIST OF FIGURES

Figure 2.1 Discharging of different waste material to the water sources [36]	6
Figure 2.2 Sources and sinks of heavy metals [56].	8
Figure 2.3 Health effect Cr (VI) in human body [65].....	9
Figure 2.4 Methods for the remediation's of hexavalent chromium [56,86].....	13
Figure 2.5 Three stages of adsorption mechanisms.....	15
Figure 2.6 The mechanism of Cr (VI) bio sorption by natural biomaterials [94].	16
Figure 2.7 Synthesis of AC from wheat bran.....	19
Figure 2.8 Synthesis of MAC from mixture of peanut shells and $\text{FeCl}_3 \cdot 6\text{H}_2\text{O}$	20
Figure 3.1 Synthesis method of activated carbon.....	28
Figure 3.2 The synthesized activated carbon from BSG impregnated at 50% H_3PO_4	28
Figure 3.3 Schematic diagram for the Synthesis of magnetic activated carbon.	29
Figure 3.4 Location map of Awash tannery factory.	36
Figure 3.5 Recyclability study of magnetic activated carbon adsorbent	39
Figure 4.1 FT-IR spectra of MAC before and after adsorption of Cr (VI).....	41
Figure 4.2 SEM image of (a) AC and (b) MAC.....	42
Figure 4.3 XRD analysis of magnetic activated carbon	43
Figure 4.4 Point of zero charge analysis	44
Figure 4.5 The effect of contact time with dose 5g /l, initial concentration of 40 mg/l and pH 2 at 200 rpm.	46
Figure 4.6 The effect of pH with dose 5 g/l, contact time of 30 min and initial concentration of 40 mg/l at 200 rpm % removal of Cr (IV).	47
Figure 4.7 The effect of initial concentration at constant dose 5 g/l, contact time of 30 min and pH 2 at 200 rpm of % removal Cr (VI).	48
Figure 4.8 The effect of MAC dosage with initial concentration 40 mg/l, contact time of 30 min and pH 2 at 200 rpm % removal of Cr (VI).	49
Figure 4.9 The individual effect of (a) dosage, (b) contact time, (c) pH and (d) initial concentration of the % removal Cr (VI).	51
Figure 4.10 Graph of Predicted versus Actual.	53
Figure 4.11 2D Contour plot (a) and 3D response surface (b) of the combined effects of dosage and contact time on the (%) removal of Cr^{6+} by MAC.	54
Figure 4.12 2D Contour plot (a) and 3D response surface (b) of the combined effects of dosage and pH on the (%) removal of Cr^{6+} by MAC.	55
Figure 4.13 2D Contour plot (a) and 3D response surface (b) of the combined effects of dosage and initial concentration on the (%) removal of Cr^{6+} removal from simulated wastewater by MAC.	56
Figure 4.14 2D Contour plot (a) and 3D response surface (b) of the combined effects of contact time and pH (%) removal of Cr^{6+} removal from simulated wastewater by MAC.	57

Figure 4.15 2D Contour plot (a) and 3D response surface (b) of the combined effects of pH and initial concentration (%) removal of Cr^{6+} removal from simulated wastewater by MAC.	58
Figure 4.16 2D Contour plot (a) and 3D response surface (b) of the combined effects of contact time versus initial concentration on the percentage removal of Cr (VI).	59
Figure 4.17 Graph of calibration curve of C_e/Q_e versus C_e	61
Figure 4.18 Graph of $\log(Q_e)$ versus $\log(C_e)$	62
Figure 4.19 Graph of Q_e versus $\ln(C_e)$	62
Figure 4.20 Graph of $\log(q_e - qt)$ versus time.	63
Figure 4.21 Graph of t/qt versus time.	64
Figure 4.22 Graph of wastewater sample analysis.	66
Figure 4.23 % Removal of MAC for Cr (VI) versus recycle number.	67

CHAPTER 1 INTRODUCTION

1.1 Background of the Study

Environmental pollution is a major challenge in the entire world. It is the release of chemical, physical and biological contaminants to the environment. In recent years contamination of the environment (water, soil and air) by persistent pollutants from different activities has become an increasingly serious problem [1,2]. It has increased exponentially in the past few years and reached alarming level in terms of its effects on living creatures. Environmental pollution by toxic heavy metals is one of the most serious issues in the world [2,3]. Disposal of untreated wastewaters containing heavy metals has a detrimental impact on the ecosystem and human health. Substances containing heavy metals are considered among the pollutants that have direct effect on human and animals. With increasing industrial development, toxic heavy metals are also increasingly generated. The high toxicity of these metal ions can cause serious harm to humans and the ecosystem even at very low concentrations [4,5].

Heavy metals such as hexavalent chromium (Cr^{+6}), lead (Pb), arsenic (As), cadmium (Cd), silver (Ag), Nickel (Ni), copper (Cu), zinc (Zn), mercury (Hg) and platinum (Pt) are the major ions produced in large volumes in different industrial activities in which these metals cannot be degraded easily [6–8]. Heavy metals are naturally occurring elements having a high atomic mass and density, at least five times greater than that of water [9]. Those ions are considered by the United States Environmental Protection Agency (USEPA) as a carcinogenic pollutant, due to their accumulation and persistence in the environment.

Different industries such as electroplating, welding, automotive painting, chromated copper arsenate (CCA) production, paint and coating production, printing and ink production, Plastic colorant production and tannery industry are highly discharging hexavalent chromium to the environment [10]. Therefore, the environment problem due to the release of hexavalent chromium from the Awash tannery factory is one of the problems in our country.

There are various methods to remove heavy metals from wastewater such as ion exchange, ultrafiltration, chemical precipitation, electrochemical oxidation, coagulation-flocculation, adsorption and so on [11–13]. Among these methods, adsorption is considered as a promising technique due to its simplicity for design, easy operation and insensitivity to toxic substances [14]. There are numerous adsorbents such as zeolites, polymers, fly ash, biomasses, graphene oxide and activated carbon which have been applied for the removal of heavy metals from wastewater [9]. Among several adsorbents activated carbon is the most widely used adsorbents due to its large surface area, porosity, high adsorption capacity and low cost. As a result activated carbon (AC) has become an excellent and well known adsorbent for heavy metal removal from industrial wastewaters [15].

In recent years, many studies have been reported the production of activated carbon from agricultural wastes, such as pistachio shell, acorn shell, cotton stalks, pine cone , almond shell, bamboo , mangos teen peel, palm , coconut shell , barley husks , sunflower seed press cake, palm trunk and mangrove, sugarcane bagasse, corncob char, palm shell char and soybean straw char, municipal solid waste, paper mill sludge, orange peel, rice husk, peanut husk, sawdust etc.[3,11,16]. Most developing countries continuously produce abundant industrial by products such as brewery's spent grain (BSG), which are underexploited [17]. BSG is the major byproduct of the brewing industry representing around 85% of the total by product generated [18,19]. The brewing industry generates relatively large amounts of byproducts and wastes; spent grain, spent hops and yeast being the most common. However, most of these industrial products can be readily recycled and reused [20]. In this study, BSG has been used to prepared AC as an adsorbent to remove chromium (VI) from wastewater.

Activated carbon can be produced from BSG which can successfully remove heavy metals ions like chromium (VI) from wastewater. Although these adsorbents are effective in the adsorption of hexavalent chromium, they have a common limitation that the materials are not easily separated from the wastewater after they adsorb the hexavalent chromium, due to their granular or powdery nature which requires plenty of time to centrifuge, precipitate or filter [4]. To solve these problems, combining activated carbon

with magnetic composite has been introduced. Magnetic materials have the great advantages compared with the traditional adsorbent in such a way that separation process can be performed directly on crude samples containing suspended solid materials by external magnetic field without the need of additional centrifugation or filtration. The method makes the separation easier, faster and recover the spent activated carbon [3,14,21,22].

Thus, there is still an increasing demand for the development of cost effective and efficient magnetic carbon materials for the adsorption of Cr (VI) in tannery wastewater. Accordingly, magnetic activated carbon (MAC) can be used as an adsorbent for the remediation of harmful substances such as heavy metals, dyes and organic compounds [23,24]. It is obvious that the composite materials of MAC are not only high efficiency adsorbents for adsorption of Cr (VI) from aqueous solutions, but also easily collected magnetically after adsorption [4,25]. By introducing magnetic property into conventional adsorbents, recollection after separation could be achieved so easily that the loss of adsorbents could be lowered [26]. Magnetic separation has been shown to be a promising method to separate hazardous substances from wastewater and to be superior in its performance in comparison with previous common methods [27].

1.2 Statement of the Problem

Heavy metal contaminants from industrial waste streams that seriously threaten the human health and the environment have been recognized as an issue of growing importance in recent years. Heavy metals discharged from different factories into waterways would adversely affect human health as well as that of flora and fauna. Therefore, it is necessary to remove the heavy metal like Cr (VI) from industrial effluents before discharging into the water stream. There are many methods such as ion exchange, ultrafiltration, chemical precipitation, electrochemical oxidation, coagulation-flocculation, adsorption and so on to remove Cr (VI) from tannery wastewater. However, some of these methods are very expensive, use dangerous chemical and generate toxic sludge as a byproduct which is harmful to the environment and people. In this study, brewer's spent grain was used to produce activated carbon and used as adsorbent because it so plentiful and easily available in our country as byproduct of Beer factory. In

addition, magnetic activated carbon had been synthesized to enhance the recyclability and adsorption efficiency of the activated carbon. Therefore, the magnetic activated carbon composite material expected to be low in cost and could have good adsorption efficiency in removing the hexavalent chromium ion from industrial waste effluents.

1.3 Objectives

1.3.1 General Objective

The general objective of this work is to prepare and characterize magnetically recyclable activated carbon from brewery's spent grain and investigation of its application for hexavalent chromium remediation.

1.3.2 Specific Objectives

- ✓ To synthesize activated carbon from brewer's spent grain.
- ✓ To synthesize magnetic activated carbon (Activated carbon/Fe₃O₄ composite).
- ✓ To characterize pristine activated carbon and activated carbon/Fe₃O₄ composites.
- ✓ To optimize adsorption parameters.
- ✓ To investigate adsorption ability of hexavalent Chromium (VI).

1.4 Significance of the Study

It has been known that several researches demonstrate heavy metal removal by adsorption techniques. This particular investigation has the following particular significances:

- ✓ This study will serve for the industry to use their byproducts for other value-added projects such as wastewater treatment.
- ✓ The study will be important for the community in mitigation of heavy metals (i.e. Cr⁺⁶) remediation by using industrial byproducts.
- ✓ It will add more knowledge on heavy metal waste mitigation process in magnetically recycling activated carbon adsorbent.
- ✓ It provides an alternative way for researchers and environmental scientists on heavy metal removal and material recycling methods in wastewater treatment.
- ✓ It will be an important input for the academic community for future study.

CHAPTER 2 LITERATURE REVIEW

2.1 Water Contaminants

Water contamination is a common problem worldwide. The types and concentrations of natural contaminants depend on the nature of the geological materials through which the groundwater flows and quality of the recharge water [28]. Discharge of domestic and industrial effluent wastes, leakage from water tanks, marine dumping, radioactive waste and atmospheric deposition are major causes of water pollution [29]. Studied improvements are needed in ensuring access to clean water and sanitation worldwide. Currently, based on the report of the WHO about two billion people are use fecal contaminated water worldwide [30]. Hundreds of thousands of people die every year because they are forced to drink contaminated water. As a result, WHO is recommending large investments to provide universal access to safe drinking water. There are different sources of water pollutants discharged in to water sources as shown in **Figure 2.1** as an example.

2.2 Wastewater from Tannery Industries

Tanneries come under oldest process industries consume huge amount of water in several stages. Wastewater generated from tannery industries having large amount of suspended solid, organic, inorganics and heavy metals [31]. This waste product is converted into desirable and useful leather products [32]. Ethiopia is one of the leather producing nations in Africa, which simultaneously produces remarkable amount of cowhide waste [33]. In leather tanning, various cycles are performed utilizing an enormous number of synthetic compounds, for example, surfactants, acids, colors, normal or engineered tanning specialists, sulfonated oils, salts and so forth, to change over creature skin into an unalterable and morally sound item. Thinking about the utilization of these low biodegradable synthetic compounds, tannery wastewaters cause unaffected natural issues. A few specialists consider the tannery wastewater as one of the ten most hurtful substances for nature [34,35].



Figure 2.1 Discharging of different waste material to the water sources [36]

2.3 Environmental Impact of Tannary Industry Wastewater

The tannery industry belongs to one of the most polluting industrial sectors. Almost every tannery industry uses significant amounts of chemicals in the process of transforming animal hides into leather [37]. Environmental impact of tannery wastewater containing, hazardous chemicals such as chromium, synthetic tannins, oils, resins, biocides, detergents has created a negative image on tannery industry [38]. Chrome containing tannery waste is carcinogenic in nature and it causes clinical problems like respiratory tract ailments, ulcers, perforated nasal septum, kidney malfunction and lung cancer [39,40]. Generation of huge amount of liquid and solid wastes, from tannery also emits obnoxious smell because of degradation of proteinous material of skin and generation of gases such as NH_3 , H_2S and CO_2 [41]. During leather processing various air pollutants including SO_2 and Cl_2 fume of formic acid and volatile organic compounds are discharged into atmosphere, Cl_2 is produced in liming, de-liming and pickling operations of leather finishing process [42].

2.4 Heavy Metals

Heavy metal pollution has natural causes as well as human causes [43]. Heavy metals are elements having atomic weights between 63.5 and 200.6, and a specific gravity greater than 5 g/cm^3 [44]. Heavy metal pollution is an inorganic chemical hazard, which is mainly caused by hexavalent chromium (Cr (VI)), arsenic (As), cadmium (Cd), mercury (Hg), zinc (Zn), lead (Pb), copper (Cu), cobalt (Co), and nickel (Ni) [45]. Five metals among them, Cr (VI), As, Cd, Pb, and Hg are the key heavy metal pollutants. These

heavy metals are classified as strong carcinogens by the international agency for research on cancer [7]. Rapid development of industries such as metal plating facilities, mining operations, casting, electroplating, painting, fertilizer industries, tanneries, batteries, paper industries and pesticides increasingly discharged heavy metal polluted wastewaters directly or indirectly into the environment , especially in developing countries [9,43]. If heavy metals such as hexavalent chromium, lead, etc. are present in quantities above certain limits, they can cause adverse effects on the health of living organisms [8,46]. For this reason, lowering the heavy metal concentrations below the certain limits is important to protect the health of humans and all other organisms [43].

Heavy metals exhibit toxic effects towards soil biota by affecting key microbial processes and decrease the number and activity of soil microorganisms. Even low concentration of heavy metals may inhibit the physiological metabolism of a plant. Uptake of heavy metals by plants and subsequent accumulation along the food chain is a potential threat to animal and human health [8]. The heavy metal present in wastewater does not possess a property to degrade naturally and are also very toxic to aquatic life even at low concentrations and hence it is essential to remove heavy metals from wastewater [46]. Chromium is one of the most extensively used heavy metal in industrial applications such as in leather tanning, pigments and stainless-steel production. This element can be found in metal alloys as well as Cr containing compounds [47].

2.5 Source of Heavy Metals

Heavy metals exist in rocks, as ores, such as sulphides (iron, arsenic,, lead, zinc, cobalt, gold, silver and nickel sulphides), oxides (aluminum, manganese, gold and selenium) and both sulphides and oxides from which they are recovered as minerals [48–50]. Basically, there are two main sources of heavy metals in wastewater. These are natural and human sources. The natural factors include soil erosion, volcanic activities, urban run offs and aerosols particulate [11,51]. The human factors include effluents from textile, leather, tannery, electroplating, galvanizing, pigment and dyes, battery manufacturing, metallurgical and paint industries at small and large scale sector [11,13,46,52–54]. Electroplating process, such as, electro less depositions, conversion coating, milling and etching generate heavy metals (such as hexavalent chromium, cadmium, zinc, lead,

nickel, copper, vanadium, platinum, silver, and titanium) [55]. Industries, agriculture, mining and metallurgical processes and runoffs also lead to the release of pollutants to different environmental compartments as shown in **Figure 2.2** [56,57].

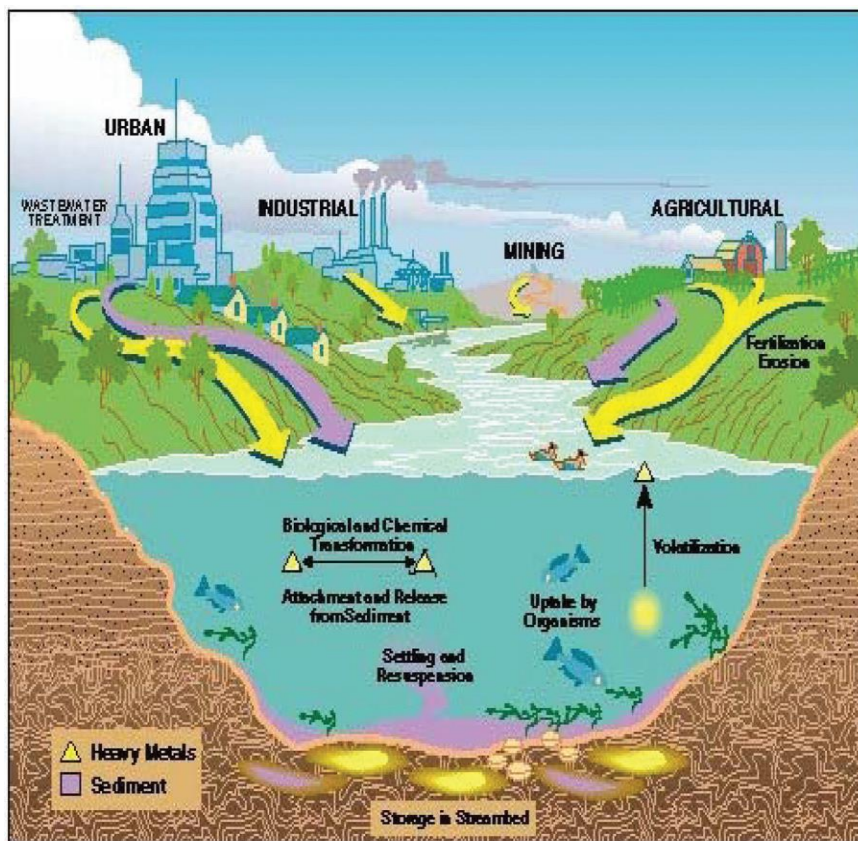


Figure 2.2 Sources and sinks of heavy metals [56].

2.6 Toxicity of Heavy Metals

Heavy metals contamination is becoming a serious issue of concern around the world as it has gained momentum due to the increase in the use and processing of heavy metals during various activities to meet the needs of the rapidly growing population. Soil, water and air are the major environmental compartments which are affected by heavy metals pollution [58]. Heavy metal pollution is a great threat facing to human health due to the solubility, mobility, bio-accumulation and non-biodegradability of toxic metal ions. Chromium is a first-row d-block transition metal of group VIB in the periodic table with the following properties: atomic number 24, atomic mass 52, density 7.19 g cm^{-3} , melting point $1875 \text{ }^{\circ}\text{C}$ and boiling point $2665 \text{ }^{\circ}\text{C}$. It is one of the less common elements and does not occur naturally in elemental form [59,60].

Chromium is present in many oxidation states, mainly chromium (VI) and chromium (III), which are found in industrial effluents. It is more toxic in hexavalent form as compared to trivalent form in which Cr (III) is essential trace element used for glucose metabolism. Among the 10 major chemical contaminants authenticated by the WHO hexavalent chromium is accepted as one of the highly threatening substances accumulated in human body [61]. Hexavalent chromium can exert highly toxicity and carcinogenicity to human beings associated with a variety of detrimental health effects such as skin rash, weakened immune system, nose irritations and nosebleed, ulcers, allergic reactions, kidney and liver damage, genetic material alteration, gastric damage, and even deaths as shown in **Figure 2.3**. Hence, the decontamination of Cr (VI) from sewage has been a severe task for human being which affect human leg, skin and dermatitis [62]. Due to the aforementioned health effects related to Cr (VI) toxicity, numerous studies have focused on developing methods for the removal of Cr (VI) compounds from various matrices [63,64]. On the other hand, Cr (VI) hydrolyzes to $\text{Cr}_2\text{O}_7^{-2}$, CrO_4^{-2} and HCrO_4^- which are strong oxidants [64].



Figure 2.3 Health effect Cr (VI) in human body [65].

The generation of heavy metals from different industrial activities in to the environment is major concern because of their toxicity, bio-accumulating tendency and threat to human life and the environment through a process of bio magnification, they further accumulate in food chains as shown in **Table 2.1** [66].

Table 2.1 Source and impact of heavy metal with their WHO limit in ppm

S.No	Heavy Metals	Source	Impact	WHO limit in ppm	Ref.
1	Hg	Enters the environment through leaching of soil due to acid rain.	Damage to nervous system, kidneys and vision.	0.001	[48,67]
2	Pb	Paint, mining wastes, incinerator ash, water from lead pipes, solder and automobile exhaust.	Causes damage to kidneys, nervous system and red blood cells.	0.01	[68–70]
3	Cd	Electroplating, mining and plastic industries, sewage.	Causes kidney disease.	0.003	[49,71]
4	Cr (VI)	Cement industry, effluents from chemical plants and contaminated landfill.	Pulmonary, fibrosis, lung cancer.	0.05	[72–74]
5	As	Enters the environment through Herbicides, wood preservatives, and mining industry.	Cause damage to skin, eyes and liver. May also cause cancer.	0.01	[48,75]
6	Ni	Porcelain enameling, nonferrous metal, paint formulation and electroplating	Headache, dizziness, vomiting, chest pain, tightness of the chest.	0.05	[76]

The existence of hexavalent chromium, mercury, nickel, copper, cadmium, lead, arsenic and others metals has a possibly damage effect on human physiology and other biological systems when the tolerance levels are exceeded beyond limits. Hence, there is the need for proper understanding of the conditions, such as the concentrations and oxidation states, which make them harmful and how toxicity occurs [49,52].

2.7 Importance of Heavy Metals

Heavy metals are important for both microorganism and plant health. Certain heavy metals such as Ca, Cu, Zn, Co, Mg and Fe are essential to man, their daily medicinal and dietary for survival and growth of microbes. The metallic element could be used as a nutrient for plant health however, there are two principles used to describe metals as important nutrients for healthy plant which contain: (a) it would be essential by the plants to complete its life cycle and (b) it must be part of crucial plant constituent [77]. The tolerance limits of drinking and potable waters have been described in **Table 2.2**. Though, some heavy metals like As, Cd, Pb and methylated forms of Hg have been written to have unknown function in human

biochemistry, physiology and consumption even at very low concentrations can be toxic. Any level of concentration of silver in drinking water has been disallowed both by the WHO and national agency for food and drugs administration and control (NAFDAC) [49]. Zn and Cu are the two vital elements for plants, humans, animals and microorganisms. The connection between soil and water contamination and metal uptake by plants is determined by many chemical and physical soil factors as well as the physiological properties of the crops [59].

Table 2.2 Guideline in drinking water by the WHO and national agency for food and drugs administration and control (NAFDAC) for heavy metals [49]

Heavy metal	WHO in mg/l	Max. acceptable conc. (NAFDAC) in mg/l
Zn	5	5
Mg	50	30
Ca	50	50
As	0.01	0.0
Cd	0.003	0.0
Pb	0.01	0.0
Ag	0.0	0.0
Cr(VI)	0.0	0.0
Hg	0.001	0.0

2.8 Guide Line of Heavy Metal Discharge to the Environment

The maximum contaminant level (MCL) standards for heavy metals discharging established by USEPA [78]. Hexavalent chromium is one of the toxic heavy metal in the environment released from various sources like electroplating, leather tanning, mining, textile and fertilizer industries. The maximum permissible limit of hexavalent chromium in drinking water and inland surface water according to US EPA are 0.05 and 0.1 mg/l, respectively [47,74]. **Table 2.3** describe the permissible limits of various toxic heavy metals in different standards discharge different country to minimize the health and environmental burden of toxic heavy metal.

Table 2.3 Permissible limits of various toxic heavy metals in different country standards [77]

Metals	Permissible limits for portable water (mg/l)				
	Indian standard			USEPA	EU Standard
	Inland surface water	Public surface water	Marine coastal areas		
Ni	3	3	5	0.1	0.02
Zn	5	15	15	5	-
Cu	3	3	3	1.3	2
Cd	2	1	2	0.005	0.005
Pb	0.1	1	2	0.015	0.01
Total Cr	2	2	2	0.1	0.05
As	0.2	0.2	0.2	0.1	0.01
Hg	0.01	0.01	0.01	0.002	0.001
Mn	2	2	2	0.05	0.05

2.9 Common Wastewater Remediations

Advanced wastewater remediation is defined as any process designed to produce an effluent of higher quality than normally attained by secondary treatment processes. Advanced wastewater remediation used to remove toxic materials in water such as; additional organic and suspended solids, nitrogenous oxygen demand, and toxic heavy metals. Common methods for removal of heavy metals pollutant from industrial effluents including: ion exchange, chemical precipitation, Electro-chemical, Membrane filtration process, flocculation and coagulation, reverse-osmosis, adsorption etc. as shown in **Figure 2.4** [79–83].

Chemical precipitation is one of the most widely used for heavy metal removal from inorganic effluent discharged from different industry due to its simple operation. Lime and lime stone are the most commonly employed precipitant agents due to their availability and low-cost most countries [84,85].

Reverse osmosis (RO): a pressure-driven membrane process, water can pass through the membrane, while the heavy metal is retained and pressure is the major parameter that affects the extent of heavy metal removal by RO. Nano-filtration (NF): can effectively remove metal at a wide pH range of 3–8 and at pressure of 3–4 bars. The limitation of NF method is that it is costly and prone to membrane fouling.

From this mentioned methods adsorption is a recent method to remove heavy metals like hexavalent chromium (VI). Some advantage of common remediation methods such as, nano-filtration, reverse osmosis and membrane filtration are: large number of applications and module configurations, small space requirement, simple, rapid and efficient even at high concentrations, produces a high-quality treated effluent, no chemicals required, low solid waste generation and eliminates all types of heavy metals. On the other hand, some of the disadvantages of the common remediation techniques include; high energy requirements, high maintenance and operation costs, rapid membrane clogging, are often too high for small and medium industries, limited flow rates, etc. [29].

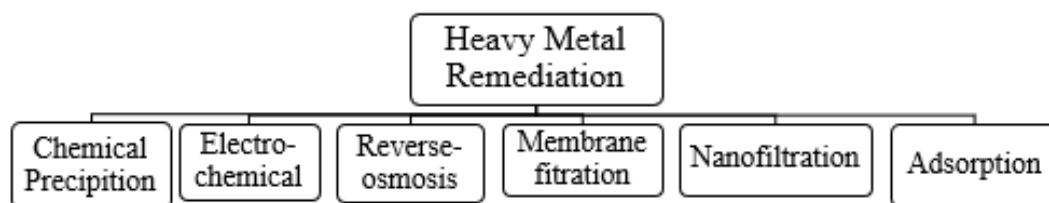


Figure 2.4 Methods for the remediation's of hexavalent chromium [56,86].

2.9.1 Adsorption Methods

Adsorption method is a method that uses solid adsorbent materials with good porosity and high specific surface area as an adsorbent to adsorb heavy metal from wastewater [87]. Adsorption is a widely used method for the treatment of industrial wastewater having heavy metals like Cr (VI), color and other inorganic and organic impurities. The benefits of adsorption process are its simplicity in operation, inexpensive and easily available [78]. Adsorption refers to the attachment of substances from a liquid or gaseous phase to solids. The solid is referred to as the adsorbent. The substance taken up is called the adsorbate. Adsorption has important for industries which use for removal of metal from industrial wastewater. In general, there are three main steps involved in pollutant sorption onto solid sorbent such as; (i) the transport of the pollutant from the bulk solution to the adsorbent surface (ii) adsorption on the particle surface and (iii) transport within the adsorbent particle.

Various low cost adsorbents derived from agricultural waste, industrial by product, natural material, or modified biopolymers have been recently developed and applied for

the removal of heavy metals from metal contaminated wastewater [88,89]. The attachment of atoms or molecules of adsorbate on the surface of solids and liquids may be through two types of forces, physical or chemical. Depending upon the types of forces involved in adsorption it may be divided into two types, physical adsorption or physisorption and chemical adsorption or chemisorption's [90].

I. Chemical adsorption: the adsorbate can form a monolayer. It is also utilized in catalytic operations. In general, the main steps involved in adsorption of pollutants on solid adsorbent are:

(a) Transport of the pollutant from bulk solution to external surface of the adsorbent. Internal mass transfer is carried by pore diffusion from outer surface of adsorbent to the inner surface of porous structure.

(b) Adsorption of adsorbate on the active sites of the pores of adsorbent. The overall rate of adsorption is decided by either film formation or intra-particle diffusion or both as the last step of adsorption are rapid as compared to the remaining two steps.

II. Physical adsorption: occurs in any solid/liquid or solid/gas system. Physical adsorption is a process in which binding of adsorbate on the adsorbent surface is caused by van der Waals forces of attraction [78].

2.9.2 Adsorption Mechanism

Classical mechanisms of adsorption are divided into three stages as shown in **Figure 2.5**. Stage (a) is the diffusion of adsorbate to adsorbent surface. It occurs by the dispersion of adsorbate on the adsorbent surface by intermolecular powers among adsorbate and adsorbent, stage (b) migration into pores of adsorbent includes relocation of adsorbate into pores of adsorbent. During the last stage (c) a monolayer of adsorbate builds up on the adsorbent when the adsorbate particles are appropriated on a superficial level and topped off the volume of pores. Particles adsorbate are developing the monolayer responded molecule, ion and atom to the dynamic destinations of adsorbent [91].

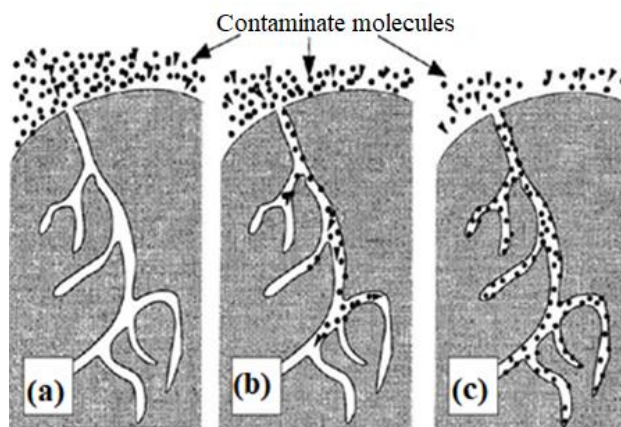


Figure 2.5 Three stages of adsorption mechanisms.

2.9.3 Adsorption Mechanism of Cr (VI)

Many studies have claimed that Cr (VI) could be removed from the aqueous phase through an adsorption mechanism, whereby anionic Cr (VI) ion species bind to the positively charged groups of nonliving biomasses. According to Park and his coworker the removal of Cr (VI) from an aqueous system follows the direct reduction (Mechanism I) and indirect reduction (Mechanism II) as shown in **Figure 2.6** [92]. In the direct reduction Cr (VI) is directly reduced to Cr (III) in the aqueous phase by contact with the electron donor groups of the biomass that is, groups having lower reduction potential values than that of Cr (VI). The indirect reduction consists of three steps: (1) the binding of anionic Cr (VI) ion species to the positively charged groups present on the biomass surface, (2) the reduction of Cr (VI) to Cr (III) by adjacent electron donor groups and (3) the release of the Cr (III) ions into the aqueous phase due to electronic repulsion between the positively charged groups and the Cr (III) ions or the complexation of the Cr (III) with adjacent groups capable of Cr binding. Amino and carboxyl groups take part in direct mechanism [92]. As the pH of the aqueous phase is lowered, the large number of hydrogen ions can easily coordinate with the amino and carboxyl groups present on the biomass surface. Thus, low pH makes the biomass surface more positive. The more positive the surface charge of the biomass, the faster the removal rate of Cr (VI) in the aqueous phase, since the binding of anionic Cr (VI) ion species with the positively charged groups is enhanced [93].

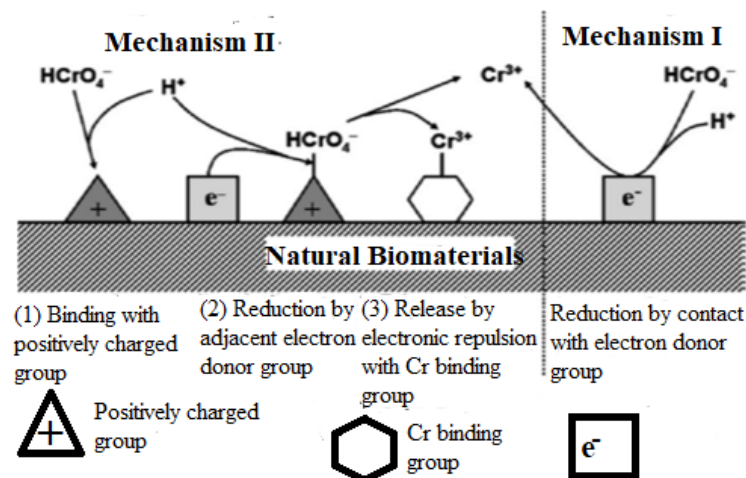


Figure 2.6 The mechanism of Cr (VI) bio sorption by natural biomaterials [94].

The low pH likewise quickens the decrease response in both immediate and backhanded systems. The arrangement pH is the most significant controlling mechanism in the utilization of nonliving biomass in the adsorption cycle. Henceforth, it is of centrality that the pH of wastewaters containing substantial metals is commonly acidic. Then, if there are few electron contributor bunches in the biomass or protons in the fluid stage, the chromium bound to the biomass can stay in the hexavalent state [92,94].

2.10 Adsorbent Materials

The adsorbent materials that are profitable and effective have opened walks for investigators to attempt almost any material of industrial byproduct like BSG used in adsorption of hexavalent chromium ions. Due to their plentiful accessibility, biodegradability and inexpensive cost, many adsorbents from diverse sources such as sawdust, pinecone biomass, almond green hull, grape peelings, nutshells, lemon peel powder and fungal biomass [64]. Adsorbent materials can be categorized under the following biomaterials such as industrial wastes/by product, activated charcoal, algae, bacteria, fungi, animal products, agricultural wastes and cellulose based materials [11,95].

2.10.1 Agricultural Wastes

Agricultural wastes such as corn cob, coconut shell, jatropha, oil palm fiber, wood sawdust and date stone are of interest to be converted into activated carbons because of their hardness and high strength in which these desired properties are due to its high

lignin, high carbon content and low ash content of the materials [96,97]. Agricultural waste remains a sustainable and reproducible material which can be used to synthesis carbonaceous mass called activated carbon [98].

2.10.2 Industrial Byproducts/Wastes

Industrial by products and plant wastes have been used as the unconventional and cheapest adsorbents for heavy metals from aqueous solutions [99,100]. These materials are produced either as byproducts or leftover materials from the industrial operations. Industrial byproducts/wastes include brewer's spent grain, lignin, fly ash, sludge, blast furnace slag and red mud have been applied for the removal of heavy metals from water/wastewater [101]. They have very high strength, resistance, electrical products such as fly ash, waste iron, metallic iron, hydrous titanium oxide, blast furnace sludge, waste slurry and red mud have been used as effective adsorbents during the past for their technical feasibility to remove toxic heavy metals from contaminated water [11,99].

2.10.2.1 Brewer's Spent Grain

Beer is the fifth most consumed beverage in the world next to tea and it continues to be a popular drink with an average consumption of 23 liters per person per year by population aged above 18. The brewing industry has an ancient tradition and is still a dynamic sector open to new developments in technology and scientific progress [100]. The brewing process uses malted barley (cereals), unmalted grains (sugar/corn syrups), hops, water and yeast to produce beer [102]. Most brewers use malted barley as their principal raw material. From this process, various byproducts are generated. The three most common byproducts are spent grains, spent hops and surplus yeast, which are generated from the main raw materials. These three brewery byproducts are available in large quantities throughout the year, but their use has still been limited, to being basically sold to local dairy farmers to be used as cattle feed, charcoal production, energy production, adsorbent material and raw material for paper and pulp production [103].

However, as most of these are agricultural products, they can be readily recycled and reused. BSG is available at low or no cost throughout the year and is produced in large quantities [20]. Brewery spent grain is a lignocellulosic material rich in protein and fiber,

which account for around 20 % and 70 % of its composition, respectively. The main components of these fibrous tissues are arabinoxylan, lignin and cellulose [104].

2.11 Metal Adsorption by Magnetic Activated Carbon

2.11.1 Activated Carbon

AC is one of the most commonly used adsorbents due to its high specific surface area, porosity, chemical resilient and thermal stability. However, the used activated carbon often suffers from serious problems of separation in liquid solid phase processes. Among many adsorbents, AC is a kind of black porous solid adsorption material with unique properties [11]. Due to its large surface area, surface chemistry and porous structure, AC has shown excellent efficiency for contaminant removal in the liquid phase. To become a sustainable process and to reduce the preparation costs of AC, waste materials like walnut shells, pine cones, palms, almond wastes, pomegranate peels, orange peels and leaves have been used in order to prepare AC [105,106].

Attia *et al*, examined that AC was synthesized from olive stones and utilized as an adsorbent for the removal of Cr (VI) from aqueous solution with the adsorption capacity of 71 mg/g [107]. In similar study, Dula *et al*, reported that the adsorption of hexavalent chromium from aqueous solutions using activated carbon prepared from bamboo waste by KOH activation. Adsorption efficiency and capacity of hexavalent chromium were found to be 98.28% at pH 2 and 59.23 mg/g at 300 K [108]. In other study, Katenta *et al*, showed that bio-char was synthesized from date palm seed to remove chromium (VI) ions from aqueous solutions by adsorption was investigated. The maximum percent removal of chromium (VI) ions at pH 2 was 86 % [109]. Madhu *et al*, synthesized AC from wheat bran in adsorption of heavy metals using biodegradable adsorbent as indicating **Figure 2.7**. The maximum overall removal efficiency of chromium is 10.41 mg/g [45]. However, many researchers are still working on the modification of AC to increase the efficiency.

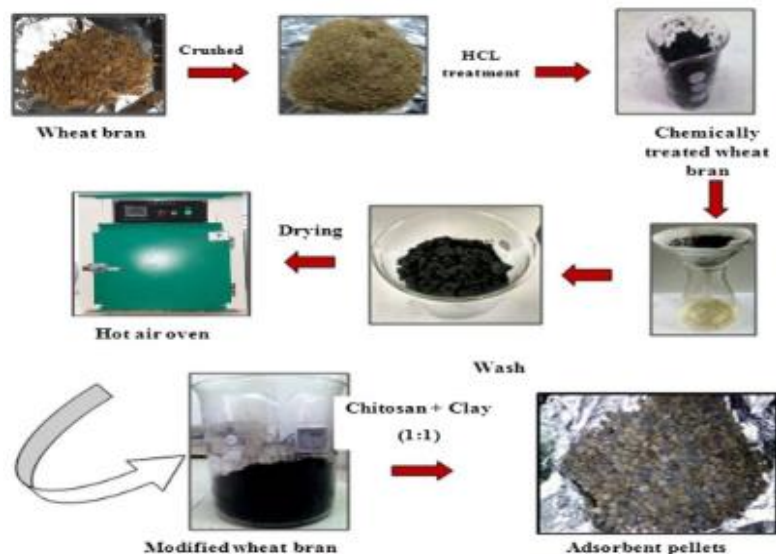


Figure 2.7 Synthesis of AC from wheat bran

2.11.2 Magnetic Activated Carbon

Magnetic technology makes it possible to effectively separate and recover the spent activated carbon by a simple magnetic process. In recent years preparation and application of magnetic activated carbon (MAC) have been given more and more attention [22]. At present, MAC is mainly prepared by a two-step method, which combines activated carbon with magnetic material by mixing, adsorption, chemical co-precipitation and reactivation. At two-step method has several disadvantages of complicated and costly process and the loss of adsorption capacity. In contrast, MAC made by a one-step method can maintain high specific surface area and stable magnetic properties because the magnetic additive is added to the raw material and involved in the whole process of preparing activated carbon [110]. Magnetic adsorbent is commonly used to describe the materials derived from iron (particles of $\gamma\text{-Fe}_2\text{O}_3$, Fe_3O_4 and CoFe_2O_3) or composites prepared from different types of matrix modified with iron compounds, which could be used in the adsorption of water contaminants [111].

In recent years, researchers have combined AC with magnetite particles (Fe_3O_4) to overcome this barrier. In the presence of Fe_3O_4 , the magnetic activated carbon (MAC) adsorbent and adsorbed contaminants could be easily separated from treatment systems by an external magnetic field. Magnetic particles, especially Fe_3O_4 , are easy to prepare and inexpensive [112]. Furthermore, Fe_3O_4 particles itself can increase the number of

adsorption sites and enhance the adsorption capacity towards pollutants. Although the MAC materials exhibit as potential adsorbents for removing heavy metal ions from contaminated water improvements of their adsorption are still needed to make them more practicable [113].

Recently, introduction of magnetism in activated carbon has gained great concern as it helps in separating AC from aqueous solutions along with the pollutants simply using a magnetic separator. It has been recognized that magnetic filtration is a promising water treatment technology which overcomes the disadvantages of filter blockage and secondary pollution caused by the tradition lengthy filtration steps and realizes rapid and efficient contaminant removal from wastewater. MAC is a kind of modified activated carbon which possesses both high adsorption capacity and magnetic property. MAC with super paramagnetic particles can be recovered very quickly by external magnetic field and reuse without losing the active sites, which is of great interest to provide the basis for the recycling and reuse of adsorbents [21]. Magnetic adsorbents can easily be manipulated by low strength external magnetic fields, permitting easy recovery from contaminated water which is high in suspended solids and oil and grease [80]. Guo *et al*, demonstrated that MAC was prepared from using the mixture of $\text{FeCl}_3 \cdot 6\text{H}_2\text{O}$ and biomass waste (peanut shells) by modified one-step method under CO_2 atmosphere as shown in **Figure 2.8** [21].



Figure 2.8 Synthesis of MAC from mixture of peanut shells and $\text{FeCl}_3 \cdot 6\text{H}_2\text{O}$

2.12 Synthesis Methods of Activated Carbon and Magnetic Activated Carbon

2.12.1 Activation of Activated Carbon

There are two type of activation of activated carbon. Those are physical and chemical agents. BSG was transformed in to activated carbon by physical or chemical activation, the preceding one being more sufficiently used than physical activation, since it involves lower activation temperatures and gives higher product [114]. Chemical activation is used

for the treatment of the BSG with a chemical agent such as H_2SO_4 , ZnCl_2 , H_3PO_4 , KOH , NaOH , ferric chloride (FeCl_3), magnesium chloride (MgCl_2) and calcium chloride (CaCl_2) with heating at 450 – 900 °C therefore carbonization and activation happen instantaneously [115]. Among the above chemical agents that can be used in this method, H_3PO_4 is commonly utilized due to economic and environmental reasons, since it requires relatively low activation temperatures (nearly 400–500 °C) or 400-600 °C and can be recovered at the end of the process [106,116].

2.12.2 Preparation Methods of Magnetic Activated Carbon

MAC can be synthesized; using a variety of methods, the most widely used of which include chemical co-precipitation, hydrothermal, impregnation, one-step and ball milling from this method magnetite was formed in chemical co-precipitation due to the simplicity design and low cost. The co-precipitation method has been extensively used by the earlier investigators and is usually conducted in an alkaline solution via the precipitation of ferric and ferrous salts in the presence of AC. This is usually followed by heating the prepared solution to precipitate iron oxides into the pores of AC. Magnetite (Fe_3O_4) are usually formed by this technique. At a pH rate, ranging between 8-14, it is quite expected of Fe_3O_4 to be created in a non-oxidizing setting, where in the ratio of Fe^{3+} to Fe^{2+} is equal to 2:1 as shown in **Equation 1** [105].



2.13 Factors Affecting Adsorption

There are many factors which affect the efficiency of adsorbents for heavy metal removal from wastewater. The main factors are initial concentration, adsorbent dose, pH and contact time [11,76,117].

Effect of solution pH: The pH of the metal ion solution is an important parameter for adsorption of metal ions because it affects in the solubility of the metal ions, concentration of the counter ions on the functional groups of the adsorbent and the degree of ionization of the adsorbate [118]. Therefore, pH of solution influences the nature of biomass, binding sites and metal solubility.

Initial solute concentration: The initial concentration provides an important driving force to overcome all mass transfer resistance of metal between the aqueous and solid phases [102]. Increasing amount of metal adsorbed by the biomass will be increased with initial concentration of metals. It is generally agreed that the adsorption capacity increases as the initial metal ion concentration in the solution increases, whereas the metal removal percentage (also called removal efficiency) decreases by increasing the metal ion initial concentration. Research findings shows that the removal efficiency of Cr (VI) decreases as the initial Cr (VI) concentration increases [119].

Adsorbent dosage: The amount of biomass added in the solution during adsorption process also affects the specific metal uptake. In principle, the amount of adsorbent present, on the adsorbate the available adsorption sites also increase [120]. At low biomass dosage the number of ions adsorbed per unit adsorbent weight is high. Adsorption capacity is reduced when the biomass dosage increases as a result of lower adsorbate to binding site ratio where the ions are distributed onto larger amount of biomass binding sites [121].

Contact time: A contact time during which an adsorbate could be completely adsorbed onto an adsorbent is important for design and control of adsorption systems. The removal efficiency increased with an increase in contact time before equilibrium is reached. The amount adsorbed at the equilibrium time reflects the maximum adsorption capacity of the adsorbent under the operating conditions [122].

2.14 Adsorption Isotherms

The adsorption isotherm is important to describe how the adsorbate interacts with the adsorbent [123]. The adsorption capacity of the adsorbent is a very important factor for designing an adsorption system. Adsorption equilibrium isotherm correctly establishes the relationship between adsorbate and adsorbent at a fixed temperature. Adsorption isotherm is an empirical relationship used to predict how much solute can be adsorbed by adsorbent. Adsorption isotherms provide information about the effects of the solution concentration on the adsorption capacities of the metal ions and interaction of adsorbate molecules with adsorbent [124]. Distribution of metal ions between the liquid phase and

the solid phase can be described by the well-known isotherms such as Freundlich, Langmuir and Temkin adsorption isotherm.

Langmuir isotherm model assumes monolayer adsorption onto a surface containing a finite number of adsorption sites of uniform surface [125]. When a site is filled, no additional adsorption occurs and the model is expressed as **Equation 2**.

$$\frac{C_e}{q_e} = \frac{1}{K_L q_L} + \frac{C_e}{q_L} \dots \dots \dots (2)$$

Where K_L (l/mg) = adsorption constant, which reflects the affinity between the adsorbent and adsorbate. q_L and K_L were determined from the slope and x or y intercept of the plots of C_e/q_e versus C_e .

The characteristics of Langmuir isotherm can be stated in term of dimensionless separation factor and described the type of isotherm defined by **Equation 3**.

$$R_L = \frac{1}{1 + K_L q_L} \dots \dots \dots (3)$$

Where, K_L and q_L is the Langmuir constant. The value indicates the nature of the adsorption. The R_L value of Langmuir models where, $R_L = 1$ liner, $R_L = 0$ Unfavorable, $0 < R_L < 1$ favorable.

Freundlich isotherm is introduced as an empirical model, where q_e represents the amount adsorbed per amount of adsorbent at the equilibrium (mg/g), C_e represents the equilibrium concentration (mg/l), and K_f and n are parameters that depend on the adsorbate and adsorbent [126]. This model describes systems where the adsorption is done on heterogeneous surfaces with interactions between the adsorbed molecules as given by in **Equation 4**.

$$\log q_e = \log K_F + \frac{1}{n} \log C_e \dots \dots \dots (4)$$

K_F and n are Freundlich constants, which represent adsorption capacity and adsorption intensity, respectively. The Freundlich constants were determined from the slope and intercept of a plot of $\log q_e$ versus $\log C_e$.

Temkin isotherm model considered the effects of indirect adsorbate/adsorbent interactions on adsorption isotherms. The heat of adsorption of all the molecules in the layer would decrease linearly with coverage due to adsorbate /adsorbent interactions. It contains a factor that explicitly takes into the account of adsorbing species in adsorbent interactions. The linear form of this isotherm is given by **Equation 5**.

$$q_e = B_1 \ln K_T + B_1 \ln C_e \dots \dots \dots (5)$$

Where, $B_1 = RT/b$. T is the absolute temperature (Kelvin) and R is the universal gas constant ($J \text{ mol}^{-1} \text{ K}^{-1}$). B is the Temkin constant related to the heat of adsorption and K_T is the equilibrium binding constant (l/mg) corresponding to the maximum binding energy [127].

2.15 Adsorption Kinetics

Several kinetic models have been applied to examine the controlling mechanism of metal ion adsorption from aqueous solution. To understand the rate and type of adsorption on adsorbents, there are kinetic models [128]. Different kinetic models like pseudo first order and pseudo second order kinetic models were applied for the fitting of the experimental data [129].

The pseudo first order model identifies the adsorption based on the adsorption capacity of solids. The form of pseudo first order is given by **Equation 6**.

$$\log (q_e - q_t) = \log q_e - \frac{K_1 t}{2.303} \dots \dots \dots (6)$$

Where q_e and q_t represent the amount of metal ions adsorbed at equilibrium and at time, t, respectively, k_1 is pseudo first order rate constant.

Pseudo second-order adsorption kinetic rate equation can be expressed in **Equation 7**.

$$\frac{t}{q} = \frac{1}{K_2 q_e^2} + \frac{t}{q_e} \dots \dots \dots (7)$$

Where k_2 (g/mgmin) is the rate constant of the pseudo-second-order adsorption, q_e is the amount of metal ion adsorbed on the adsorbent at equilibrium (mg/g) and q_t is the amount of metal ion adsorbed on the adsorbent at any time, t (mg/g).

2.16 Spectrophotometric Method of Cr (VI) Analysis

Several methods are available for the analytical determination of Cr (VI) such as, AAS (Atomic absorption spectroscopy), ICPS (Inductively coupled plasma spectroscopy), UV–Visible spectrophotometry etc. UV-Visible spectrophotometry is a well-established technique for the selective determination of Cr (VI) with good detection power. The standard method for the selective determination of Cr (VI) is based on the formation of a red violet colored complex with 1, 5 diphenyl carbazide under acidic conditions, which can be detected spectrophotometrically at 540 nm. In order to achieve good reproducibility, several conditions such as temperature or amount of reagent and acids must be kept strictly constant [130].

CHAPTER 3 MATERIALS AND METHODS

3.1 Apparatus and Instruments

Furnace (XMT-F9), SEM (INSPECT F 50), XRD (XRD-700 X-RAY), BET (SA9603), UV-Vis spectroscopy (Biochrom, England), FT-IR (PerkinElmer, USA), Bar magnet, COD (HI83099), BOD (BOD direct), Funnel, Oven (Fisher scientific, 40GCEMD), pH meter (Eutech & HI 83141) and Hot plate (AM5250A), Electronic balance (AUW 320), Orbital shaker (KT 4000 IC), Magnetic stirrer (Auto Science, AM 5250A), Zipper plastic bags, Whatman Filter Paper, Mesh size sieves and Vacuum filtration had been used in this work.

3.2 Chemicals and Reagents

The chemicals and reagents which have been used in this study are: Phosphoric acid (H_3PO_4) (85 wt%, Sigma-Aldrich, USA), Sodium hydroxide (98%, Sigma-Aldrich, USA), hydrochloric acid (HCl) (37%, Sigma-Aldrich, USA), Ferrous tetrahydrate ($\text{FeCl}_2 \cdot 4\text{H}_2\text{O}$) (99 % , Loba chemie plc., India), Ferric chloride hexahydrate ($\text{FeCl}_3 \cdot 6\text{H}_2\text{O}$) (97%, Sigma-Aldrich ,USA), Potassium dichromate ($\text{K}_2\text{Cr}_2\text{O}_7$) (99.9% , Sigma-Aldrich, USA), 1,5 Diphenyl carbazide ($\text{C}_{13}\text{H}_{14}\text{N}_4\text{O}$) (Sigma-Aldrich, USA), Distilled water, Ethanol (99.4% ,Addis Ababa, Ethiopia), Sulphuric acid (H_2SO_4) (98% Sigma -Aldrich ,USA), Acetone (99% , Sisco research laboratory plc., India), Perchloric acid (HClO_4) (70%, Loba chemie plc., India) and Concentrated HNO_3 (70% , Central drug house plc., India). All chemicals had been in analytical grade.

3.3 Sampling and Sample Preparations

3.3.1 Spent Grain Sample Collection

The fresh brewery spent grain sample was collected from Heineken brewery share company (HBSC) located at Kilito near to Addis Ababa Science and Technology University using polyethylene bag. After collection, the brewery spent grain was washed repetitively 5 times with distilled water to remove impurity and dried in the oven at 60°C for 24 hr. The dry sample was stored at room temperature using plastic container for further experiment.

3.3.2 Preparation of Activated Carbon

The brewer's spent grain (BSG) was ground, sieved and to be used for the prepared activated carbon. A weighed amount (60 g) of BSG were transferred into three conical flasks containing different concentrations of H_3PO_4 , i.e., 10% wt/wt., 30% wt/wt., and 50% wt/wt., [131]. The content of the three flasks were covered with aluminum foil and left over for 24 hr. The BSG was then impregnated with an aqueous solution of H_3PO_4 at a ratio of 1:2 for 24 hr as shown in **Figure 3.1**. The three treated samples (with 10, 30, and 50% H_3PO_4) were washed thoroughly with distilled water, transferred into 12 labeled clean dry crucibles and dried at 105°C oven for 24 hr, kept in desiccator to remove moisture to perform carbonization. Then the samples in the crucibles were placed in furnace at 200°C for 30 min to initiate the carbonization process. The carbonization process was held at four different temperature (400 , 450 , 500 and 550°C) for 2 hr and the contents were allowed to cool to room temperature. Each sample were thoroughly washed and rinsed using vacuum filtration with hot distilled water to remove all the excess acid until the pH of the filtrate was approximately 7. Then dried in an oven at a temperature of 105°C for 24 hr and kept in desiccator for further analysis [116]. The activated carbon prepared using 50% H_3PO_4 soaked BSG at carbonization temperature of 400°C was indicated in **Figure 3.2**.

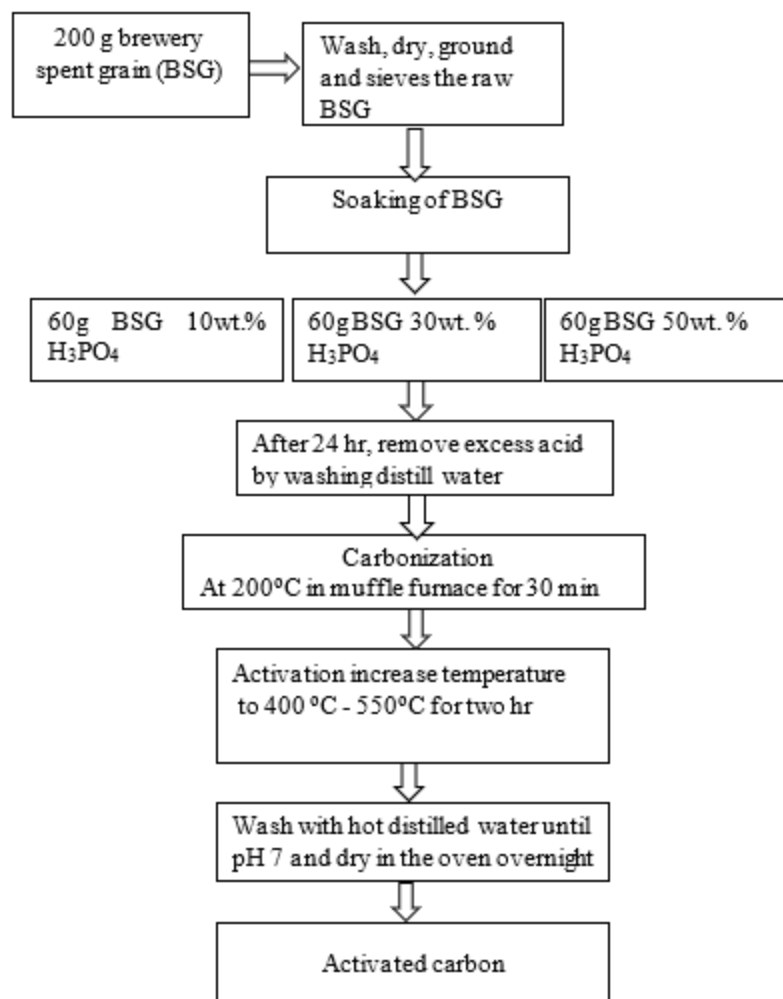


Figure 3.1 Synthesis method of activated carbon.



Figure 3.2 The synthesized activated carbon from BSG impregnated at 50% H₃PO₄.

3.3.3 Preparation of Magnetic Activated Carbon

Magnetic activated carbon was prepared from activated carbon, ferric chloride hexahydrate ($\text{FeCl}_3 \cdot 6\text{H}_2\text{O}$) and ferrous chloride tetra hydrate ($\text{FeCl}_2 \cdot 4\text{H}_2\text{O}$). First, 6 g AC was dissolved in 200 ml distilled water in 500 ml beaker (solution A). Then, 3 g of $\text{FeCl}_3 \cdot 6\text{H}_2\text{O}$ dispersed in 100 ml distilled water and 1.5 g of $\text{FeCl}_2 \cdot 4\text{H}_2\text{O}$ dissolved in 50 ml distilled water was mixed in 500 ml beaker (solution B). Thereafter, solution A and solution B were mixed in 500 ml beaker and stirred for 1 hr [14,131,132]. After mixing, the pH of the solution was adjusted into pH 11 by adding 0.1M of NaOH solution drop wise and heated to a temperature of 70°C followed by vigorous stirring using magnetic stirrer. Then, after cooling to room temperature and aging for 24 hr the produced MAC was separated using magnet and washed using distilled water and ethanol until the pH of the filtrate was approximately 7 as shown in **Figure 3.3**. Finally, the prepared MAC was labeled and dried at 50°C in the oven overnight.

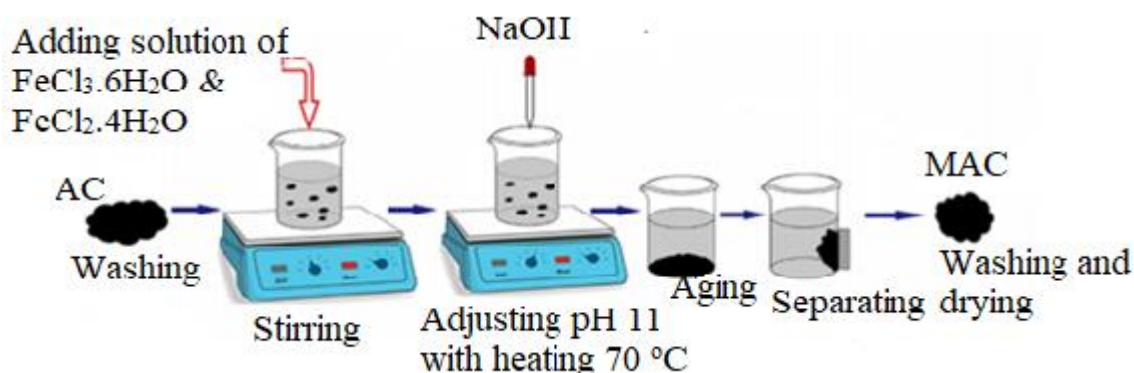


Figure 3.3 Schematic diagram for the Synthesis of magnetic activated carbon.

3.4 Characterization Methods of Adsorbent

3.4.1 Proximate Analysis of Activated Carbon and Magnetic Activated Carbon

Proximate analysis performed to determine the amount of moisture, volatile matter, fixed carbon and ash content in activated carbon and MAC.

3.4.1.1 Moisture Content Determination

The moisture content determination was developed by following ASTM named as oven drying test method. Sample of activated carbon (2 g) was placed in to a dry, closed capsule and weighed accurately using electronic balance sensitive to 0.01 mg. The

capsule opened and placed with the lid in a preheated oven. The sample was dried to constant weight at 105 °C for 3 hr, then removed out from the oven and with the capsule closed, then cooled to ambient temperature [133]. The closed capsule was weighed again accurately. The moisture content was determined as in weight % as follows in **Equation 8**.

$$\text{MC, \%} = \frac{W_2 - W_3}{W_2 - W_1} * 100 \dots \dots \dots (8)$$

Where, W_1 is weight of capsule with cover (g), W_2 is weight of capsule plus original sample (g), W_3 is weight of capsule with cover plus dried sample (g)

3.4.1.2 Ash Content Determination

To determine the total ash content of activated carbon the procedure was followed according to ASTM for activated carbon test method. First 1 g AC was measured and then placed in the dry and known weight of crucible. Then the crucible was placed in the furnace and it was then ignited at 650°C for 3 hr. After igniting to the required temperature and time, the crucible was removed out from the furnace and cooled to room temperature and reweighed [134,135]. The weight of the ash content was expressed as a percentage of the AC sample in **Equation 9**.

$$\text{Total ash, \%} = \frac{D - B}{C - B} * 100 \dots \dots \dots (9)$$

Where, B is weight of crucible with cover (g), C is weight of crucible with cover plus original activated carbon sample (g), D is weight of crucible plus ash sample (g).

3.4.1.3 Volatile Matter Content Determination

Determination of volatile mater for the AC was conducted according to the procedure specified by ASTM for activated carbon. The sample (1 g AC) was measured carefully and placed in the crucible which was dry, clean and known weight. And then the crucible was closed and placed in the furnace as it was closed to avoid contact between the air and sample. The sample was ignited in the furnace at 950°C for 7 min. After seven minute the sample was removed from furnace and cooled to room temperature and then weighted by using electronic balance which was sensitive to 0. 01 mg [136]. Then the volatile mater was calculated by using the following **Equation 10**.

$$\text{Volatile Mater, \%} = \frac{D - B}{C - B} * 100 \dots \dots \dots (10)$$

Where, D is weight of crucible and ignited sample (g), C is weight of crucible and original sample (g), B is weight of crucible (g).

3.4.1.4 Fixed Carbon Determination

Fixed carbon was calculated as the resultant summation of percentage of all proximate analysis (moisture content, volatile matter and ash content) and subtracted from 100 [135]. The fixed carbon was determined by using in **Equation 11**.

$$\text{Fixed carbon (\%)} = 100 - (\text{moisture, \%} + \text{volatile matter, \%} + \text{ash, \%}) \dots \dots \dots (11)$$

3.4.2 Scanning Electron Microscope (SEM)

The morphological structure of AC and magnetic activated carbon was investigated using SEM (INSPECT F50).

3.4.3 BET (Brunauer Emmett Teller) Analysis

The surface area of AC and MAC were measured using BET (SA9603) by N₂ adsorption and desorption at temperature of 200°C for 1 hr under 2 bars.

3.4.4 FT-IR (Fourier Transform Infrared) Analysis

The functional groups on the surface of the MAC (before and after adsorption) were studied using FT-IR (PerkinElmer, USA). Typically, the sample was prepared by mixing 2 g of MAC with 0.3 g of anhydrous KBr and the mixture was pressed under vacuum (hydraulic press 15). Then, the spectrum was recorded in a spectral range of 400-4000 cm⁻¹ [137].

3.4.5 XRD (X-ray Diffraction) analysis

The crystalline structures of the as prepared samples were studied using an XRD (Pan Analytical X'PRO MRD X-ray diffractometer) equipped with Cu K α - radiation (λ = 1.5406 Å) in 2θ range of 10 to 80° continuously with a step of 0.013° and 30.35 seconds /step. The sample was pressed into the holder before analysis. The operating voltage and current were 40 kV and 30 mA, respectively at ambient temperature.

3.4.6 Point Zero Charge Determination

The pH value, at which the surface charge is zero, is called the point of zero charge (PZC) by using 0.1N KNO₃. Batch equilibrium method was used to determine point zero charge. To each flask 0.1 g adsorbent was added in to 45 ml of 0.1N KNO₃ solution in the pH range of 1, 2, 4, 6, 8 and 10. The initial pH solution was adjusted by adding drops of 0.1 N NaOH and 0.1N HCl solutions. Each flask was sealed and shaken thoroughly for 48 hr at room temperature. Finally, the pH was measured and recorded. The total charge adsorbed (Δ pH on MAC surface was determined by the difference between initial pH and pH after 48 hr. The pH values are plotted along the x-axis and Δ pH along y-axis, the data obtained from the experiment are plotted and the intersection point is taken as a reference for determining the pH PZC value [138].

3.4.7 UV-Vis Spectrophotometry

The concentration of Cr (VI) ions in solution was measured using UV–Visible spectroscopy after reaction with 1.5-diphenyl carbazide and 0.2 N Sulphuric acids [139]. The procedure was performed following a standard method introduced by UV–Visible spectrophotometer at wave length of $\lambda = 540$ nm.

3.4.7.1 Preparation of Diphenyl Carbazide

A 0.25 g diphenyl carbazide was weighed and then dissolved into 25 ml acetone and mixed until it was completely dissolved. The solution was then made up with deionized water to a final volume of 50 ml. This reagent was then stored in an amber glass bottle and kept in refrigerator discarded if the solution was discolored [139].

3.4.7.2 Preparation of Cr (VI) Stock Solution

Potassium dichromate (K₂Cr₂O₇) was used as a source for hexavalent chromium. All the required solution was prepared with analytical reagents and distilled water. 2.835 g of 99% K₂Cr₂O₇ crystals was dissolved accurately in 1.0-liter of double distilled water to obtain 1000 ppm (mg/l) of Cr (VI) stock solution. Different concentration hexavalent chromium standard working solutions were prepared from the stock solution by dilution [118].

3.5 Batch Adsorption Experiment

Batch mode adsorption studies were conducted at room temperature (25°C) using 250 ml conical flasks. A known amount of dried and powdered MAC was added to 100 ml of known concentration of Cr (VI) solutions. pH of Cr (VI) solutions was adjusted by using 0.1 N NaOH and HCl solutions prior to mixing with the adsorbent [140]. The mixture was then agitated at 200 rpm using orbital shaker depending upon the contact time of interest, allowing sufficient time for mixing. After the desired time the mixture was filtered using bar magnet. The concentrations of Cr (VI) in the filtrates were then measured from the calibration curve of UV-Vis spectra of the developing purple color while 1,5- diphenyl carbazide forms complex in the presence of 0.2 N Sulphuric acid.

The residual Cr^{+6} concentrations were determined by UV-Vis spectrophotometry. All of the experiments were performed in triplicated and the mean values were used. The percentage removal was determined in **Equation 12**.

$$\% \text{ Removal of Cr(VI)} = \frac{C_o - C_f}{C_o} * 100 \dots \dots \dots (12)$$

Where C_o is initial concentration of metal ion and C_f is the final concentration of metal ion after adsorption. The results are plotted on a line graph. The adsorption at equilibrium, q_e (mg/g) was determined by using **Equation 13**.

$$q_e = \frac{(C_o - C_f)V}{m} \dots \dots \dots (13)$$

Where, C_o is initial concentration and C_f is the final (equilibrium) chromium (VI) concentration (mg/l), respectively; V is the adsorbate volume (l) and m is the mass of adsorbent (g).

3.6 Effect of Adsorbent Parameters

3.6.1 Effect of Adsorbent Dose

The effect of adsorbent dosage on the removal of Cr (VI) was investigated by keeping the other parameters constant. Typically, the dosage of adsorbent was varied from 0.1 - 2 g and other parameters (i.e. contact time 30 min, pH 2, initial concentration working solution of Cr (VI) standard and 200 rpm) remain constant.

3.6.2 Effect of pH

The effect of initial pH on adsorption property of the as prepared adsorbents was determined at different pH values (1–6). The pH values of the solutions was adjusted by addition of 0.1 M HCl and NaOH solution. Experimental condition such as; adsorbent dose, contact time and initial concentration were as fixed constant.

3.6.3 Effect of Contact Time

The time intervals for contact time was varied from 10 to 90 min keeping other parameters constant [109].

3.6.4 Effect of Initial Concentration of Metal ions

Effect of initial concentration Cr (VI) was investigated by changing initial concentration from 20 to 120 mg/l keeping other parameters constant.

3.7 Experimental Design

The experimental data were analyzed using statistical software called Design Expert software version 12.00. For regression analysis and the evaluation of the statistical significance of the results. Central composite design (CCD), a broadly used statistical technique built on the multivariate nonlinear model for the optimization of process variables of adsorption is used. The optimization process involves three major steps these are performing the statistically designed experiments, estimating the coefficients in a mathematical model and predicting the response and checking the adequacy of the model [141]. It is also used to determine the regression of model equations and operating conditions from the appropriate experiments. It is useful in studying the interactions of the various factors affecting the process [142]. The interaction effect of the four optimization parameters and the effect they have on the adsorption percentage removal of hexavalent chromium had been studied by setting four levels for each of the parameters as shown in **Table 3.1**.

Table 3.1 Factors and corresponding levels for CCD experiments

Factors	Factor Code	Unit	Low level	High level
Dosage	A	g/ l	3	7
Time	B	min	20	40
pH	C	-	1	3
Initial concentration	D	mg /l	20	60

3.8 Description of Study Area

Wastewater sample was taken from Awash tannery factory which is found in Addis Ababa Akaki kaliti sub city. The factory manufactures different kind of leather products such as leather footwear, leather bags, leather garments, wallet, bag etc. The location map of Awash tannery factory is shown in **Figure 3.4**. The factory produces maximum of 900 kg of soaking lime input and 25000 square feet finished product of leather per day as a result it generates about 42500 liters of liquid waste on average per day. Untreated wastewater had been discharging into the Akaki river since its establishment. Tannery wastewater is one of the most complexes, troublesome with a strong industrial effluent having high COD, TSS, BOD, TDS, TS and pH. **Figure 3.4** describes the geographical location of study area with geographic coordinates 473800 E to 474000 E and 989190 N to 989340 N, longitude and latitude respectively.

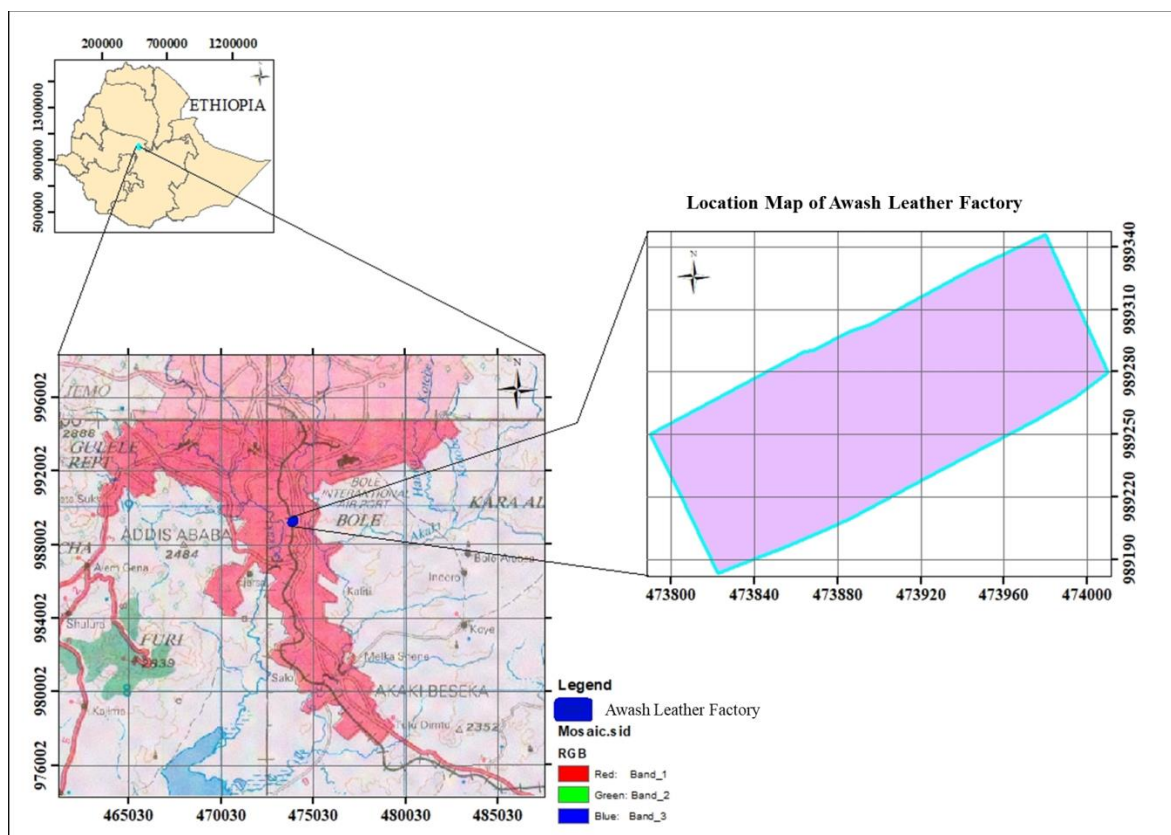


Figure 3.4 Location map of Awash tannery factory.

3.8.1 Sampling Techniques

The effluent samples were collected from Awash tannery factory. The wastewater samples were collected from the equalization tank. Samples were collected two times a day one in the morning (4AM- 9AM) in which most of the effluent from night work is released and one in the afternoon (3PM-4PM) in which the effluent from the day times work is released and this were repeated three times in three days interval. Polypropylene bottle 1.5 litter was used to collect the samples. Sampling bottles were thoroughly cleaned with hydrochloric acid, tap water and distilled water twice to render free acids, aluminum foil cover was used to protect sunlight during transportation period and finally the samples were stored in refrigerator at a temperature below 4°C (HRB 339HS).

The pH and dissolved oxygen (DO) were determined immediately by using DO meter and pH meter. Other parameters were analyzed later, samples were preserved by adding 1.5 ml of concentrated nitric acid per litter of sample as stated by environmental sampling and analysis for pollutants [143]. Sampling equipment's were cleaned before sampling

and at the end of sampling. All samples were mixed by stirring before laboratory test to make a homogeneous system.

3.8.2 Characterization and Analysis of Wastewater

The wastewater parameter analysis was selected before conducting experiment. The selected tannery industry wastewater parameters are: pH, DO, BOD, COD, TSS and TDS of tannery industry effluent. The wastewater parameters analysis was done in the field at time of sampling and at Addis Ababa Sciences and Technology University (in Department of Industrial Chemistry laboratory, Central laboratory and Environmental Engineering laboratory).

pH was directly measured on spot at the sampling site in the field using portable pH meter (HI 83141) HANNA calibrated with buffer standard of pH 4, 7 and 10. Analysis of BOD₅, COD, TSS, TDS and conductivity were carried out at Addis Ababa Science and Technology University. BOD incubator seated at room temperature for five days with adding 157 ml wastewater in beaker by adjusting 0.1 N NaOH and HCl to have pH 6-8. Then adding 3 drop of nitrification reagent and 2 drops of KOH in BOD bottle so as to measure the value by using BOD photometer [143]. COD determination was carried out with an open reflux method and done by CR 4200 digester and HANNA (HI83099) COD photometer analyzer according to APHA.

Residue left after the evaporation and subsequent drying in an oven at temperature range of 103-105°C of a known volume of sample were taken as total solids (TS).

The dry weight of empty crucible was weighed (W_1) and 20 ml of sample was added in to crucible. Then the sample was placed inside the oven (103 to 10°C) for at least 1 hr, after that cool at room temperature [144,145]. Lastly the final weight of crucible was measured and TS was calculated by using **Equation 14**.

$$TS \left(\frac{\text{mg}}{\text{l}} \right) = \frac{(W_2 - W_1)}{v} 1000 \times 1000 \dots \dots \dots (14)$$

Where W_2 is the final weight of crucible, W_1 is the dry weight of empty crucible and V is the volume of the sample (20 ml).

Total dissolved solid (TDS): The dry weight of empty crucible was measured (W_1) then the sample was filtered with bar magnet and 10 ml of filtrate sample was added in to crucible then place inside the oven (103°C to 105°C) for 1 hr, after that the final weight of the crucible(W_2) was weighed and the TDS was calculated by **Equation 15** [144].

$$\text{TDS} \left(\frac{\text{mg}}{\text{l}} \right) = \left(\frac{W_2 - W_1}{V} \right) 1000 \times 1000 \dots \dots \dots (15)$$

Where W_1 is the weight of empty crucible, W_2 is the weight of crucible after evaporation; V is the volume of sample (10 ml).

Total suspended solid was calculated by using **Equation 16**.

$$\text{TSS} = \text{TS} - \text{TDS} \dots \dots \dots (16)$$

3.8.3 Awash Tannery Industry Wastewater Sample Digestion

100 ml of wastewater collected from Awash tannery industry was digested by adding 5 ml of 65% HNO_3 and then the mixture was boiled gently for 30–45 min. After cooling 2.5 ml of 70% HClO_4 was added and the mixture was gently boiled until dense white fumes appeared. The mixture was then allowed to cool and 10 ml of deionized water was added followed by further boiling until the fumes were totally released [146,147].

Instrument Calibration

A series of four working standard solutions containing 0.01, 0.05, 0.25 and 1.25 ppm of hexavalent chromium in pH 2 including a blank solution were prepared from the stock solution. Furthermore a 0.25 g of DPC, which is a common complexing agent for chromium (VI), was prepared. A freshly prepared 1 ml DPC solution and 2 ml of 0.2 M H_2SO_4 were then added to each working standard and a pink color was immediately developed except the blank solution. The blank and standard solutions were then analyzed using the UV–Visible spectrophotometer at a wave length of 540 nm [148].

3.9 Determination of Adsorption Isotherms and Kinetics

3.9.1 Isotherms Study

The equilibrium isotherms were studied by taking 200 ml of Cr (VI) solutions at different initial concentrations 20 – 100 mg/l in 250 ml erlenmeyer flasks and pH solutions was adjusted to 2. 0.5 g of MAC was added to the solutions and agitated at 200 rpm for 30

min. To establish the adsorptions capacity of MAC experimental data was fitted against isotherm equations of Langmuir, Freundlich and Temkin [107].

3.9.2 Kinetics Study

Kinetic study was conducted by taking 200 ml of Cr (VI) solutions with initial concentrations of 40 mg/l in 250 ml erlenmeyer flasks and adjusting the pH to 2. Then 0.5 g of MAC was added and the solution was agitated at 200 rpm. Solutions was sampled at time interval of (10-80) min and the filtrate was analyzed for the remaining Cr (VI) concentration. Experimental data were analyzed against kinetic models, which explain the mechanism of the adsorptions processes. The kinetics of Cr (VI) adsorptions on MAC were analyzed using pseudo first-order and pseudo second-order kinetic models [107].

3.10 Recyclability Study of Magnetic Activated Carbon

0.5 g adsorbent was added to 100 ml solution in a rotary shaker (200 rpm) for 12 hr in a beaker. The precipitate was collected by bar magnet and then washed several times with deionized water until pH of the filtrate reached 7.0. Then, Cr (VI) loaded adsorbent was added into 400 ml, 0.005 M NaOH solution and shaken for 12 hr. The adsorbent was recollected by bar magnet and reused for adsorption again. The supernatant solutions were analyzed by UV–Vis spectra at 540 nm [149]. The adsorption desorption processes were successively conducted for five cycles as shown in **Figure 3.5**.

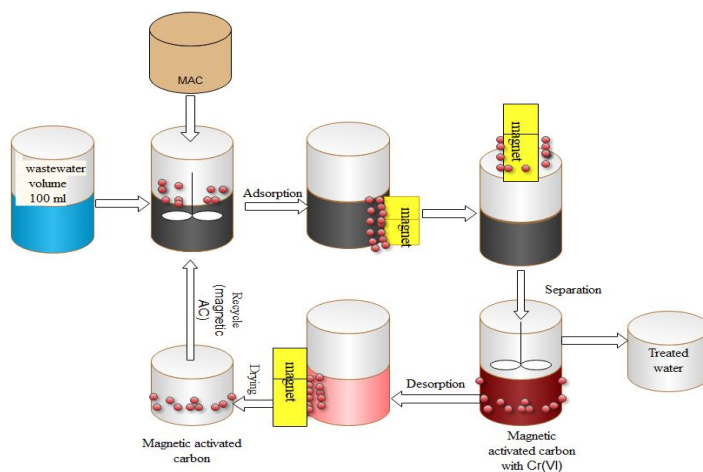


Figure 3.5 Recyclability study of magnetic activated carbon adsorbent

CHAPTER 4 RESULTS AND DISCUSSIONS

4.1 Physio-Chemical Characterization of AC and MAC

The physico-chemical properties of the as prepared AC and MAC were studied and the results are shown in **Table 4.1**. The ash content for the MAC shows a slight decrement in contrast to the ash content of the non-magnetized AC. High ash content has a consequence in a diminished efficiency on the adsorptive capability of the activated carbon. Dula *et al*, studied the physio-chemical characterization (volatile matter, fixed carbon, moisture and ash contents) of AC from bamboo. The report reveals that the moisture content of the carbon has no effect on its adsorptive power; it dilutes the carbon which is necessary for the use of additional weight of carbon during the treatment process. Accordingly, the lower ash content and volatile matter is attributed to lower inorganic content and higher fixed carbon as obtained from the result of moisture content 9.56%, volatile matter 4.66%, ash content 21.66% and fixed carbon 73.68%. Higher value of fixed carbon shows that the adsorbent is having more efficiency and stability [108].

Table 4.1 Physico-chemical characteristic of AC and MAC

Characterstics	Activated carbon	Magnetic activated carbon
Moisture Content (%)	5.13	4.2
Volatile Content (%)	22.93	18
Ash content (%)	7.6	5.1
Fixed Carbon (%)	64.29	71.4
pH	6.7	6.5

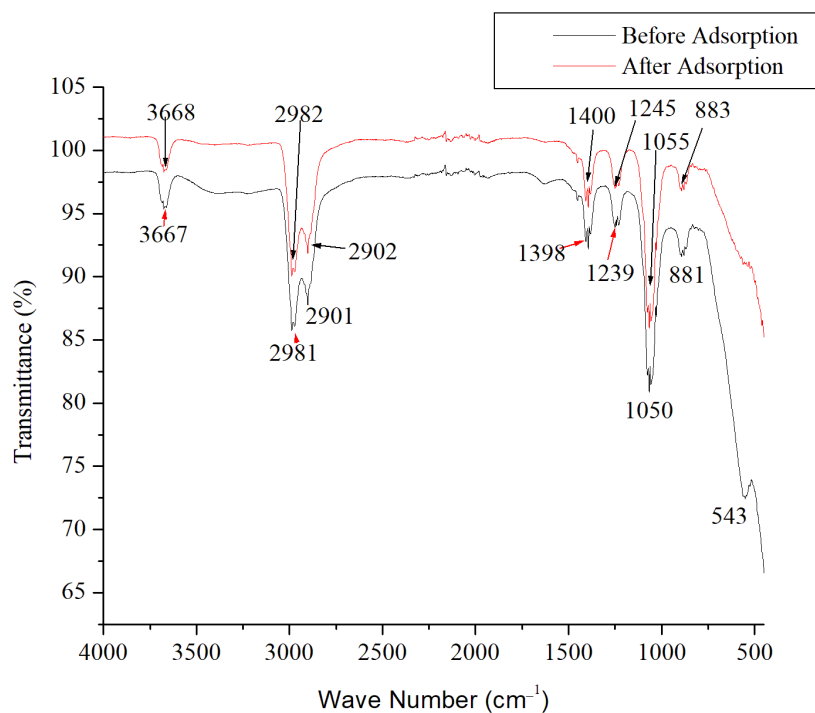
4.2 Fourier Transformation Infrared Spectroscopy (FTIR) Analysis

FT-IR analysis was made to perceive evidence on the nature of the bonds and to recognize diverse functional groups existing on the adsorbent surface. **Figure 4.1** shows the FT-IR spectra of MAC and the peaks at 1398, 2901, 2981 cm^{-1} corresponds to C-H bending of alkane. The peak at 3667 cm^{-1} represents the –OH stretching as shown in **Table 4.2**.

Table 4.2 Characteristic IR adsorption frequencies of MAC functional groups

Wave number (cm ⁻¹)	Functional groups	Compound class	Intensity
881	C-H bending	1,2,4-trisubstituted	strong
1050	C-O	Primary alcohol	Strong
1239	C-O stretching	alkyl aryl ether	Strong
1398	-C-H bending	alkane	Weak
2901	-C-H bending	alkane	Strong
2981	-C-H bending	alkane	Strong
3667	O-H (hydrogen bonded) stretching	alcohol	Weak

The spectra before and after adsorption of Cr (VI) are slight shift. The **Figure 4.1** illustrated that the functional group determination of magnetic activated carbon before and after adsorption of hexavalent chromium from wastewater. The obtained result was comparable to the study of hexavalent chromium (Cr (VI)) functional group analysis by H. Baylie [150].

**Figure 4.1** FT-IR spectra of MAC before and after adsorption of Cr (VI)

4.3 BET Analysis

To identify the porous texture of the synthesized AC and MAC, N₂ adsorption desorption technique was sought using micrometrics apparatus. The surface area of AC and MAC measured by the N₂ adsorption/desorption instrument was described. As shown in **Table 4.3** the surface area of activated carbon (AC) 694.210 m²/g was greater than that of MAC (Fe₃O₄/AC) 495.461 m²/g. This may be due to the incorporation of Fe₃O₄ in the micropores of AC and there was some space 102.02 m²/g which is not occupied by hexavalent chromium. The found result was similar to the study of hexavalent chromium (Cr (VI)) BET analysis by Wenmei and his friends [151].

Table 4.3 The surface area of AC and MAC

Adsorbent	Surface area
AC	694.210 m ² /g
MAC	495.461 m ² /g
MAC after adsorption	102.02 m ² /g

4.4 Scanning Electron Microscope

The morphology of the AC and MAC were investigated using SEM and the SEM images are displayed in **Figure 4.2** (a) and (b). As can be seen from the SEM images, the AC is more porous than the MAC. This result is consistent with the BET result. In **Figure 4.2** (a) sated the surface morphology of activated carbon with the 20 µm pore size and this pore size is efficient to over loaded magnetite particle. The obtained result was equivalent to the study of hexavalent chromium (Cr (VI)) SEM analysis by Helton *et al*, [47].

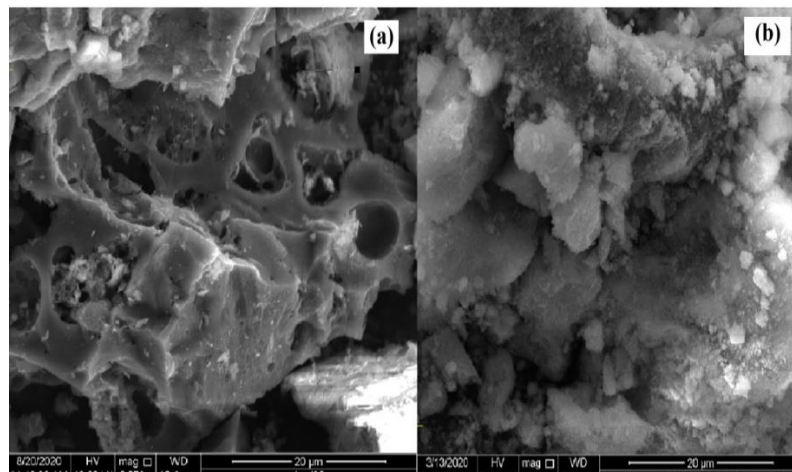


Figure 4.2 SEM image of (a) AC and (b) MAC

4.5 XRD Analysis

The crystalline structure of AC and MAC was investigated using XRD. **Figure 4.3** shows the XRD pattern of MAC. The peaks at 2θ value of 14, 30, 35, 43.24, 57.12, and 74.14⁰ were recognized as the (78), (118), (108), (82), (98), and (38) planes of Fe₃O₄ respectively (JCPDS card no. 019-0629 Iron Oxide (Magnetite, syn)). Whereas, the peaks at 2θ value of 53.46 and 62.56⁰ corresponding to (58) and (104) planes of graphite respectively (JCPDS card no. 026-1079 Carbon (Graphite-3R, syn)). Therefore, the XRD result shows the MAC contains graphite and magnetite minerals. Furthermore, the average particle size of Fe₃O₄ was 3.81 nm as calculated from (311) diffraction peak according Scherrer equation **17**.

$$D = \frac{K\lambda}{B\cos\theta} \dots \dots \dots (17)$$

Where, K proportionality constant, is usually 0.94, $\lambda = 1.54 \text{ \AA}$ & B is taken as full width at half maximum (FWHM) [152].

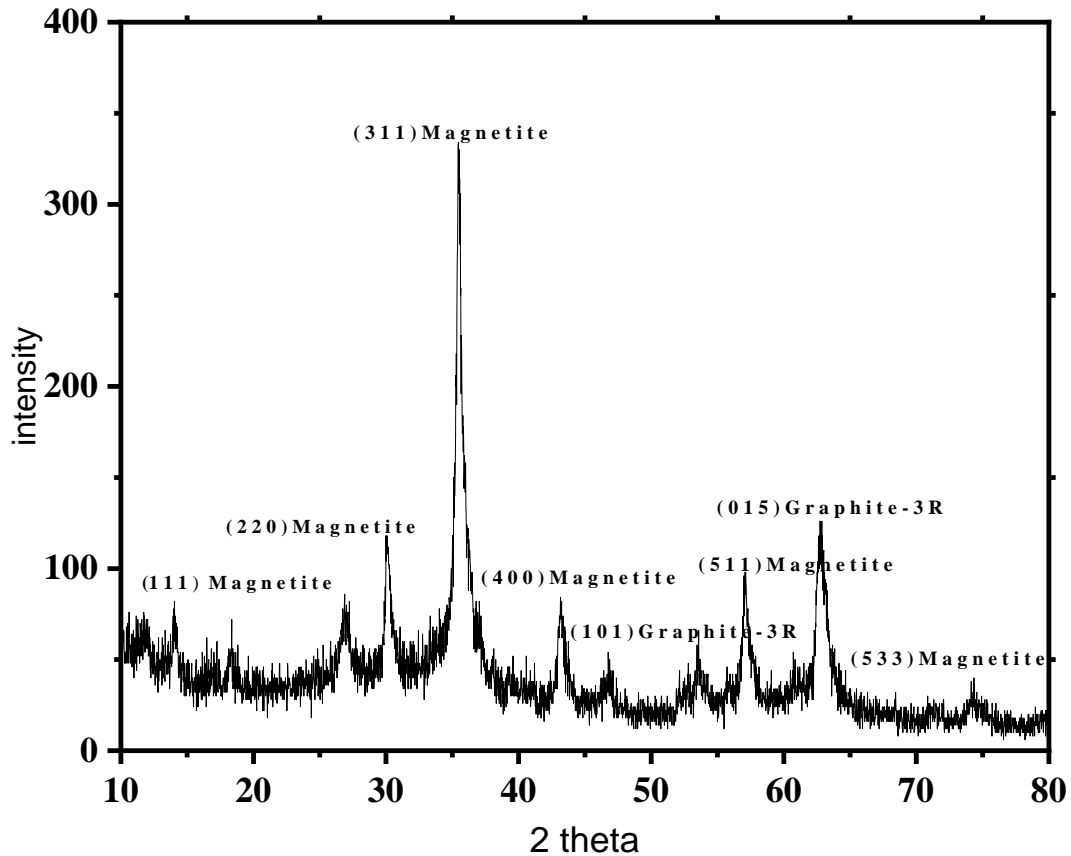


Figure 4.3 XRD analysis of magnetic activated carbon

4.6 Point Zero Charge Analysis

The adsorption of cations on any adsorbent would be expected to increase at pH value higher than the point zero charge while anions adsorption would be favorable at pH values lower than the point zero charge. As shown in **Figure 4.4**, the reduction in the value of the point zero charge for the phosphoric acid treated AC may be caused by removal of acid soluble material from the AC and addition of magnetite compounds during preparation of MAC biomass and protonation of surface functional groups like the carboxylic group. The point zero charge value for the MAC was obtained to be almost one. At pH values below PZC, MAC had a net positive charge, since the electrostatic attraction between positively charged adsorption sites and positively charged hexavalent chromium causes a decrease in % removal. Moreover, with a decreasing pH value, the fraction of neutral chromium hexavalent species increases, leading to a decreased adsorption. The obtained result was equivalent to the study of hexavalent chromium (Cr (VI)) analysis of point of zero charge by Labied *et al*, [151].

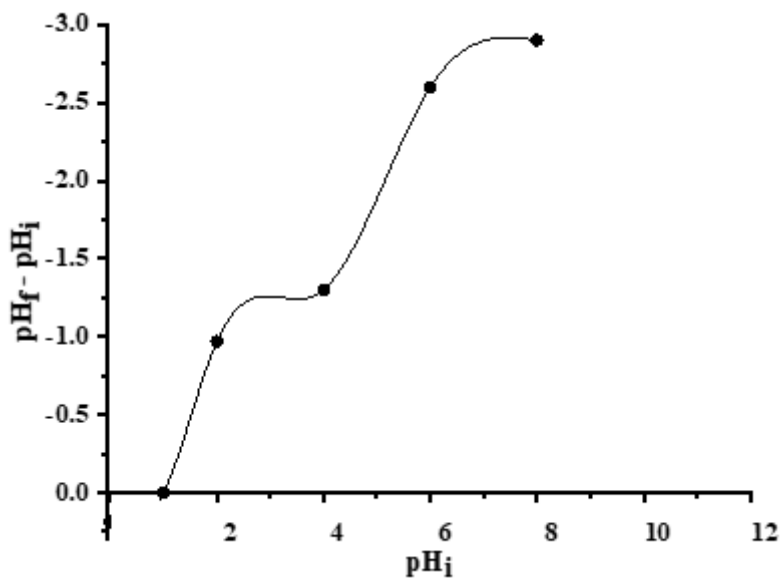


Figure 4.4 Point of zero charge analysis

4.7 Comparison of Percentage Removal of Cr (VI) by Different Ratio of Phosphoric Acid to AC

Comparison of the removal efficiency of prepared magnetic activated carbon was conducted in simulated wastewater with different percent ratio of phosphoric acid

(10,30,and 50%), temprature of 400, 450 and 500 at initial concentration of 20-80 mg/l, pH 2-6, contact time 10-100 min and diferent dosage 1-11g/l of magnetic activated carbon. The maximum hexavalent chromium removal of 98.5% was found for 50% H₃PO₄ soaked BSG at 40 mg/l, pH 2, 30 min, in 5 g/l. Therefore, comparatively good result was obtained for 50% H₃PO₄ soaked BSG at carbonization temprature of 400 °C. The other MAC (10 and 30%) however showed less removal efficiency when compared to 50% concentration. With this regared 30% MAC showed 92.40,87.21 and 84.50% hexavalent chromium removal at the temprature of 400,450 and 500°C respectively. The removal efficiency of 10% MAC on the other hand were 70.01,68.90 and 65.86 % at the study temprature of 400,450 and 500°C respectively. MAC prepared with 50% concentration showed relatively good removal efficiency when compared to the other studied concentration (98.5%).

4.8 Optimization of Adsorption Parameters

4.8.1 Effect of Contact Time

Figure 4.5 shows the profile of time versus percent removal Cr (VI) by magnetic activated carbon constant pH of 2, concentration of 40 mg/l and dosage of 5 g/l. It can clearly be seen that when adsorption time increased from 10 min to 30 min the removal capacity of the magnetic activated carbon rose rapidly from 55 to 97%. However, the removal capacity becomes constant above 30 min. This is mainly due to the adsorption process reached equilibrium point where the adsorbent adsorbed enough of adsorbate. Monika *et al*, [153], found that the removal efficiency of Cr (VI) using Fe₃O₄/AC at pH of 2 is 95.5%, and the percent removal almost remains constant after 45 min. An adsorbent which provide a large adsorption amount and produces a fast process is considered to be the best one. MAC, the removal efficiency of Cr (VI) increases better rapidly when the contact time rises from 5 to 30 min. in addition, Joseph *et al*, [109] showed that, the increase in contact time that is allowed for chromium (VI) ions and active sites on the AC/Fe₃O₄ interaction causes an increase in the percentage removal of chromium (VI) at pH 2. The availability of many free active on the adsorbent surface causes the rapid increase in the adsorption percentage for the time up to 30 min.

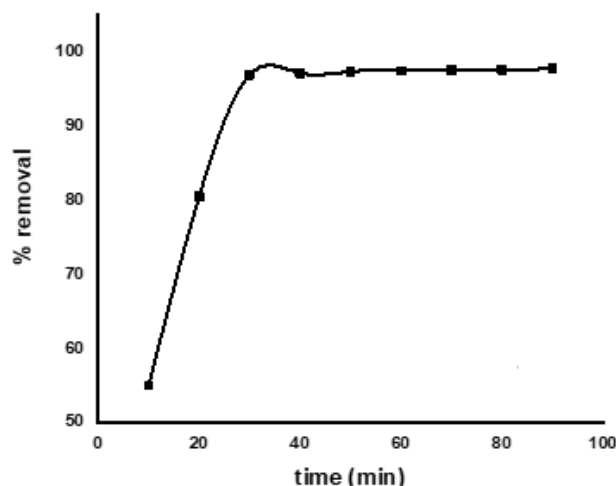


Figure 4.5 The effect of contact time with dose 5g /l, initial concentration of 40 mg/l and pH 2 at 200 rpm.

4.8.2 Effect of pH

The effect of pH on the removal efficiency of MAC was studied by varying the pH from pH 1 to pH 6 by keeping the other parameters MAC dose 5 g/l, contact time 30 min, and initial concentration of Cr (VI) 40 mg/l constants. As shown in **Figure 4.6**, the removal efficiency of magnetic activated carbon was found be higher at low pH values. When the pH increased from 2 to 6, the percent removal gradually decreased from 96.6 % to 48 %. Therefore, the optimum pH was found to be 2. Turkan *et al*, described that the percentage removal of Cr (VI) was highest at the pH 2.00 for MAC. Adsorption percentages at this pH values is 95% for Fe₃O₄/AC. When the pH increased to 2.97, the percentage of adsorption decreased to 60% for Fe₃O₄/AC and the percentage of adsorption decreased as the pH increased. The reason why adsorption is efficient at low pH is the protonation of the functional groups such as -NH₂ and -OH on the adsorbent surface at acidic pH. Cr(VI) ions are retained by the positively charged adsorbent surface due to the electrostatic attractions, because Cr(VI) present in the solution as anionic components such as HCr₂O₇⁻, HCrO₄⁻, CrO₄²⁻ and Cr₂O₇²⁻ [154].

Furthermore, Katenta *et al*, reported that effect of pH on the percentage of adsorption Cr (VI) was (97%) was at pH 1 and an increase in pH beyond 2 resulted into a rapid decrease in both adsorption percentage and adsorption capacity. This may be attributed to

the fact that at pH 2 and below, the dominant species in the solution is hydrogen chromate ions (HCrO_4^-) and at such low pH, the concentration of protons in the solution is high, which causes the active sites of the adsorbent to become positively charged due to protonation of the functional groups which may be amines and carboxyl in nature [109].

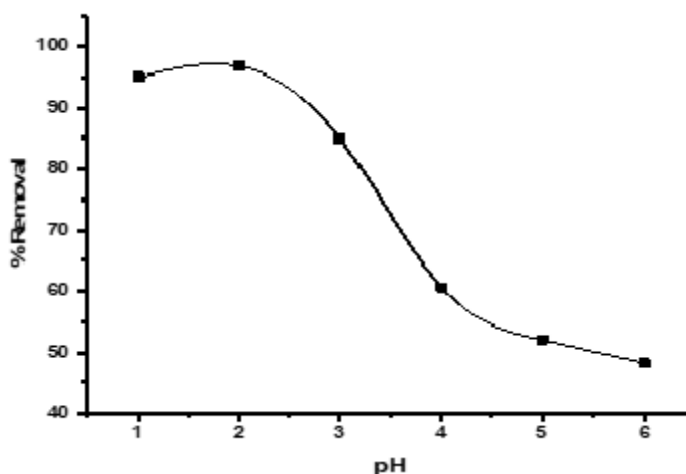


Figure 4.6 The effect of pH with dose 5 g/l, contact time of 30 min and initial concentration of 40 mg/l at 200 rpm % removal of Cr (IV).

4.8.3 Effect of Initial Cr (VI) Concentration

Keeping the pH 2, contact time 30 min, and dose of MAC 5 g/l constants, the effect of varying initial concentration of Cr (VI) from 20 mg/l to 120 mg/l was studied. As the initial concentration increased from 20 mg/l to 40 mg/l the removal efficacy of magnetic activated carbon was remained constant (97.5%) as shown in **Figure 4.7**. However, as the initial concentration increased above 40 mg/l, the removal capacity fell at high rate down from 97.5% to 48.3%. Shreosi *et al*, examined that the effect of initial concentration of Cr (VI) by changing it from 10 to 50 mg/l at the usual reaction conditions. Through this increase in Cr (VI) concentration, the removal capacity meaningfully decreased from 96.33 to 4.09%. The reduction in removal efficiency was caused due to ended overload of binding sites. Generally, the removal efficiency of hexavalent chromium ion decreases as the initial concentration increased [155].

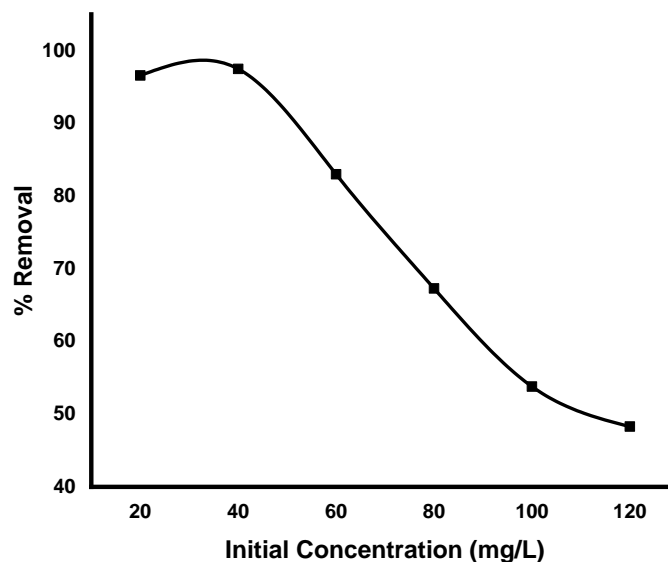


Figure 4.7 The effect of initial concentration at constant dose 5 g/l, contact time of 30 min and pH 2 at 200 rpm of % removal Cr (VI).

4.8.4 Effect of Adsorbent Dose

As shown in **Figure 4.8**, the magnetic activated carbon adsorbent was effective at 5 g/l of dosage to remove Cr (VI) from simulated wastewater (aqueous solution). The removal efficiency of hexavalent chromium ions increases for an increase in the dosage value of MAC from 1 g/l to 5 g/l. This increment in percentage removal of Cr (VI) is due to the increment of active sites or adsorbent surfaces to adsorb the pollutant. As adsorbent dose increases from 1-5 g/l, the hexavalent chromium removal efficiency increased from 71 to 95% as shown in **Figure 4.8**. For the adsorbent dosage above 5 g/l, the percentage removal remains almost a constant maximum value due to incorporation of active site by Cr (VI). Therefore, the optimum dose is then 5 g/l, with 95% removal efficiency of hexavalent chromium. Turkan and his co-workers reported that adsorption of metal ions was found to increase with an increase in the amount of MAC. The maximum adsorption for Cr (VI) was found to be above 95% at 3 g/l adsorbent. Overall, the adsorption was found to increase with the increasing of the adsorbent dosage, possibly due to the maximum number of active sites, which may be responsible for the removal of more ions at their surfaces [154].

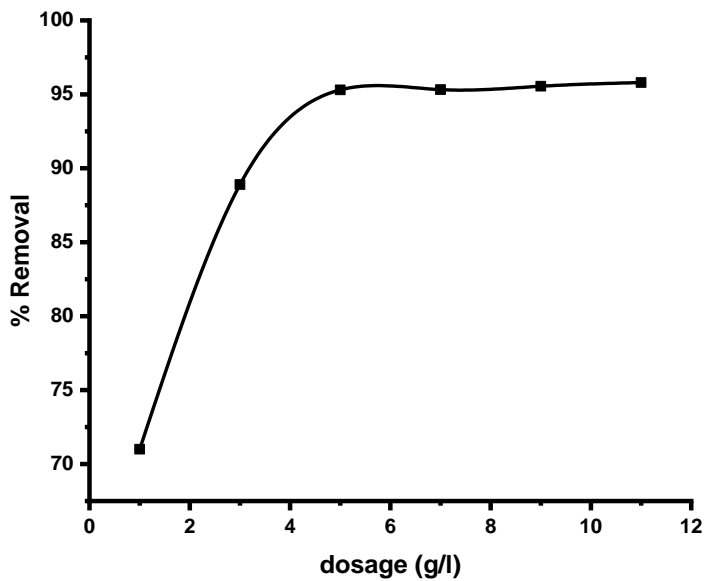


Figure 4.8 The effect of MAC dosage with initial concentration 40 mg/l, contact time of 30 min and pH 2 at 200 rpm % removal of Cr (VI).

4.9 Modelling and Optimization

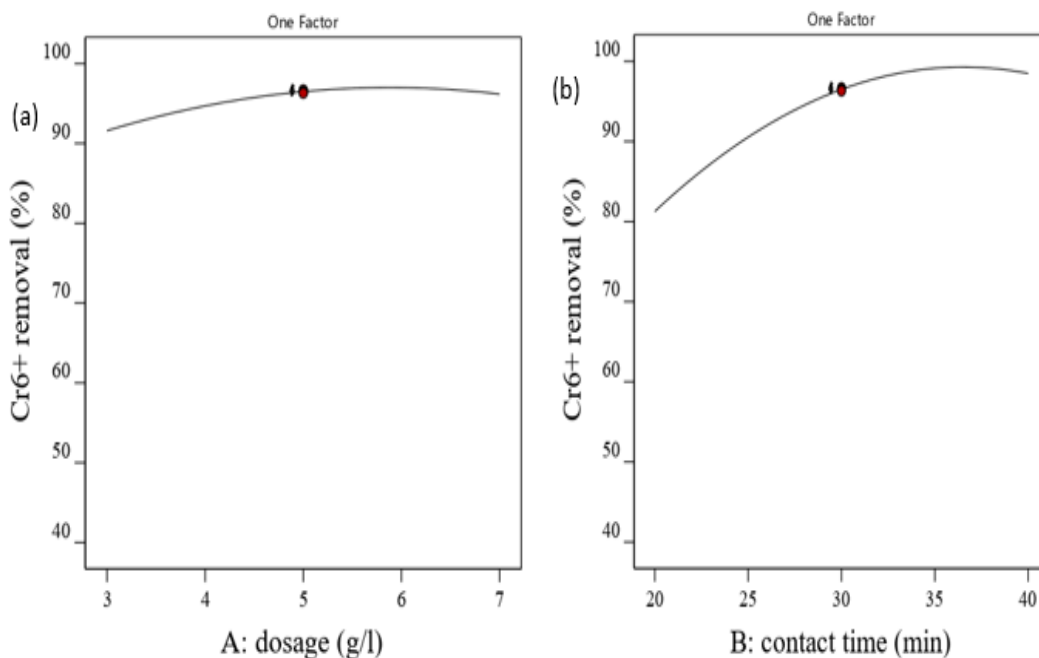
4.9.1 Effect of Individual Variables on Adsorption of Cr (VI)

Individual interaction effect of dosage, contact time, pH and initial concentration in turn can affect the removal efficiency of Cr (VI) ion using magnetic activated carbon. **Figure 4.9**, illustrated that the percentage removal of Cr (VI) increase when the dosage and contact time rise until it reaches equilibrium and after equilibrium attained the percentage removal almost remains constant. But the percentage removal of hexavalent chromium decreases when the pH and initial concentration increase. Even though removal efficiency decreases with increase in initial concentration and pH then the change is high. This shows that initial concentration and pH has only a very little effect on adsorption.

As is shown clearly in **Figure 4.9** (a) the percentage removal of chromium hexavalent increases as dosage increases from 3–5 g/l. However, beyond 5 g/l the removal efficiency of magnetic activated carbon remains almost constant. This is so because the amount of adsorbate available was already adsorbed and 5 g/l adsorbent was enough to remove 96.5 % of it. As a result, 5 g/l was found to be optimum value for this process. As is mentioned in **Figure 4.9** (b), the percentage elimination of hexavalent chromium rises as contact time increment from 20-30 min. Although after 30 min the removal competence

of MAC remains constant. Since the amount of adsorbable available was previously adsorbed and 30 min was enough to remove 96.55 % of it. Consequently 30 min was starting to be the optimum value for this procedure.

Figure 4.9 (c), revealed that the percentage removal efficiency of hexavalent chromium was increased as the pH increases from 1-2. But right after pH 2, the removal efficiency of magnetic activated carbon was fell rapidly. Therefore, the highest amount of adsorption took place at pH of 2. At pH 2 maximum removals (96.5 %) have occurred. As described in **Figure 4.9** (d), the percentage removal efficiency of hexavalent chromium was increased when the initial concentration increases from 20-40 mg/l. At 40 mg/l maximum removal (96.7 %) has happened. However, beyond 40 mg/l the removal efficiency of MAC was decreased. For a given amount of adsorbent, it is crystal clear that the removal capacity diminishes as adsorbate concentration ups. There would be no space (site) available for extra concentration after it had adsorbed enough amount of adsorbate. Generally, the result of optimization value of Cr (VI) (**Figure 4.9** a-d) in design expert software was consistent with the result of the effect of one variable at a time as shown in **Figure (4.5-4.8)**.



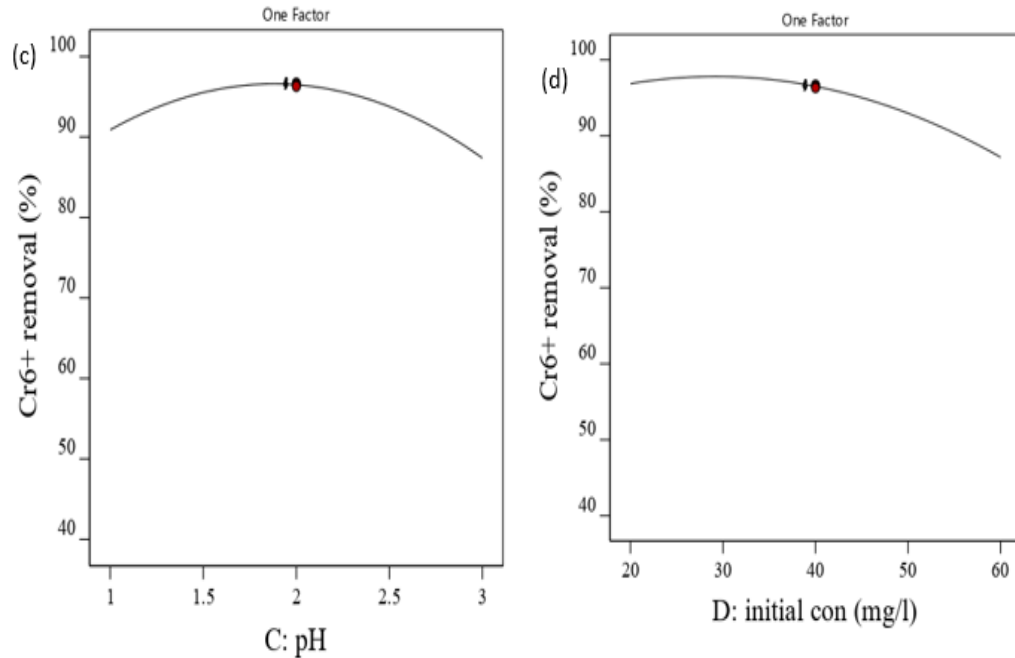


Figure 4.9 The individual effect of (a) dosage, (b) contact time, (c) pH and (d) initial concentration of the % removal of Cr (VI).

4.9.2 Development of Adsorption Percentage Model Prediction

Twenty-two unique experimental conditions and eight central replicates, total of thirty experimental runs were carried out. Each of experimental runs was conducted according to procedure defined above in methodology section 3.7. Predicted value which indicates the expected value of surface response method of design expert software suggested validating the experimental value on the adsorption of hexavalent chromium. For each experimental procedure, chromium (VI) removal efficiency was determined using the procedure described in section 3.7. The central composite experimental matrix, experimental and predicted values of adsorption efficiency obtained under different experimental conditions are presented **Appendix 8G(b)**. The final obtained equation for prediction of response variable based on coded factors is as follows in **Equation 18**.

$$\text{Cr}^{6+} \text{ removal} = -19.48326 + 16.43911A + 4.53834B + 3.40198C - 0.380557D - 0.260031A*B - 0.542188 A * C + 0.069984 A * D + 0.270063C* B + 0.014797B*D + 0.085031C*D - 0.720130A^2 - 0.059055B^2 - 4.69677C^2 - 0.009554D^2 \dots\dots\dots(18)$$

Where **A** is dosage, **B** is contact time, **C** is pH and **D** is initial concentration.

To assess the adequacy of a model, the coefficient of determination and the lack of fit test were commonly used. Coefficient of determination refers to the changes described by the model to the overall changes. Therefore, whatever R^2 is closer to 1, the power of fitted model is greater to describe the response changes as a function of the independent variables. From the model summary statistics, it can be seen that, the **Predicted R^2** of 0.9355 is in reasonable agreement with the **Adjusted R^2** of 0.9581; i.e. the difference is less than 0.2. **Adequate Precision** measures the signal to noise ratio. A ratio greater than 4 is desirable. The ratio of 25.1389 indicates an adequate signal. So that, this model can be used to navigate the design space as shown in **Table 4.4**.

Table 4.4 R^2 squared value for the model

Std. Dev.	3.08	R^2	0.9783
Mean	81.71	Adjusted R^2	0.9581
C.V. %	3.77	Predicted R^2	0.9355
		Adeq Precision	25.1389

The statistical implication of the model was explored by analysis of variance (ANOVA). The significance of the model and model terms are known by applying the p-test. The p-values signify the usefulness of the model and its terms. They are important in understanding the outlining of shared interactions between the variables. The larger the magnitude of F-test and smaller the p value, the more significant is the corresponding model and model terms as shown in **Appendix 8G :(a)**. As seen from **Equation 18** in terms of coded factors can be used to make predictions about the response for given levels of each factor. By default, the high levels of the factors are determined the range of low and high value of independent variable. The coded equation is useful for identifying the relative impact of the factors by comparing the factor coefficients.

The adequacy and significance of the quadratic model was justified by the analysis of variance (ANOVA). The model p-value observed was less than 0.0001 enlightening that the model was significant. In this study the probability of model p-value of the experimental work was less than 0.0001 indicating that the model suggested by the software was highly significant. In this work P-values obtained from the experiment less than 0.0500 indicate model terms are significant. In this case AB, BC, AD, BD, CD, A^2 ,

B^2 , C^2 , D^2 , are significant model terms. Values greater than 0.0500 indicate the model terms are not significant. If there are many insignificant model terms (not counting those required to support hierarchy), model reduction may improve your model. Additionally, the fitting of the experimental data to the regression model was seen and adequately explained by the value of the adjusted determination coefficient ($R^2_{Adj} = 0.9581$). This result means that 95.81 % of the total variation on Cr (VI) adsorption data can be clarified by the selected model. The adequate precision ratio of 25.1389 indicates an appropriated signal to noise ratio. Moreover, the relationship between actual values and predicted values showed that the actual values are distributed relatively near to the straight line, indicating good fitness of the model. This was an indication of better fitment of the model with the experimental data as described in **Figure 4.10**.

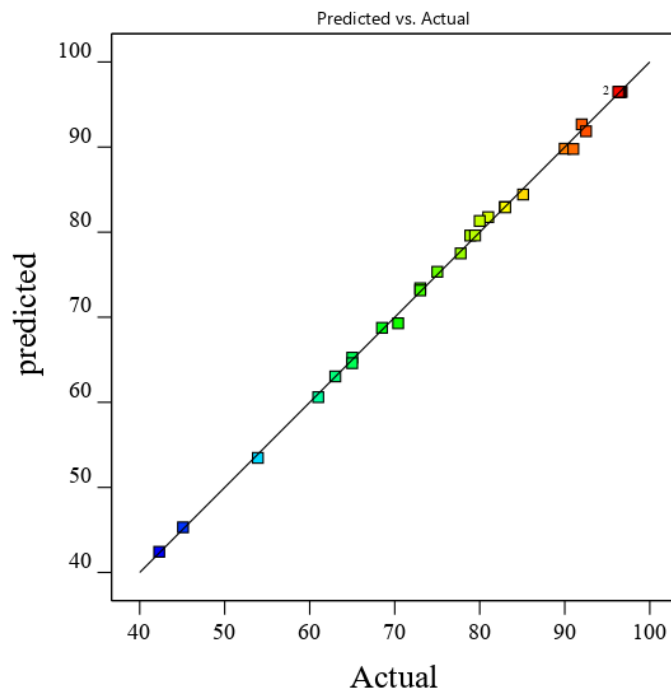


Figure 4.10 Graph of Predicted versus Actual.

4.10 Combined Effect of the Factors

As discussed in the above sections, the decisive objective of CCD method applied in this study was to find out the substantial effects of the process parameters initial concentration, pH, adsorbent dose and contact time on the removal efficiency of Cr (VI). Three-dimensional response surface and 2D contour plots were used to investigate the effect of all the factors on the responses.

4.10.1 Combined Effect of Adsorbent Dosage and Contact Time

Figure 4.11 presented the interaction effect of adsorbent dose and contact time on the percent removal of Cr (VI). From the plot it can be seen that, maximum Cr (VI) removal was obtained at adsorbent dose range of 3 to 5 g/l then slightly increase from 6-7 g/l. The removal of Cr (VI) increased with the rise of the adsorbent amount up to a certain level and increasing contact time resulted in the increment of percent removal of Cr (VI). The maximum removal efficiency, which is 96.55 %, as it can be observed from the **Figure 4.11**, is at the intersection point of 5 g/l adsorbent dosage and 30 min contact time.

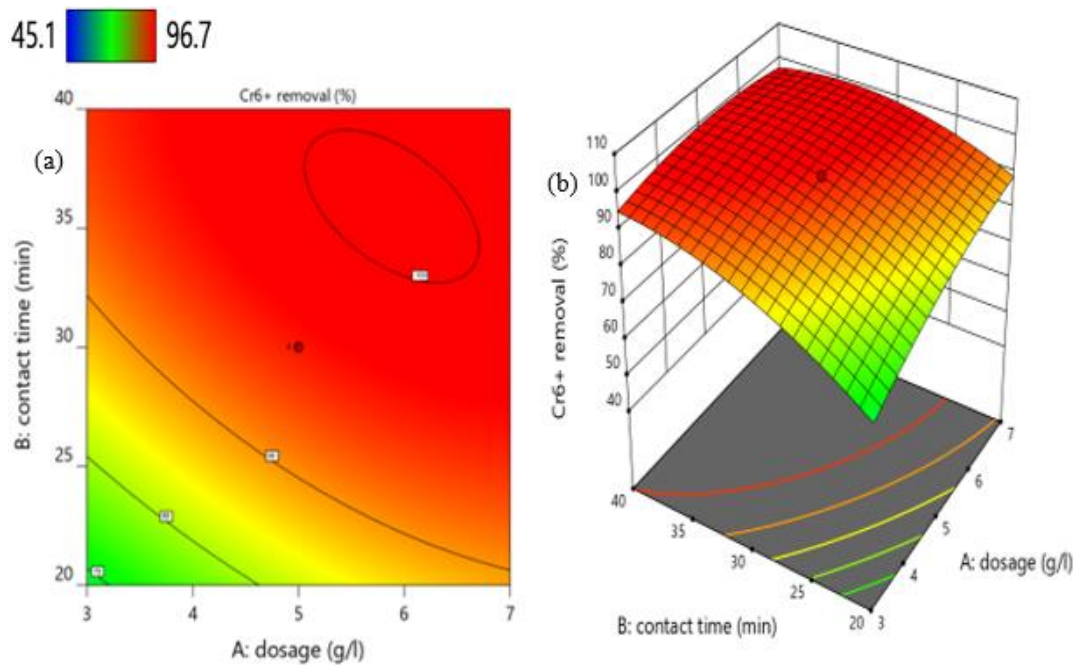


Figure 4.11 2D Contour plot (a) and 3D response surface (b) of the combined effects of dosage and contact time on the (%) removal of Cr⁶⁺ by MAC.

4.10.2 Combined Effect of Dosage and pH

The interaction between pH and adsorbent dose on Cr (VI) removal is presented in **Figure 4.12**. It was detected that a direct decrease in the Cr (VI) ion removal occurred when the pH value of the solutions changed from 1 to 3. The maximum adsorption of Cr (VI) ions is found at pH 2. The decrease in Cr (VI) ion removal efficiency at higher pH might be due to the competition between OH⁻ and chromate ions (CrO₄²⁻), where the former being the dominant species wins the race. The increment in the adsorbent dose increase the removal efficiency of Cr (VI), the maximum removal efficiency was found at

a dose between 3 to 5 g/l. The peak value of removal efficiency is observed for the values of dosage 5 g/l and pH 2 to be 96.5 %.

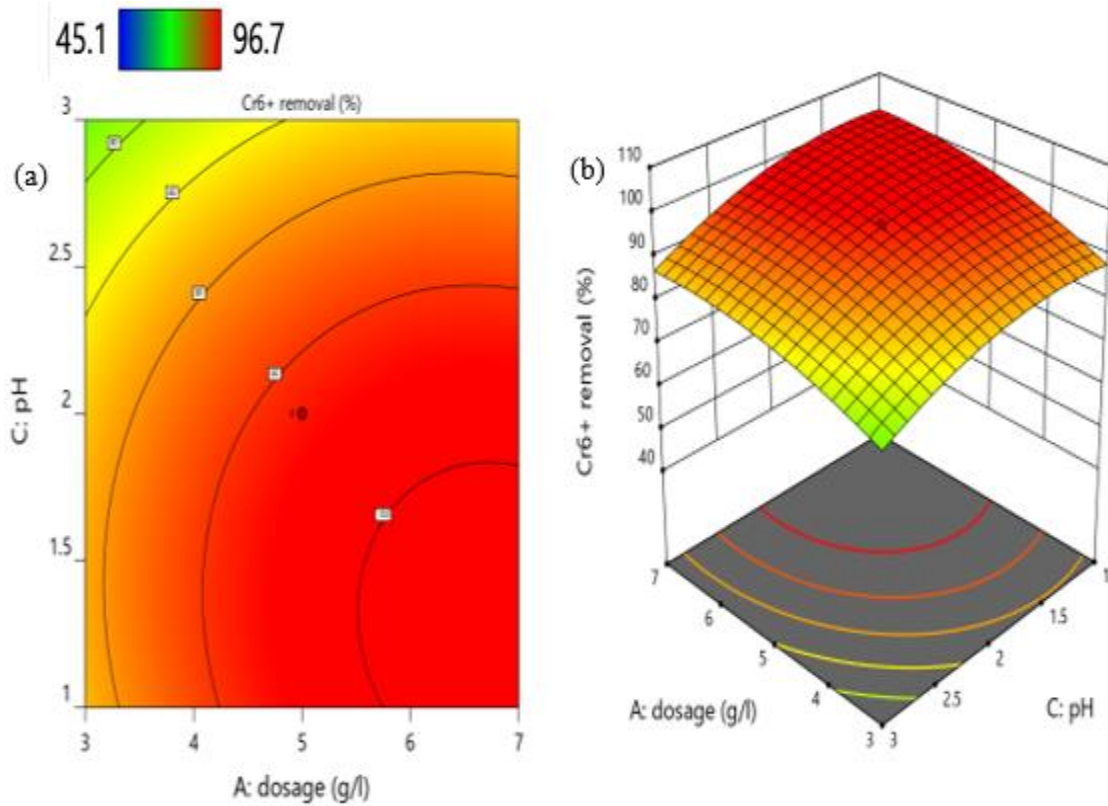


Figure 4.12 2D Contour plot (a) and 3D response surface (b) of the combined effects of dosage and pH on the (%) removal of Cr⁶⁺ by MAC.

4.10.3 Combined Effect of Dosage and Initial Concentration

The interaction effect of initial Cr (VI) concentration and adsorbent dose on the percentage removal of chromium (VI) is revealed in **Figure 4.13**. From the **Figure 4.13**, it can be seen that, the initial Cr (VI) concentration and adsorbent dose leads to the central point's (i.e. 20-40 mg/l and 3 to 5 g/l) maximization in percent removal of chromium (VI), while the minimum and maximum points in initial Cr (VI) reaching maximum point it decrease percentage removal of Cr (VI) whereas the increment of adsorbent dose leads to rise the percentage removal of Cr (VI) until it reaches equilibrium and it remains constant. The reason behind the decrement in removal efficiency when metal ion concentration increased is the increase in coverage of more surface sites due to an increase in metal ion concentration. This implies that when metal ion concentration gets higher, the adsorption capacity of the iron particles gets exhausted due to non-

availability of free binding sites. Thus, it results in a decrease in the overall removal efficiency. It is therefore evident that, at low concentration ranges, the percentage of adsorption is high because of the availability of more active sites on the surface of MAC. Thus, the peak value of the percentage removal of Cr (VI) for the combined effect of initial concentration and dosage, with values of 40 mg/l and 5 g/l, respectively, is found to be 96.5 %.

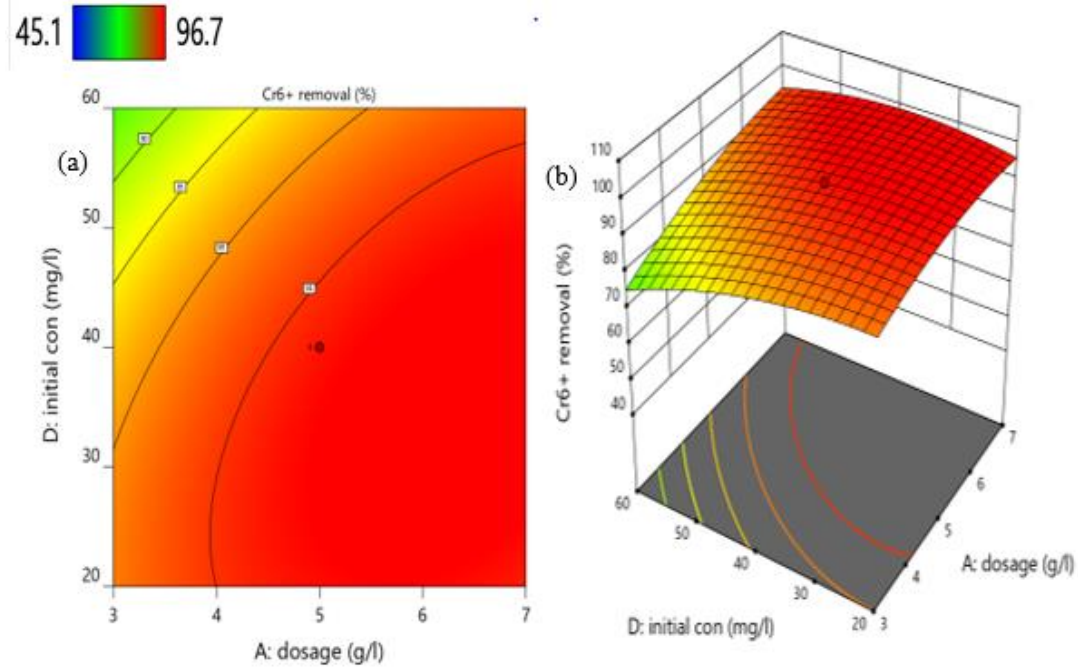


Figure 4.13 2D Contour plot (a) and 3D response surface (b) of the combined effects of dosage and initial concentration on the (%) removal of Cr⁶⁺ removal from simulated wastewater by MAC.

4.10.4 Combined Effect of Contact Time and pH

Figure 4.14 shows the effect of solution pH and adsorption contact time on the percentage removal of Cr (VI) ions by the magnetic activated carbon. From the three-dimensional interaction plot it could be seen that, with increase in contact time, the percentage removal of Cr (VI) increases, while the increase in pH causes a decrement in percentage removal of Cr (VI). This phenomena is observed because pH has more effect on the removal efficiency of it than time. The maximum adsorption efficiency was obtained at a pH value of 1-2. And for the contact time interval of 10-30 min, there is a rapid increase in adsorption efficiency. The peak value for it is then observed at pH of 2 and 30 min contact time to be 96.7%.

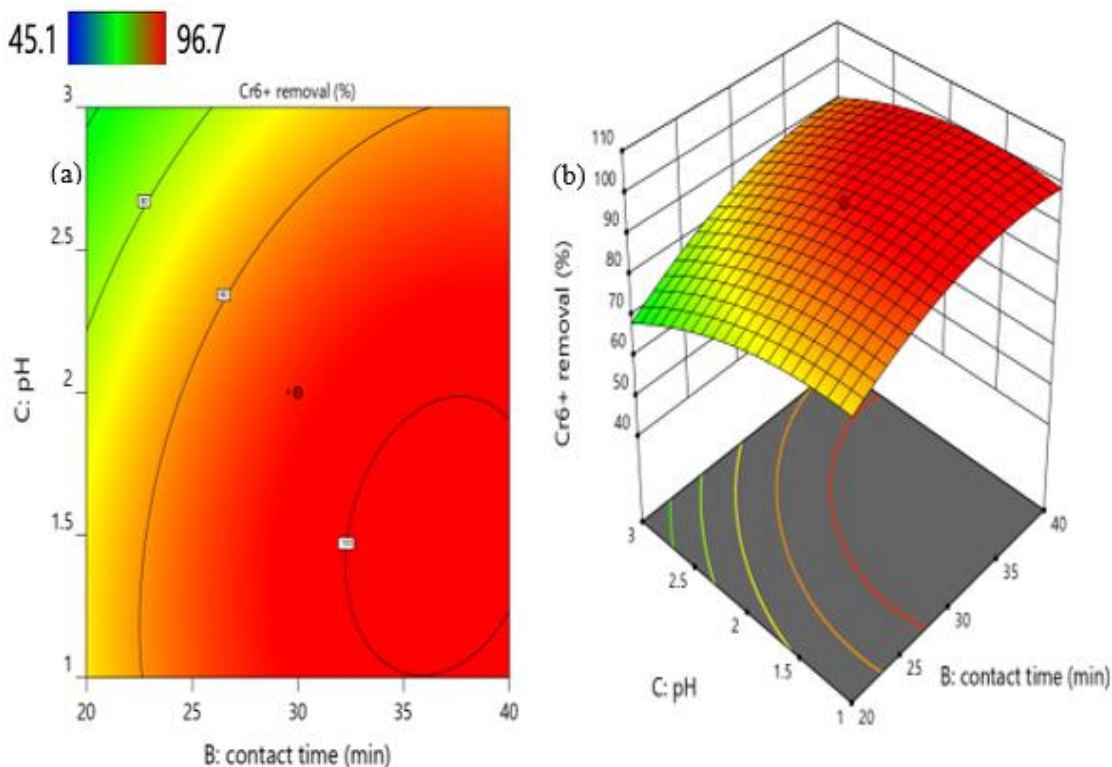


Figure 4.14 2D Contour plot (a) and 3D response surface (b) of the combined effects of contact time and pH (%) removal of Cr⁶⁺ removal from simulated wastewater by MAC.

4.10.5 Combined Effect of pH and Initial Concentration

The mutual effect of pH and initial concentration on removal efficiency of Cr (VI) at constant dose and adsorption time is represented in **Figure 4.15**. The percentage removal of Cr (VI) ion is enhanced with minimizing the initial concentration of Cr (VI) ions as well as pH. This can be clarified by the fact that all adsorbents have a limited number of active sites and at some concentration these active sites become saturated. It is also clear from the **Figure 4.15**, that the removal efficiency decreases with increase in pH after 2 and initial concentration after 40 mg/l. The results show that at a fixed adsorbent dosage and contact time, as the amount of Cr (VI) concentration increases, the percentage of adsorption becomes small. This is due to the fact that at lower concentrations, the ratio of number of Cr (VI) ions to the available adsorption sites is almost occupied and subsequently the adsorption becomes greater. At higher concentrations of metal ions, however, the available pores on MAC for adsorption are fixed and hence the removal of chromium (VI) depends on the concentrations of Cr (VI) and it decreases with an increase in initial Cr (VI) concentration. The peak value of removal efficiency for the

combined effect of pH and initial concentration at their value of 2 and 40 mg/l respectively, was observed to be 96.7 %, alike other combined effects.

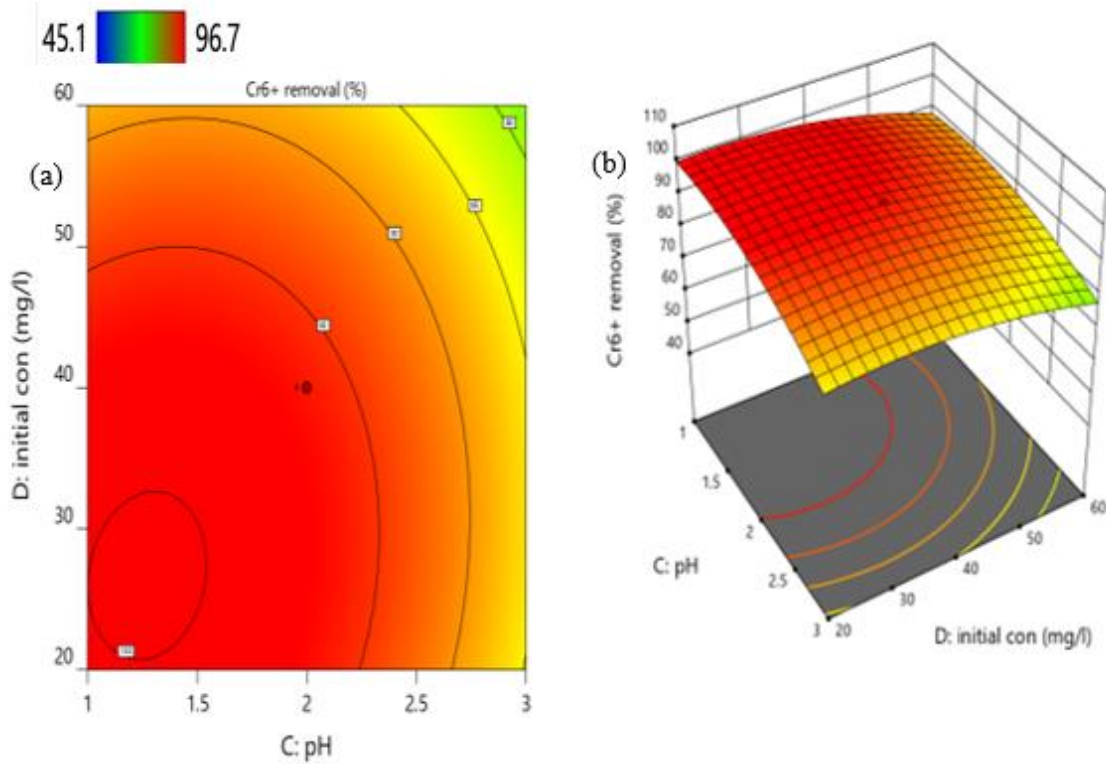


Figure 4.15 2D Contour plot (a) and 3D response surface (b) of the combined effects of pH and initial concentration (%) removal of Cr⁶⁺ removal from simulated wastewater by MAC.

4.10.6 Combined Effect of Initial Concentration and Contact Time

The combined effect of contact time and initial adsorbate concentration on the percent removal of Cr (VI) is shown in **Figure 4.16**. The result proved that, the collaboration of contact time and initial metal Cr (VI) concentration at low contact time had no significant effect on the removal of Cr (VI). This is because at small contact time there will be higher percentage of Cr (VI) removal due to the protonation of surface functional groups. This result is also supported by the ANOVA analysis which proved that the interaction of contact time and initial metal Cr (VI) concentration have significant effect on Cr (VI) removal with the p- value less than 0.05. The maximum value for the percentage removal is then observed for the intersection of initial concentration and contact time values of 40 mg/l and 30 min respectively, to be 96.55% for their combined effects.

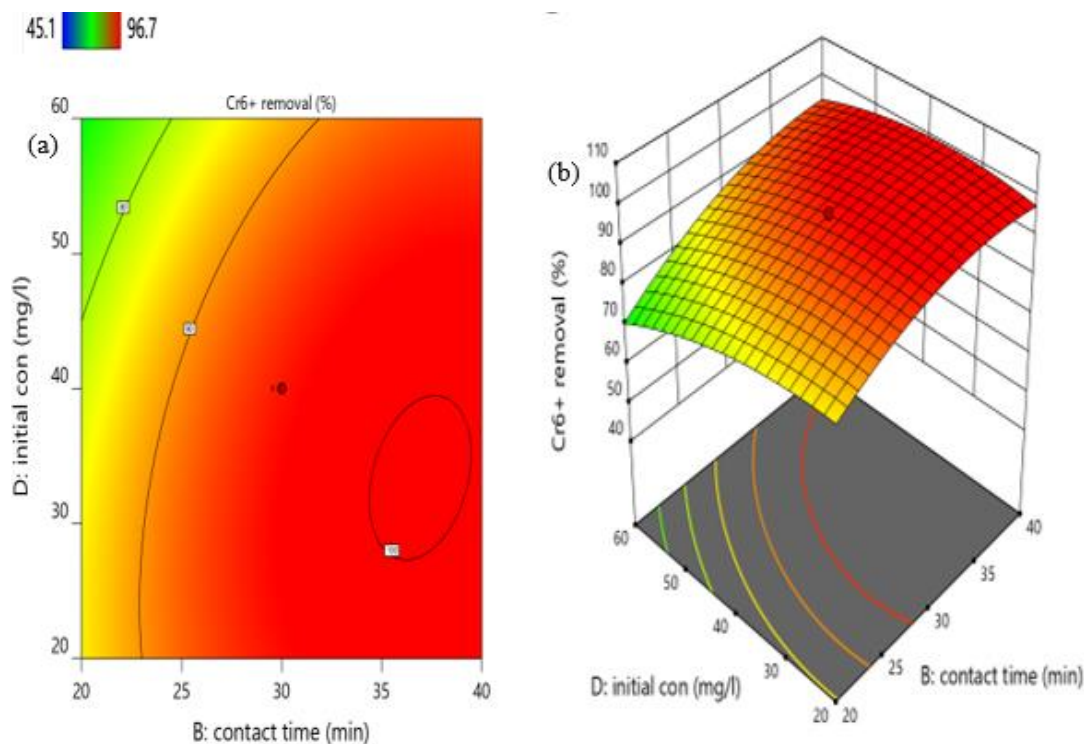


Figure 4.16 2D Contour plot (a) and 3D response surface (b) of the combined effects of contact time versus initial concentration on the percentage removal of Cr (VI).

4.11 Process Optimization and Evaluation

The experimental design and response surface analysis is an efficient tool for the development and optimization of the processes. The overall model in ANOVA was used to recognize the significant factors between the specified factors. The optimization plot is interactive, in which case the input variables can be adjusted on the plot to find for more necessary solutions. In this study, the maximum adsorption removal efficiency was quantified as the response, together with pH, dose of adsorbent, contact time and initial concentration were provided as the factors.

The criteria indicated that pH, adsorbent dose, initial concentration of adsorbate and contact time was minimized, by maximizing the amount of Cr (VI) removal efficiency. When optimal conditions are selected from the above, the developed method is subjected to a validation procedure in case it will be used for quantitative purposes. As it can be seen from the **Table 4.5** for the optimum values of the factors given to the software as an input, the percentage removal of Cr (VI) is found to be 96.55%. This value is almost similar to the experimental value.

Table 4.5 Optimum condition for Cr (VI) removal by MAC adsorbents from the model

Parameter	Optimum value
Adsorbent dose (g/l)	5
pH	2.0
Initial concentration(mg/l)	40
Contact time (min)	30
% Removal of Cr (VI)	96.55
Desirability	1

4.12 Study of Adsorption Isotherm Models

Adsorption isotherms are mathematical models used to clearly describe the distribution of adsorbate species among liquid and adsorbent. Using the assumptions mainly related to the heterogeneity or homogeneity of adsorbents, there are types of coverage and possibility of interaction between adsorbate species. In this study batch adsorption characteristics of Cr (VI) removal by magnetic activated carbon were studied and the results obtained from the experimentation were used to determine the better isotherm model that the adsorption process follows as Langmuir, Freundlich or Temkin [156].

Applicability of Langmuir isotherm model for Cr (VI) removal was analyzed using the data obtained from batch adsorption experiment by plotting C_e/q_e versus C_e . **Figure 4.17** shows Langmuir plot of Cr (VI) adsorption at room temperature, pH of 2, adsorbent dosage of 5 g/l, contact time of 30 min and for different initial Cr (VI) concentrations. The values of Langmuir constants, K_L (K_L is the constant related to binding energy of adsorption) and q_m (q_m is the maximum amount of metal ion adsorbed capacity in mg/g) were calculated from the intercept and slopes of the linear plot and summarized in **Table 4.6**. The correlation coefficients (R^2) of Langmuir model for the adsorption of the Cr (VI) were 0.98524, which were slightly lower than the R^2 values of Freundlich model for Cr (VI) and Temkin isotherm ($R^2=0.99583$). The result reveals that the adsorption of Cr (VI) on MAC is well fitted to the Temkin model, meaning that MAC surfaces are homogeneous adsorption patches, on which monolayer coverage of Cr (VI) ions were formed on the outer surface. The value of RL , which is in between 0 and 1 indicating that the adsorption process was favorable.

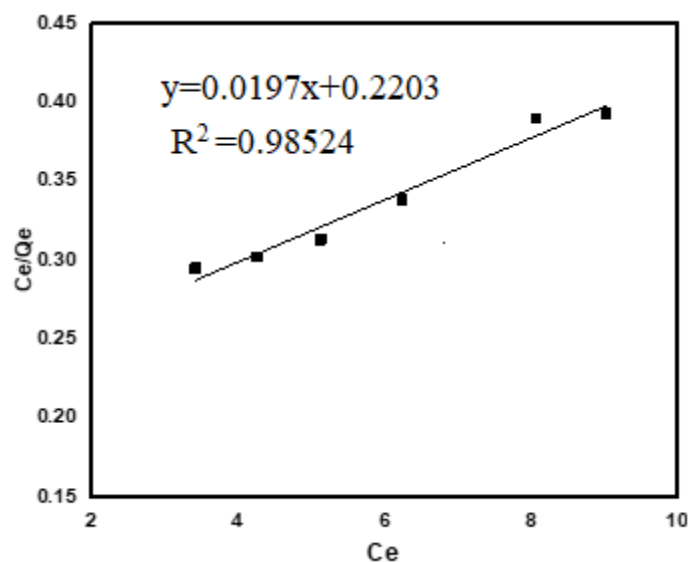


Figure 4.17 Graph of calibration curve of C_e/Q_e versus C_e .

Where C_e is equilibrium concentration in mg/L, Q_e is the amount of metal ion per unit mass of adsorbent at equilibrium (mg/g).

Table 4.6 Parameters for Langmuir, Freundlich and Temkin isotherms for the adsorption of Cr (VI) by MAC

Langmuir isotherm				Freundlich isotherm			Temkin isotherm		
R^2	$Q_m(\text{mg/g})$	R_L	k_L	R^2	N	k_f	R^2	β	k_t
0.98524	50.84	0.181	0.089	0.99306	1.504	45.40	0.99583	10.819	0.87

On the Freundlich isotherm model constant parameters, K_f and n were determined by linear regression from the plot of $\log(q_e)$ against $\log(C_e)$ shown in **Figure 4.18**. K_f is the degree of adsorption; when K_f value is low it indicates minimal adsorption of Cr (VI) whereas the higher K_f value suggests greater adsorption ability. For this specific case, K_f value for chromium (VI) ion removal was found 45.4 mg/g indicating a favorable adsorption according to Freundlich isotherm. Coming back to the n value, when $n > 1$, the adsorbate is favorably adsorbed on an adsorbent and it indicates the state of adsorption intensity. From this it could be concluded that the value of n was 1.504, suggesting a maximum adsorption of Cr (VI).

Jain *et al*, reported that the values of (R^2) 0.9907 in Freundlich model for Cr (VI) removal by AC/Fe₃O₄ were higher as compared to Langmuir model thus, indicating that Freundlich model fitted the data well confirming multilayer adsorption [74,122].

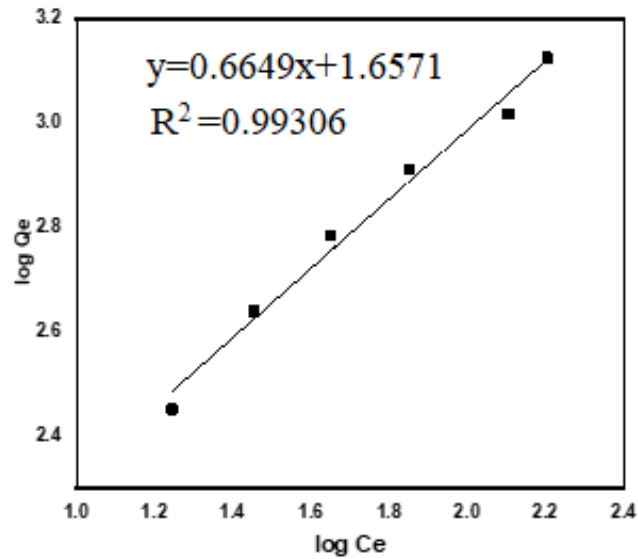


Figure 4.18 Graph of $\log (Q_e)$ versus $\log (C_e)$.

On the Temkin isotherm model constant parameters, K_t and β were determined by linear regression from the plot of q_e against $\ln (C_e)$ as described in **Figure 4.19**. The values that were found indicated that $\beta=10.81$ and $K_t=0.87$. When we compare and contrast the value of isotherm constants of Langmuir, Freundlich or Temkin the highest result obtained is 10.81 this value was indicate Temkin isotherm constant. For this specific case, these values were comfortable for chromium (VI) ion removal.

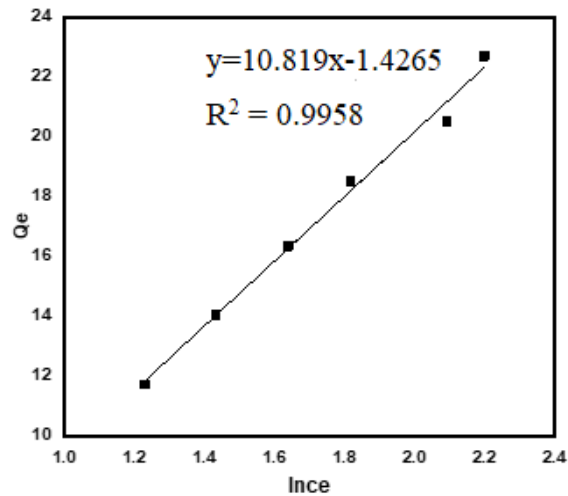


Figure 4.19 Graph of Q_e versus $\ln (C_e)$.

4.13 Study of Adsorption Kinetics

Pseudo first and second order kinetic models have been verified to fit the data obtained from different adsorption experiments of chromium (VI). The experimental and calculated q_e values, rate constants and regression coefficient of determination (R^2) values are given in **Table 4.7**. Since the plots showed linearity and the R^2 values were found to be 0.9722 and 0.99771 for first and second order kinetics, respectively as shown in **Figure 4.20** and **4.21**.

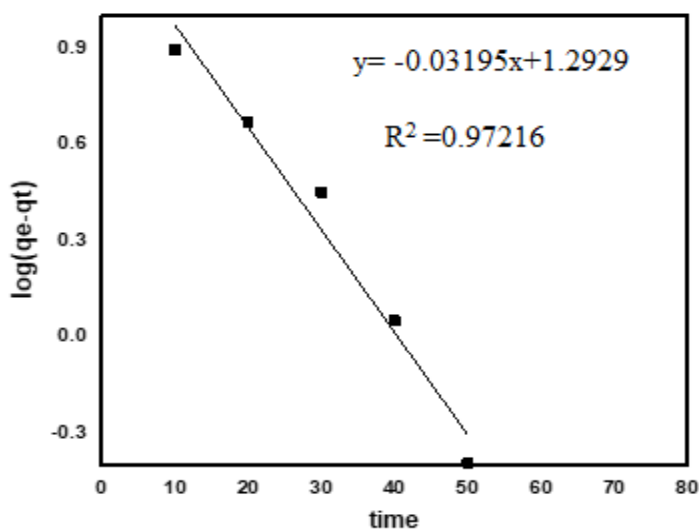


Figure 4.20 Graph of $\log(q_e - q_t)$ versus time.

Table 4.7 Kinetic parameters for 1st and 2nd order

1 st order kinetics			2 nd order kinetics		
R^2	q_e	k_1	R^2	q_e	k_2
0.9722	19.62	-0.0735	0.99771	13.31	0.1147

According to the values of correlation coefficient, R^2 obtained, fitting of adsorption experimental data using pseudo-second order model showed a higher value which showed that the kinetics of adsorption of Cr (VI) could be better described by pseudo-second order model. It can be noted that rate of the adsorption of Cr (VI) appears to be controlled by the chemical reaction. Nethaji *et al*, [127] reported that the studied adsorption process can be better studied with pseudo second-order equation. The linearity of pseudo second-order equation for the kinetic data can be $R^2 = 0.99943$. This implies

that the adsorption of Cr(VI) onto MCCAC was a chemisorption process involving valence force through sharing or exchange of electron between adsorbate and adsorbent species.

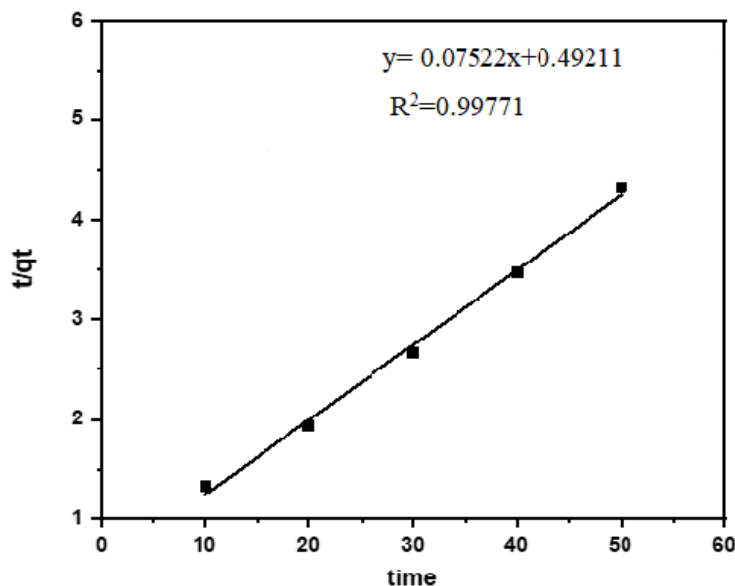


Figure 4.21 Graph of t/q_t versus time.

4.14 Real Sample Analysis

4.14.1 Physicochemical Characterization of Awash Tannery Effluent

The physicochemical characteristics of the Awash tannery wastewater were studied. The values of BOD, COD, TSS and TDS of untreated wastewater are 115 ± 10 , 1171.3 ± 104 , 1909 ± 6.21 and 2087 ± 76 mg/l, respectively. However, the recommended maximum permissible amount of BOD, COD, TSS and TDS values are 200, 500, 50 and 2000 mg/l, respectively (FEPA&EEPA) [146]. Therefore, all the untreated wastewater characteristics were beyond the provisional release limit set by the FEPA and EEPA, representing the poor remediation mechanism employed by the tannery. Furthermore, the wastewater was treated to assume values as shown in **Table 4.8** parameters within the standard. After treating the wastewater, the BOD, COD, TSS and TDS of the treated wastewater were come out be 41.3 ± 7.8 , 317.833 ± 14 , 31.4 ± 19 and 1001.34 ± 9.113 mg/l respectively.

Table 4.8 Physicochemical Characterization of untreated and treated effluent

Parameters	Untreated effluent Mean \pm SD mg/l	Treated effluent Mean \pm SD mg/l	Max permissible limit (mg/l) in EPA/FEPA
pH	4.3 \pm 1	6.5 \pm 0.146	6-9
DO	2.40 \pm 0.013	2.174 \pm 0.243	4-6
BOD5	115 \pm 10	41.3 \pm 7.8	50
COD	1171.3 \pm 104	317.833 \pm 14	500
TSS	1909 \pm 6.21	31.4 \pm 19	50
TDS	2087 \pm 76	1001.34 \pm 9.13	2000
Conductivity	56 \pm 3.5 ms/cm	44 \pm 5.3	-

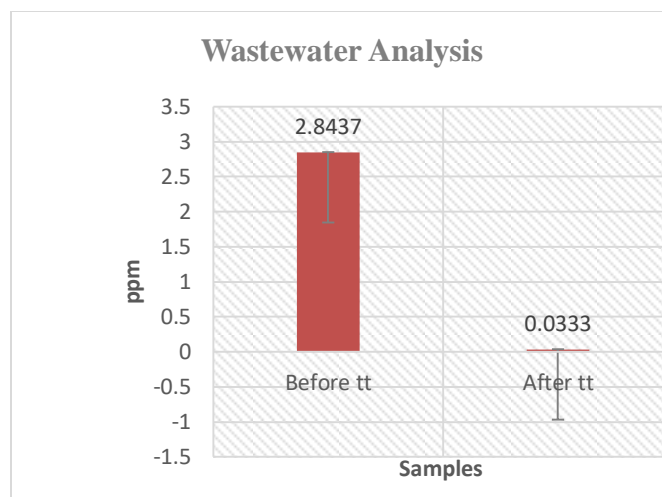
4.14.2 Cr (VI) Analysis in Awash Tannery Effluent

Our study on chromium (VI) concentration at Awash tannery factory was analyzed by double beam UV-Vis spectrophotometry. A direct relationship of absorbance (A) and concentration of Cr (VI) was attained in the concentration between 0.01–1.25 ppm with a lined regression equation as shown in (**Appendix 8E.1**).

Table 4.9 Optimum condition for Cr (VI) removal by MAC adsorbents

	Calculated concentration (ppm)			Standard deviation
	1 st	2 nd	3 rd	
Before treatment	2.746	3.051	2.734	2.8437 \pm 0.139
After treatment	0.0281	0.0304	0.0413	0.0333 \pm 0.0054

Before adsorption treatment, the concentration of Cr (VI) in the tannery wastewater is 2.8437 \pm 0.139 ppm as shown Table 4.9. But after we treat wastewater using MAC, we found to be 0.033 \pm 0.0054 ppm. This value is below the allowed value by WHO (i.e.0.05 ppm of Cr (VI)). As a result, this shows the MAC has excellent removal efficiency of Cr (VI) from the real wastewater as described in **Figure 4.22**.



tt=treatment

Figure 4.22 Graph of wastewater sample analysis.

As shown **Table 4.10** various researchers reported adsorption capacity of magnetic activated carbon to remove hexavalent chromium (Cr (VI)). For example, Jain *et al.*, reported adsorption capacity of 4.4 mg/g [74]. Arslan *et al.*, reported the adsorption capacity was 67 mg/g [157]. Nethaji *et al.*, reported the adsorption capacity was 57.37 mg/g [127]. Our result on the other hand has the comparatively good adsorption capacity of 193 mg/g at lower contact time. This is because of the high specific surface area of the as prepared MAC.

Table 4.10 Optimum condition for Cr (VI) removal by MAC adsorbents.

Adsorbent	dosage (g/l)	Initial conc (mg/l)	Time (min)	pH	Q _m (mg/g)	Reference
Fe ₃ O ₄ /AC	5	50	45	2	4.4	[74]
magnetic particles-loaded chitin micro cages Cr (VI)	0.25	10	60	1.75	67	[157]
MCCAC	5	50	65	2	57.37	[127]
MAC	5	40	30	2	193	This study

4.15 Recycling of Magnetic Activated Carbon Adsorbent

The MAC can be recycled numerous times keeping great adsorption capacity there by making water contaminate treatment processes cost effective and sustainable. It is shown that in **Figure 4.23** the percentage removal efficiency decreased from the 96.34-75.00% from runs one to run five due to the presence of adsorbent amount reduced respectively compared with their initial removal efficiency Cr (VI). The results display that MAC

presents good cyclic adsorption performance with easy separated characteristic after adsorption due to its excellent magnetic properties, which can better meet the treatment requirements for industrial wastewater.

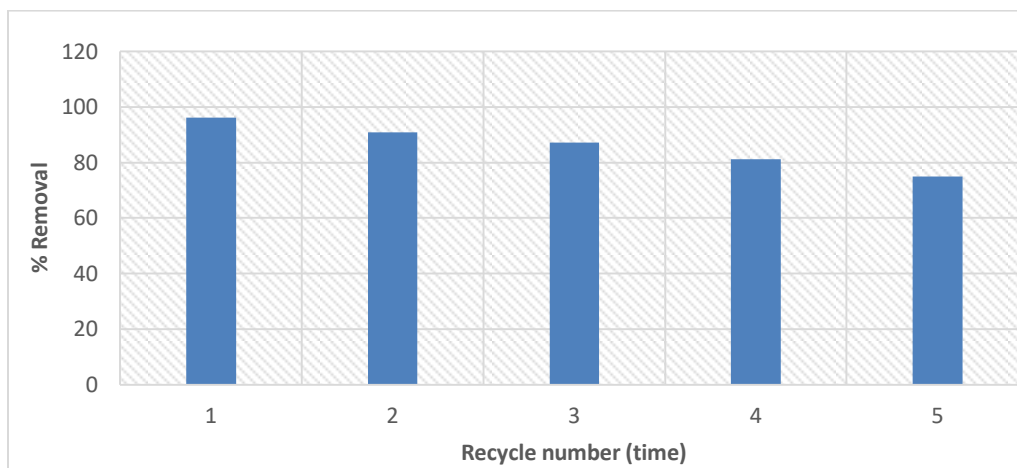


Figure 4.23 % Removal of MAC for Cr (VI) versus recycle number.

The decrease in the desorption and recycle capacity of adsorbent as shown in **Figure 4.23** due to the permanent alteration of functional groups afterward exposure of desorbing agent and Cr (VI) solution. Ajmani *et al*, reported that great reduction in the percentage removal of upright desorption was due to the inaccessibility (unavailability) of binding sites for chromium (VI) ions [158].

CHAPTER 5 CONCLUSION AND RECOMMENDATIONS

5.1 CONCLUSION

In this study, AC was synthesized from BSG and MAC was synthesized from AC derived from BSG and magnetite (Fe_3O_4). The adsorbent was tested and evaluated for removal of hexavalent chromium ion in aqueous solution using batch adsorption experiment and RSM. FT-IR analysis was made to perceive evidence on the nature of the bonds and to recognize diverse functional groups existing on the adsorbent surface. SEM analysis was determined surface morphology of MAC and AC with the $20\mu\text{m}$ pore size and this pore size is efficient to over loaded magnetite particle. The surface areas of adsorbent were $694.210\text{ m}^2/\text{g}$, $495.461\text{ m}^2/\text{g}$ and $102.02\text{ m}^2/\text{g}$ for AC, MAC and MAC after adsorption respectively. The optimum condition for removal of Cr (VI) has been obtained as Dosage 5 g/l, pH 2, contact time 30 min and initial concentration 40 mg/l. The predicted removal of 96.55 % for the concentration of 40 mg/l. In the isotherms analysis the Temkin isotherms was found to fit best for the adsorption of Cr (VI) by MAC with constant value 10.189. The adsorption kinetics of MAC was found to fit better with a pseudo-second-order model. The recycling of MAC adsorbent percentage removal efficiency decreased from the 96.34-75.00% from run one to run five and the % adsorption removal of Cr (VI) in the real wastewater showed significant adsorbent potential ranging from 2.8437 ± 0.139 to 0.0333 ± 0.0054 ppm. Finally, the study was as stepping stone for further field experiments.

5.2 RECOMMENDATION

After conducting different experimental work during preparation of AC and MAC in current studies, the following recommendation was drawn for further experimental work.

- ✓ The prepared MAC adsorbent can be used by tannery industries.
- ✓ The removal efficiency of the MAC should be studied for other heavy metals.
- ✓ EDX analysis is needed to study the elemental composition of adsorbed species in the MAC.
- ✓ Effective disposal of the adsorbent needs further investigation.

REFERENCES

- [1] K.M. Dimpe, J.C. Ngila, P.N. Nomngongo, Application of waste tyre-based activated carbon for the removal of heavy metals in wastewater, *Cogent Eng.* 4 (2017). <https://doi.org/10.1080/23311916.2017.1330912>.
- [2] M.A. Atieh, Removal of phenol from water different types of carbon – a comparative analysis, *Asia-Pacific Chem. Biol. Environ. Eng.* 10 (2014) 136–141. <https://doi.org/10.1016/j.apcbee.2014.10.031>.
- [3] E. Altıntığ, H. Altundag, M. Tuzen, A. Sarı, Effective removal of methylene blue from aqueous solutions using magnetic loaded activated carbon as novel adsorbent, *Chem. Eng. Res. Des.* 122 (2017) 151–163. <https://doi.org/10.1016/j.cherd.2017.03.035>.
- [4] C. Albertina, B. Staack, N. Nedelko, Ś. Anna, D. Piotr, A. Kaleta, R. Minikayev, T. Strachowski, L. Lipi, J. Dal, C. Antonio, Preparation , characterization and application of magnetic activated carbon from termite feces for the adsorption of Cr (VI) from aqueous solutions, *Powder Technol.* 354 (2019) 432–441. <https://doi.org/10.1016/j.powtec.2019.06.020>.
- [5] R. Abdeldayem, A preliminary study of heavy metals pollution risk in water, *Appl. Water Sci.* 10 (2020) 1–4. <https://doi.org/10.1007/s13201-019-1058-x>.
- [6] R. Bisht, M. Agarwal, Methodologies for removal of heavy metal ions from wastewater : an overview Methodologies for removal of heavy metal ions from wastewater , *Interdiscip. Environ. Rev.* 18 (2017) 1–20. <https://doi.org/10.1504/IER.2017.10008828>.
- [7] H. Hu, Q. Jin, P. Kavan, A Study of Heavy metal pollution in china: current status, pollution-control policies and countermeasures, *Sustainability.* 6 (2014) 5820–5838. <https://doi.org/10.3390/su6095820>.
- [8] S. Jiwan, K.A. S, Effects of heavy metals on soil, plants, human health and aquatic life, *Int. J. Res. Chem. Environ.* 1 (2011) 15–21.
- [9] M. Ruthiraan, N.M. Mubarak, E.C. Abdullah, M. Khalid, An overview of magnetic material : preparation and adsorption removal of heavy metals from wastewater, *Magn. Nanostructures.* (2019) 131–159. <https://doi.org/10.1007/978-3-030-16439-3>.
- [10] A. Banchhor, M. Pandey, P.K. Pandey, A review of hexavalent chromium contamination in India, *Res. J. Chem. Sci.* 7 (2017) 39–44.
- [11] A.E. Burakov, E. V. Galunin, I. V. Burakova, A.E. Kucheroval, S. Agarwal, A.G. Tkachev, V.K. Gupta, Adsorption of heavy metals on conventional and nanostructured materials for wastewater treatment purposes: A review, *Ecotoxicol. Environ. Saf.* 148 (2018) 702–712. <https://doi.org/10.1016/j.ecoenv.2017.11.034>.
- [12] S. Mohanty, B. Bal, A. Das, Adsorption of hexavalent chromium onto activated carbon, *Austin J Biotechnol Bioeng.* 1 (2014) 1–5.

- [13] S. Demcak, M. Balintova, M. Demcakova, I. Zinicovscaia, N. Yushin, M. V. Frontasyeva, Using of wooden sawdust for copper removal from waters, *Nov. Biotechnol. Chim.* 18 (2019) 66–71. <https://doi.org/10.2478/nbec-2019-0009>.
- [14] Z.J. Harandi, S.G. Nasab, A. Teimouri, Synthesis and characterisation of magnetic activated carbon/diopside nanocomposite for removal of reactive dyes from aqueous solutions : experimental design and optimisation, *Int. J. Environ. Anal. Chem.* 00 (2019) 1–27. <https://doi.org/10.1080/03067319.2019.1597867>.
- [15] K.S. Obayomi, J.O. Bello, J.S. Nnoruka, A.A. Adediran, P.O. Olajide, J.O. Bello, J.S. Nnoruka, A.A. Adediran, P.O. Olajide, Development of low-cost bio-adsorbent from agricultural waste composite for Pb (II) and As (III) sorption from aqueous solution, *Cogent Eng.* 6 (2019) 1–17. <https://doi.org/10.1080/23311916.2019.1687274>.
- [16] E. Bernard, A. Jimoh, J.O. Odigure, Heavy metals removal from industrial wastewater by activated carbon prepared from coconut shell, *Res. J. Chem. Sci.* 3 (2013) 3–9.
- [17] T. Rocha, P. Paulo, M. De Mello, Solid wastes in brewing process : A review, *J. Brew. Distill.* 5 (2014) 1–9. <https://doi.org/10.5897/JBD2014.0043>.
- [18] B.O. Aregbesola, O. A. and Omafuvbe, Production of aspergillus niger biomass from aqueous extract of brewer's spent grain, *J. Sci.* 16 (2014) 527–532.
- [19] S.B. Onofre, I.C. Bertoldo, D. Abatti, D. Refosco, Physiochemical characterization of the brewers ' spent grain from a brewery located in the Southwestern Region of Parana - Brazil, *Int. J. Environ. Agric. Biotechnol.* 2 (2017) 277–280.
- [20] S.I. Mussatto, G. Dragone, I.C. Roberto, Brewers ' spent grain : generation , characteristics and potential applications, *J. Cereal Sci.* 43 (2006) 1–14. <https://doi.org/10.1016/j.jcs.2005.06.001>.
- [21] F. Guo, X. Li, X. Jiang, X. Zhao, C. Guo, Z. Rao, Characteristics and toxic dye adsorption of magnetic activated carbon prepared from biomass waste by modified one-step synthesis, *Colloids and Surfaces.* 555 (2018) 43–54. <https://doi.org/10.1016/j.colsurfa.2018.06.061>.
- [22] S. Zhang, L. Tao, M. Jiang, G. Gou, Z. Zhou, Single-step synthesis of magnetic activated carbon from peanut shell, *Mater. Lett.* 157 (2015) 281–284. <https://doi.org/10.1016/j.matlet.2015.05.117>.
- [23] J.C. Xu, P.H. Xin, Y.B. Han, P.F. Wang, H.X. Jin, D.F. Jin, X.L. Peng, B. Hong, J. Li, H.L. Ge, Z.W. Zhu, X.Q. Wang, Magnetic response and adsorptive properties for methylene blue of CoFe₂O₄ / Co_xFe_y / activated carbon magnetic composites, *J. Alloy. Compd.* 617 (2014) 622–626. <https://doi.org/10.1016/j.jallcom.2014.08.059>.
- [24] G. Zhang, H. Liu, A.T. Cooper, R. Wu, CuFe₂O₄ / activated carbon composite : A novel magnetic adsorbent for the removal of acid orange II and catalytic regeneration, *Chemosphere.* 68 (2007) 1058–1066.

<https://doi.org/10.1016/j.chemosphere.2007.01.081>.

- [25] A. Phetrak, S. Sangkarak, S. Ampawong, S. Ittisupornrat, D. Pihusut, Kinetic Adsorption of hazardous methylene blue from aqueous solution onto iron-impregnated powdered activated carbon, *Environ. Nat. Resour. J.* 17 (2019) 78–86. <https://doi.org/10.32526/enrj.17.4.2019.33>.
- [26] R. Juang, Y. Yei, C. Liao, K. Lin, H. Lu, Synthesis of magnetic Fe₃O₄/activated carbon nanocomposites with high surface area as recoverable adsorbents, *J. Taiwan Inst. Chem. Eng.* (2018) 1–10. <https://doi.org/10.1016/j.jtice.2017.12.005>.
- [27] A.B. Cundy, L. Hopkinson, R.L.D. Whitby, Use of iron-based technologies in contaminated land and groundwater remediation: A review, *Sci. Total Environ.* 400 (2008) 42–51. <https://doi.org/10.1016/j.scitotenv.2008.07.002>.
- [28] S. Sharma, A. Bhattacharya, Drinking water contamination and treatment techniques, *Appl. Water Sci.* 7 (2017) 1043–1067. <https://doi.org/10.1007/s13201-016-0455-7>.
- [29] G. Crini, E. Lichtfouse, Advantages and disadvantages of techniques used for wastewater treatment, *Environ. Chem. Lett.* 17 (2020) 145–155. <https://doi.org/10.1007/s10311-018-0785-9>.
- [30] R.K. Koshal, Water pollution and human health, *Water. Air. Soil Pollut.* 5 (1976) 289–297. <https://doi.org/10.1007/BF00158344>.
- [31] K. Mohammed, O. Sahu, Recovery of chromium from tannery industry waste water by membrane separation technology: health and engineering aspects, *Sci. African.* 4 (2019) 1–9. <https://doi.org/10.1016/j.sciaf.2019.e00096>.
- [32] S. Dixit, A. Yadav, P.D. Dwivedi, M. Das, Toxic hazards of leather industry and technologies to combat threat: A review, *J. Clean. Prod.* 87 (2015) 39–49. <https://doi.org/10.1016/j.jclepro.2014.10.017>.
- [33] A. Teklay, T.Y. and T.P.S. G. Gebeyehu, T. Getachew, Quantification of solid waste leather generation rate from the Ethiopian leather sector - a contributing perspective to waste management approach, *Innov. Energy Res.* 7 (2018) 1–5. <https://doi.org/10.4172/2576-1463.1000208>.
- [34] S. Aber, D. Salari, M.R. Parsa, Employing the taguchi method to obtain the optimum conditions of coagulation – flocculation process in tannery wastewater treatment, *Chem. Eng. J.* 162 (2010) 127–134. <https://doi.org/10.1016/j.cej.2010.05.012>.
- [35] M. Chowdhury, M.G. Mostafa, T.K. Biswas, A.K. Saha, Treatment of leather industrial effluents by filtration and coagulation processes, *Water Resour. Ind.* 3 (2013) 11–22. <https://doi.org/10.1016/j.wri.2013.05.002>.
- [36] S. Hudda, River pollution: causes and actions “for a better tomorrow, act today,” *Janhit Found.* (2011) 1–15.
- [37] M. Chowdhury, M.G. Mostafa, T.K. Biswas, A. Mandal, A.K. Saha,

- Characterization of the effluents from leather processing industries, *Environ. Process.* 2 (2015) 173–187. <https://doi.org/10.1007/s40710-015-0065-7>.
- [38] T. Qiang, L. Chen, Q. Zhang, X. Liu, A sustainable and cleaner speedy tanning system based on condensed tannins catalyzed by laccase, *J. Clean. Prod.* 197 (2018) 1117–1123. <https://doi.org/10.1016/j.jclepro.2018.06.257>.
- [39] C. Sethuraman, K. Srinivas, G. Sekaran, Double pyrolysis of chrome tanned leather solid waste for safe disposal and products recovery, *Int. J. Sci. Eng. Res.* 4 (2013) 61–67.
- [40] J. Mushahary, V. Mirunalini, Waste management in leather industry environmental and health effects and suggestions to use in construction purposes, *Int. J. Civ. Eng. Technol.* 8 (2017) 1394–1401.
- [41] N.. C.B. and S.. S. J. Kanagaraj, K .Velappan, Solid wastes generation in the leather industry and its utilization for cleaner environment-A review, *J. Sci. Ind. Res.* 65 (2016) 1–9. <https://doi.org/10.1002/chin.200649273>.
- [42] M.S. Sajid, M. Malik, G.J. Hashmi, G. Dastageer, Z. Ali, M.F. Malik, I. Liaqat, Leather industry and environment: Pakistan Scenario, *Int. J. Appl. Biol. Forensics.* 1 (2017) 20–25. <https://www.researchgate.net/publication/317381731>.
- [43] T. Altun, H. Ecevit, Cr (VI) removal using Fe₂O₃-chitosan-cherry kernel shell pyrolytic charcoal composite beads, *Korean Soc. Environ. Eng.* 112 (2019) 0–36.
- [44] F. Fu, Q. Wang, Removal of heavy metal ions from wastewaters : A review, *J. Environ. Manage.* 92 (2011) 407–418. <https://doi.org/10.1016/j.jenvman.2010.11.011>.
- [45] M. Agarwal, K. Singh, R. Gupta, R.K. Dohare, Continuous fixed-bed adsorption of heavy metals using biodegradable adsorbent : modeling and experimental study, *J. Environ. Eng.* 146 (2020) 1–14. [https://doi.org/10.1061/\(ASCE\)EE.1943-7870.0001636](https://doi.org/10.1061/(ASCE)EE.1943-7870.0001636).
- [46] V. Bobade, N. Eshtiagi, Heavy metals removal from wastewater by adsorption process : A Review Introduction Heavy Metals and Industrial Waste water, *APCCHE.* 1 (2015) 1–6.
- [47] H.P. Nogueira, S.H. Toma, A.T. Silveira, A.A.C. Carvalho, A.M. Fioroto, K. Araki, Efficient Cr (VI) removal from wastewater by activated carbon superparamagnetic composites, *Microchem. J.* 149 (2019) 104025. <https://doi.org/10.1016/j.microc.2019.104025>.
- [48] G. Matta, G.K. Vishwavidyalaya, L. Gjiyli, Mercury , lead and arsenic : impact on environment and human health, *I J. Chem. Pharm. Sci.* 9 (2016) 1–9.
- [49] J. Duruibe, J. Ekwurugwu, Heavy metal pollution and human biotoxic effects, *Int. J. Phys. Sci.* 2 (2016) 1–8.
- [50] H.K. Alluri, S.R. Ronda, V.S. Settalluri, J. Singh, V. Suryanarayana, P. Venkateshwar, Biosorption : An eco-friendly alternative for heavy metal removal,

African J. Biotechnol. 6 (2007) 2924–2931.

- [51] O. Akpor, D.A. Otohinoyi, T.D. Olaolu, J.B.I. Aderiye, A. Ekiti, pollutants in wastewater effluents : impacts and remediation, *Int. J. Environ. Res. Earth Sci.* 3 (2014) 1–9.
- [52] H.E. Bin, Y.U.N. Zhaojun, S.H.I. Jianbo, J. Guibin, Research progress of heavy metal pollution in China : Sources , analytical methods , status , and toxicity, *Chinese Sci. Bull.* 58 (2015) 134–140. <https://doi.org/10.1007/s11434-012-5541-0>.
- [53] S.S. Ahluwalia, Waste biomaterials for removal of heavy metals – an overview, *Dyn. Biochem. Process Biotechnol. Mol. Biol.* 6 (2012) 1–6.
- [54] W.K. Buah, J.R. Dankwah, Sorption of Heavy metal ions from mine wastewater by activated carbons prepared from coconut husk , *Ghana Min. J.* 16 (2016) 2–7.
- [55] C. Bradu, N. Morin-crini, B. Sancey, Pollutant removal from industrial discharge water using individual and combined effects of adsorption and ion-exchange processes : Chemical abatement, *J. Saudi Chem. Soc.* 20 (2016) 185–194. <https://doi.org/10.1016/j.jscs.2013.03.007>.
- [56] V.M. and K.L. Muedi, Environmental contamination by heavy metals, *Clarivate Anal.* (2018) 116–133.
- [57] A. Selvi, A. Rajasekar, J. Theerthagiri, A. Ananthaselvam, K. Sathishkumar, J. Madhavan, P.K.S.M. Rahman, Integrated remediation processes toward heavy metal removal/recovery from various environments-A review, *Front. Environ. Sci.* 7 (2019) 1–15. <https://doi.org/10.3389/fenvs.2019.00066>.
- [58] W.R. García-niño, J. Pedraza-chaverri, Protective effect of curcumin against heavy metals-induced liver damage, *Food Chem. Toxicol. J.* 69 (2014) 182–201. <https://doi.org/10.1016/j.fct.2014.04.016>.
- [59] R.A. Wuana, F.E. Okieimen, Heavy metals in contaminated soils : a review of sources , chemistry , risks and best available strategies for remediation, *Int. Sch. Res. Netw.* (2011) 1–21. <https://doi.org/10.5402/2011/402647>.
- [60] A.D. Dayan, A.J. Paine, Human & experimental toxicology mechanisms of chromium toxicity , carcinogenicity and allergenicity : Review of the literature from 1985 to 2000, *Hum. Exp. Toxicol.* 20 (2001) 1–14. <https://doi.org/10.1191/096032701682693062>.
- [61] J. Rull-barrull, G. Bretel, E. Le Grogne, Chemically modified cellulose filter paper for heavy metal remediation in water, *ACS Sustain. Chem. Eng.* 5 (2017) 1965–1973. <https://doi.org/10.1021/acssuschemeng.6b02768>.
- [62] D. Guo, Q. An, Z. Xiao, S. Zhai, D. Yang, Efficient removal of Pb (II), Cr (VI) and organic dyes by polydopamine modified chitosan aerogels, *Carbohydr. Polym.* 202 (2018) 306–314. <https://doi.org/10.1016/j.carbpol.2018.08.140>.
- [63] R. Jobby, P. Jha, A.K. Yadav, N. Desai, Chemosphere biosorption and biotransformation of hexavalent chromium [Cr (VI)]: A comprehensive review,

- [64] V.E. Pakade, T. Tavengwa, L.M. Madikizela, Recent advances in hexavalent chromium removal from aqueous solutions by adsorptive methods, *R. Soc. Chem.* 9 (2019) 26142–26164. <https://doi.org/10.1039/c9ra05188k>.
- [65] P. Sharma, V. Bihari, S.K. Agarwal, V. Verma, C.N. Kesavachandran, B.S. Pangtey, N. Mathur, K.P. Singh, M. Srivastava, S.K. Goel, Groundwater contaminated with hexavalent chromium [Cr (VI)]: a health survey and clinical examination of community inhabitants (Kanpur, India), *PLoS One*. 7 (2012) 3–9. <https://doi.org/10.1371/journal.pone.0047877>.
- [66] H. Ali, E. Khan, I. Ilahi, Environmental chemistry and ecotoxicology of hazardous heavy metals : environmental persistence, Toxicity and Bioaccumulation, (2019) 1–14.
- [67] W. Zhao, H. Wei, L. Jia, S. Daryanto, X. Zhang, Y. Liu, Soil erodibility and its influencing factors on the Loess Plateau of China : a case study in the Ansai watershed, *Solid Earth*. 9 (2018) 1507–1516.
- [68] F.O.S. Pei-ntda, C. Jia, J. Zhao, L. Lei, X. Kang, R. Lu, Novel magnetically separable anhydride- stability and recyclable adsorption performance for, *R. Soc. Chem.* 9 (2019) 9533–9545. <https://doi.org/10.1039/c8ra10310k>.
- [69] R. Baby, B. Saifullah, Carbon nanomaterials for the treatment of heavy metal-contaminated water and environmental remediation, *Nanoscale Res. Lett.* 14 (2019) 1–17.
- [70] M. Abdulkarim, F.A. Al-rub, Adsorption of lead ions from aqueous solution onto activated carbon and chemically-modified activated carbon prepared from date pits, *Adsorpt. Sci. Technol.* 22 (2003) 1–16. <https://doi.org/10.1260/026361704323150908>.
- [71] H. Sharma, N. Rawal, B.B. Mathew, The characteristics , toxicity and effects of cadmium, *Int. J. Nanotechnol. Nanosci.* 3 (2015) 1–10.
- [72] D. Antivachi, C. Vasilatos, I. Megremi, Evaluation of the Cr (VI) and other toxic element contamination and their potential sources : The case of the Thiva basin (Greece), *Geosci. Front.* 3 (2012) 523–539. <https://doi.org/10.1016/j.gsf.2011.11.010>.
- [73] S.A. Obaid, Removal chromium (VI) from water by magnetic carbon nano-composite made by burned straw, *Int. Sci. Conf. Pure Sci.* 1234 (2019) 1–13. <https://doi.org/10.1088/1742-6596/1234/1/012032>.
- [74] M. Jain, M. Yadav, T. Kohout, M. Lahtinen, V. Kumar, M. Sillanpää, Development of iron oxide / activated carbon nanoparticle composite for the removal of Cr (VI), Cu (II) and Cd (II) ions from aqueous solution, *Water Resour. Ind.* 20 (2018) 54–74. <https://doi.org/10.1016/j.wri.2018.10.001>.
- [75] G. Marques, D. Giulio, A.M.B. Bedran-martins, P. Vasconcellos, W. Costa, M.

- Carmen, Mainstreaming climate adaptation in the megacity of São Paulo , Brazil, *Cities*. 72 (2018) 237–244. <https://doi.org/10.1016/j.cities.2017.09.001>.
- [76] B.K. D. Priya , C. Yu, Biosorption of Ni (II) ions from aqueous solution using leaves of *Araucaria cookie*, *Int. J. Appl. Sci.* 6 (2014) 9–16.
- [77] M.S.K. .Oves, A.Huda Qari, N.F. M, T.Almeelbi, Bioremediation & biodegradation heavy metals : biological importance and detoxification strategies, *J. Bioremediation Biodegrad.* 7 (2016) 1–15. <https://doi.org/10.4172/2155-6199.1000334>.
- [78] K.C.K.T. Matsuura, E.D.A. Ethylenediamine, Removal of heavy metals and pollutants by membrane adsorption techniques, *Appl. Water Sci.* 8 (2018) 1–30. <https://doi.org/10.1007/s13201-018-0661-6>.
- [79] M.R. Lasheen, I.Y. El-sherif, S.T. El-wakeel, Heavy metals removal from aqueous solution using magnetite Dowex 50WX4 resin nanocomposite, *J. Mater. Environ. Sci.* 8 (2017) 503–511.
- [80] D. Mohan, H. Kumar, A. Sarswat, M. Alexandre-franco, C.U. Pittman, Cadmium and lead remediation using magnetic oak wood and oak bark fast pyrolysis biochars, *Chem. Eng. J.* 236 (2014) 513–528. <https://doi.org/10.1016/j.cej.2013.09.057>.
- [81] S. Pap, V. Bezanovic, J. Radonic, A. Babic, S. Saric, D. Adamovic, M. Turk, Synthesis of highly-efficient functionalized biochars from fruit industry waste biomass for the removal of chromium and lead, *J. Mol. Liq.* 268 (2018) 315–325. <https://doi.org/10.1016/j.molliq.2018.07.072>.
- [82] A. Herrera-barros, C. Tejada-tovar, Á. Villabona-ortíz, Adsorption study of Ni (II) and Pb (II) onto low-cost agricultural biomasses chemically modified with TiO₂ Nanoparticles, 11 (2018). <https://doi.org/10.17485/ijst/2018/v11i21/123248>.
- [83] M. Lesaoana, R.P. V Mlaba, F.M. Mtunzi, M.J. Klink, P. Ejidike, V.E. Pakade, Influence of inorganic acid modification on Cr (VI) adsorption performance and the physicochemical properties of activated carbon, *South African J. Chem. Eng.* 28 (2019) 8–18. <https://doi.org/10.1016/j.sajce.2019.01.001>.
- [84] T. Agustiono, G.Y.S. Chan, W. Lo, S. Babel, Physico – chemical treatment techniques for wastewater laden with heavy metals, *Chem. Eng. J.* 118 (2006) 83–98. <https://doi.org/10.1016/j.cej.2006.01.015>.
- [85] C. Hydroxide, R. Assessment, heavy metal and phosphorus removal from waters by optimizing use of heavy metal and phosphorus, *Environ. Pollut.* 1 (2012) 1–18. <https://doi.org/10.5539/ep.v1n1p38>.
- [86] M. Yusuf, F.M. Elfghi, S.A. Zaidi, E.C. Abdullah, M.A. Khan, Applications of graphene and its derivatives as an adsorbent for heavy metal and dye removal : a systematic and comprehensive overview, *R. Soc. Chem.* 5 (2015) 50392–50420. <https://doi.org/10.1039/C5RA07223A>.
- [87] M. Han, J. Zhang, W. Chu, J. Chen, G. Zhou, Research progress and prospects of

marine oily wastewater treatment : a review, *Water Rev.* 11 (2019) 1–29.

- [88] M. Zhao, Y. Xu, C. Zhang, H. Rong, G. Zeng, New trends in removing heavy metals from wastewater, *Appl. Microbiol. Biotechnol.* 100 (2016) 6509–6518. <https://doi.org/10.1007/s00253-016-7646-x>.
- [89] M.A. Barakat, New trends in removing heavy metals from industrial wastewater, *Arab. J. Chem.* 4 (2011) 361–377. <https://doi.org/10.1016/j.arabjc.2010.07.019>.
- [90] P.C. Emenike, D.O. Omole, B.U. Ngene, I.T. Tenebe, Potentiality of agricultural adsorbent for the sequestering of metal ions from wastewater, *Glob. J. Environ. Sci. Manag.* 2 (2016) 411–442. <https://doi.org/10.22034/gjesm.2016.02.04.010>.
- [91] E. Musin, Adsorption Modeling, *Mikkeli Univ. Appl. Sci.* (2013) 577–708. <https://doi.org/10.1201/9780585418049.ch5>.
- [92] D. Park, Y.S. Yun, J.H. Jo, J.M. Park, Mechanism of hexavalent chromium removal by dead fungal biomass of *Aspergillus niger*, *Water Res.* 39 (2005) 533–540. <https://doi.org/10.1016/j.watres.2004.11.002>.
- [93] E. Malkoc, Y. Nuhoglu, Potential of tea factory waste for chromium (VI) removal from aqueous solutions : Thermodynamic and kinetic studies, *Sep. Purif. Technol.* 54 (2007) 291–298. <https://doi.org/10.1016/j.seppur.2006.09.017>.
- [94] D. Park, Y.S. Yun, M.P. Jong, Studies on hexavalent chromium biosorption by chemically-treated biomass of *Ecklonia* sp., *Chemosphere.* 60 (2005) 1356–1364. <https://doi.org/10.1016/j.chemosphere.2005.02.020>.
- [95] and G.L. Guillaume Daragon, Gwenaëlle Trouvé, Recovery of an agro-industrial vinasse by adsorption on different wood materials: parametric study at laboratory scale, *Bioresources.* 9 (2014) 7764–7781.
- [96] P.K. Sath, S. Duhan, J.S. Duhan, Agro - industrial wastes and their utilization using solid state fermentation : a review, *Bioresour. Bioprocess.* 5 (2018) 1–15. <https://doi.org/10.1186/s40643-017-0187-z>.
- [97] A.R. Hidayu, N. Muda, Preparation and characterization of impregnated activated carbon from palm kernel shell and coconut shell for CO₂ capture, *Procedia Eng.* 148 (2016) 106–113. <https://doi.org/10.1016/j.proeng.2016.06.463>.
- [98] R. Baby, Ecofriendly approach for treatment of heavy-metal-contaminated water using activated carbon of kernel shell of oil palm, *Materials (Basel).* 13 (2020) 11–13.
- [99] T.A. Kurniawan, G.Y.S. Chan, W. hung Lo, S. Babel, Comparisons of low-cost adsorbents for treating wastewaters laden with heavy metals, *Sci. Total Environ.* 366 (2006) 409–426. <https://doi.org/10.1016/j.scitotenv.2005.10.001>.
- [100] J.C. Gavaghan, Declaration of originality . Signed : Date :, *African J. Biotechnol.* 10 (2011) 324–331. <https://doi.org/10.5897/AJBx10.006>.
- [101] M. Ahmaruzzaman, Industrial wastes as low-cost potential adsorbents for the

- treatment of wastewater laden with heavy metals, *Adv. Colloid Interface Sci.* 166 (2011) 36–59. <https://doi.org/10.1016/j.cis.2011.04.005>.
- [102] A.A. Olajire, The brewing industry and environmental challenges, *J. Clean. Prod.* 30 (2012) 1–21. <https://doi.org/10.1016/j.jclepro.2012.03.003>.
- [103] S. Gupta, S. Cox, N. Abu-ghannam, Process optimization for the development of a functional beverage based on lactic acid fermentation of oats, *J. Biochem. Eng.* 52 (2010) 199–204. <https://doi.org/10.1016/j.bej.2010.08.008>.
- [104] M. Gupta, N. Abu-ghannam, Barley for brewing : characteristic changes during malting , brewing and applications of its, *Inst. Food Technol.* 9 (2010) 1–9.
- [105] P. Issn, O. Issn, W. Page, Wastewater remediation via modified activated carbon : a review, *Polution.* 4 (2018) 707–723.
- [106] O. Baytar, Ş. Ömer, C. Saka, Sequential application of microwave and conventional heating methods for preparation of activated carbon from biomass and its methylene blue adsorption, *Appl. Therm. Eng. J.* 138 (2018) 542–551. <https://doi.org/10.1016/j.applthermaleng.2018.04.039>.
- [107] A.A. Attia, S.A. Khedr, S.A. Elkholy, Adsorption of chromium ion (VI) by acid activated carbon, *Brazilian J. Chem. Eng.* 27 (2010) 183–193. <https://doi.org/10.1590/S0104-66322010000100016>.
- [108] T. Dula, K. Siraj, S.A. Kitte, Adsorption of hexavalent chromium from aqueous solution using chemically activated carbon prepared from locally available waste of bamboo (*Oxytenanthera abyssinica*), *Environ. Chem.* (2014) 1–10.
- [109] J. Katenta, C. Nakiguli, P. Mukasa, E. Ntambi, Removal of chromium (VI) from tannery effluent using bio-char of phoenix reclinata seeds, *Green Sustain. Chem.* 10 (2020) 91–107. <https://doi.org/10.4236/gsc.2020.103007>.
- [110] S. Zhang, L. Tao, Y. Zhang, Z. Wang, G. Gou, M. Jiang, C. Huang, Z. Zhou, The role and mechanism of K_2CO_3 and Fe_3O_4 in the preparation of magnetic peanut shell based activated carbon, *Powder Technol.* 295 (2016) 152–160. <https://doi.org/10.1016/j.powtec.2016.03.034>.
- [111] J. Zhou, Y. Liu, X. Zhou, J. Ren, C. Zhong, Magnetic multi-porous bio-adsorbent modified with amino siloxane for fast removal of Pb (II) from aqueous solution, *Appl. Surf. Sci.* 427 (2018) 976–985. <https://doi.org/10.1016/j.apsusc.2017.08.110>.
- [112] J. Shen, N. Wang, Y.G. Wang, D. Yu, X.K. Ouyang, Efficient adsorption of Pb(II) from aqueous solutions by metal organic framework (Zn-BDC) coated magnetic montmorillonite, *Polymers (Basel)*. 10 (2018) 1–16. <https://doi.org/10.3390/polym10121383>.
- [113] V.T. Le, M.U. Dao, H.S. Le, D.L. Tran, V.D. Doan, Adsorption of Ni (II) ions by magnetic activated carbon / chitosan beads prepared from spent coffee grounds , shrimp shells and green tea extract, *Taylor & Francis*, 2019. <https://doi.org/10.1080/09593330.2019.1584250>.

- [114] M. Li, S. Ma, X. Zhu, Preparation of activated carbon from pyrolyzed rice husk by leaching out ash content after CO₂ activation, *Bio-resources*. 11 (2016) 3384–3396. <https://doi.org/10.15376/biores.11.2.3384-3396>.
- [115] A.I. Osman, E.O. Connor, G. Mcspadden, J.K. Abu-dahrieh, C. Farrell, A.H. Al-muhtaseb, J. Harrison, D.W. Rooney, Upcycling brewer ' s spent grain waste into activated carbon and carbon nanotubes for energy and other applications via two-stage activation, *Soc. Chem. Ind.* 95 (2020) 183–195. <https://doi.org/10.1002/jctb.6220>.
- [116] S.I. Mussatto, M. Fernandes, G.J.M. Rocha, J.J.M. Órfão, J.A. Teixeira, I.C. Roberto, Production , characterization and application of activated carbon from brewer ' s spent grain lignin, *Bioresour. Technol.* 101 (2010) 2450–2457. <https://doi.org/10.1016/j.biortech.2009.11.025>.
- [117] K. Al-saad, M. El-azazy, A.A. Issa, A. Al-yafie, A.S. El-shafie, Recycling of date pits into a green adsorbent for removal of heavy metals : a fractional factorial design based approach, *Front. Chem.* 7 (2019) 1–16. <https://doi.org/10.3389/fchem.2019.00552>.
- [118] M.H. Salmani, F. Sahlabadi, H. Eslami, M.T. Ghaneian, I.R. Balaneji, T.J. Zad, Removal of Cr(VI) oxoanion from contaminated water using granular jujube stems as a porous adsorbent, *Groundw. Sustain. Dev.* 8 (2019) 319–323. <https://doi.org/10.1016/j.gsd.2018.12.001>.
- [119] G. Qu, D. Zeng, R. Chu, T. Wang, D. Liang, H. Qiang, Magnetic Fe₃O₄ assembled on nZVI supported on activated carbon fiber for Cr(VI) and Cu(II) removal from aqueous solution through a permeable reactive column, *Environ. Sci. Pollut. Res.* 26 (2019) 5176–5188. <https://doi.org/10.1007/s11356-018-3985-8>.
- [120] P. Parthasarathy, S.K. Narayanan, Effect of hydrothermal carbonization reaction parameters, *Environ. Prog. Sustain. Energy.* 33 (2014) 676–680. <https://doi.org/10.1002/ep>.
- [121] A.T. Ojedokun, O.S. Bello, Sequestering heavy metals from wastewater using cow dung, *Water Resour. Ind.* 13 (2016) 7–13. <https://doi.org/10.1016/j.wri.2016.02.002>.
- [122] J. Aravind, G. Sudha, P. Kanmani, A.J. Devisri, S. Dhivyalakshmi, M. Raghavprasad, Equilibrium and kinetic study on chromium (VI) removal from simulated waste water using gooseberry seeds as a novel biosorbent, *Glob. J. Environ. Sci. Manag.* 1 (2015) 233–244. <https://doi.org/10.7508/gjesm.2015.03.006>.
- [123] W. Boulaiche, B. Hamdi, M. Trari, Removal of heavy metals by chitin : equilibrium , kinetic and thermodynamic studies, *Appl. Water Sci.* 9 (2019) 1–10. <https://doi.org/10.1007/s13201-019-0926-8>.
- [124] V. Nejadsha, M. Reza, Adsorption capacity of heavy metal ions using sultone-modi fi ed magnetic activated carbon as a bio-adsorbent, 101 (2019) 42–52. <https://doi.org/10.1016/j.msec.2019.03.081>.

- [125] T.V. Silas, Characterization and adsorption isotherm studies of Cd (II) And Pb (II) ions bioremediation from aqueous solution using unmodified sorghum husk, *J. Appl. Biotechnol. Bioeng.* 2 (2017) 1–9. <https://doi.org/10.15406/jabb.2017.02.00034>.
- [126] M.B. Desta, Batch Sorption Experiments : Batch sorption experiments: Langmuir and Freundlich isotherm studies for the adsorption of textile metal ions onto teff straw (*eragrostis tef*) agricultural waste Waste, *J. Thermodynamics.* 2013 (2013) 1-- 6.
- [127] S. Nethaji, A. Sivasamy, A.B. Mandal, Preparation and characterization of corn cob activated carbon coated with nano-sized magnetite particles for the removal of Cr(VI), *Bioresour. Technol.* 134 (2013) 94–100. <https://doi.org/10.1016/j.biortech.2013.02.012>.
- [128] G.M. Al-senani, F.F. Al-fawzan, Adsorption study of heavy metal ions from aqueous solution by nanoparticle of wild herbs, *Egypt. J. Aquat. Res.* 44 (2018) 187–194. <https://doi.org/10.1016/j.ejar.2018.07.006>.
- [129] M.D. G.Vijayakumar , R.Tamilarasan, Adsorption, kinetic, equilibrium and thermodynamic studies on the removal of basic dye rhodamine-b from aqueous solution by the use of natural adsorbent perlite, *J. Mater. Environ. Sci.* 3 (2012) 157–170. <http://www.nb3foundation.org/our-work/nativeyouthprograms/>.
- [130] Z. Li, S. Hu, Removal of hexavalent chromium from aqueous solutions by ion-exchange resin, *Adv. Mater. Res.* 26 (2012) 1–11. <https://doi.org/10.4028/www.scientific.net/AMR.550-553.2333>.
- [131] C. Anyika, N. Asilayana, M. Asri, Z. Abdul, Synthesis and characterization of magnetic activated carbon developed from palm kernel shells, *Nanotechnol. Environ. Eng.* 2 (2017) 1–25. <https://doi.org/10.1007/s41204-017-0027-6>.
- [132] J.W. and Z.L. J. Lou, X. Xu, Y. Gao, D. Zheng, Preparation of magnetic activated carbon from waste rice husk for determination of tetracycline antibiotics in water samples, *RSC Adv.* (2016) 1–27. <https://doi.org/10.1039/C6RA24397E>.
- [133] E. Sann, S. Adeeyo, Comparative analysis of adsorption of methylene blue dye using carbon from palmkernel shell activated by different activating agents, *Univ. Conv.* (2016) 175–181. <https://pdfs.semanticscholar.org/ee8b/2c92682a183f2e38b5d36a61dfa8e359d750.pdf>.
- [134] E.S. Sanni, M.E. Emetere, J.O. Odigure, V.E. Efeovbokhan, O. Agboola, E.R. Sadiku, Determination of optimum conditions for the production of activated carbon derived from separate varieties of coconut shells, *Int. J. Chem. Eng.* (2017) 1–17. <https://doi.org/10.1155/2017/2801359>.
- [135] K.S.R. and D.S. Daniel Kibami, Chubaakum Pongener, Preparation and characterization of activated carbon from *fagopyrum esculentum* Moench by HNO_3 and H_3PO_4 chemical activation, *Der Chem. Sin.* 5 (2014) 46–55.

- [136] P. Basu, Biomass characteristics, first edit, © 2010 Elsevier Inc., 2010. <https://doi.org/10.1016/b978-0-12-374988-8.00002-7>.
- [137] B. Singha, T.K. Naiya, A.K. Bhattacharya, S.K. Das, K. Ftir, C. Vi, R. Straw, H. Roots, S. Dust, Cr (VI) ions removal from aqueous solutions using natural adsorbents — FT-IR studies, *J. Environ. Prot. (Irvine, Calif)*. 2 (2011) 729–735. <https://doi.org/10.4236/jep.2011.26084>.
- [138] M. Farahani, S. Rozaimah, S. Abdullah, Adsorption-based cationic dyes using the carbon active sugarcane bagasse, *procedia environ. Sci*. 10 (2011) 203–208. <https://doi.org/10.1016/j.proenv.2011.09.035>.
- [139] K.K. Onchoke, S.A. Sasu, Determination of hexavalent chromium (cr(vi)) concentrations via ion chromatography and uv-vis spectrophotometry in samples collected from nacogdoches wastewater treatment plant, East Texas (USA), *Adv. Environ. Chem.* (2016) 1–10. <https://doi.org/10.1155/2016/3468635>.
- [140] M.L. Mekonnen, T.S. Bogale, Biosorption of Cr (VI) From Wastewater Using Dried Leaves of *Jatropha Curcas*, *Int. J. Sci. Eng. Res.* 9 (2018) 568–589.
- [141] S.K. Behera, H. Meena, S. Chakraborty, B.C. Meikap, Application of response surface methodology (RSM) for optimization of leaching parameters for ash reduction from low-grade coal, *Int. J. Min. Sci. Technol.* 28 (2018) 621–629. <https://doi.org/10.1016/j.ijmst.2018.04.014>.
- [142] B. Sadhukhan, N.K. Mondal, S. Chatteraj, Optimisation using central composite design (CCD) and the desirability function for sorption of methylene blue from aqueous solution onto *Lemna major*, *Karbala Int. J. Mod. Sci.* 2 (2016) 145–155. <https://doi.org/10.1016/j.kijoms.2016.03.005>.
- [143] M.P. Title, E.P. Manager, K.M. Title, E.P. Manager, E. Booth, Waste Water Sampling, *Watershed Prot. Branch*. 5 (2008) 1–18.
- [144] B.I. Islam, A.E. Musa, E.H. Ibrahim, S.A.A. Sharafa, B.M. Elfaki, Evaluation and characterization of tannery wastewater , *J. For. Prod. Ind.* 3 (2014) 141–150.
- [145] D.C. B.Saritha, Evaluation and characterization of tannery wastewater, *Int. J. Pure Appl. Math.* 119 (2018) 8479–8487.
- [146] A.H. Uddin, R.S. Khalid, M. Alaama, A.M. Abdualkader, A. Kasmuri, S.A. Abbas, Comparative study of three digestion methods for elemental analysis in traditional medicine products using atomic absorption spectrometry, *J. Anal. Sci. Technol.* 7 (2016) 1–7. <https://doi.org/10.1186/s40543-016-0085-6>.
- [147] T. Hadgu, M. Amare, Assessment of the level of chromium species in the discharged effluents of haik and Debre Berhan tanneries in the Amhara Region using ICP-OES and UV-Vis spectrometry, *Journa Scicence*. 9 (2016) 123–138.
- [148] F. Zewdu, M. Amare, Determination of the level of hexavalent, trivalent, and total chromium in the discharged effluent of Bahir Dar tannery using ICP-OES and UV-Visible spectrometry, *Cogent Chem.* 4 (2018) 1–9. <https://doi.org/10.1080/23312009.2018.1534566>.

- [149] W. Cai, Z. Li, J. Wei, Y. Liu, Chemical Engineering Research and Design Synthesis of peanut shell based magnetic activated carbon with excellent adsorption performance towards electroplating wastewater, Chem. Eng. Res. Des. 140 (2018) 23–32. <https://doi.org/10.1016/j.cherd.2018.10.008>.
- [150] H. Baylie Mengstie, School of graduate studies school of chemical and bioengineering investigation of brewery spent grain as adsorbent for removal of heavy metals, 2016.
- [151] R. Labied, O. Benturki, A.Y. Eddine Hamitouche, A. Donnot, Adsorption of hexavalent chromium by activated carbon obtained from a waste lignocellulosic material (*Ziziphus jujuba* cores): Kinetic, equilibrium, and thermodynamic study, Adsorpt. Sci. Technol. 36 (2018) 1066–1099. <https://doi.org/10.1177/0263617417750739>.
- [152] K.S. Padmavathy, G. Madhu, P.V. Haseena, A study on Effects of pH, Adsorbent Dosage, Time, Initial Concentration and Adsorption Isotherm Study for the Removal of Hexavalent Chromium (Cr (VI)) from Wastewater by Magnetite Nanoparticles, Procedia Technol. 24 (2016) 585–594. <https://doi.org/10.1016/j.protcy.2016.05.127>.
- [153] J.D. Castro-Castro, I.F. Macías-Quiroga, G.I. Giraldo-Gómez, N.R. Sanabria-González, Adsorption of Cr(VI) in aqueous solution using a surfactant-modified bentonite, Sci. World J. (2020) 1–9. <https://doi.org/10.1155/2020/3628163>.
- [154] T. Altun, Cr (VI) removal using Fe₂O₃ -chitosan-cherry kernel shell pyrolytic charcoal composite beads, Environ. Eng. Res. 25 (2020) 426–438.
- [155] S. Chatterjee, S. Mahanty, P. Das, P. Chaudhuri, S. Das, Biofabrication of iron oxide nanoparticles using manglicolous fungus *Aspergillus niger* BSC-1 and removal of Cr(VI) from aqueous solution, Chem. Eng. J. 385 (2020) 123790. <https://doi.org/10.1016/j.cej.2019.123790>.
- [156] B. Choudhary, D. Paul, Isotherms, kinetics and thermodynamics of hexavalent chromium removal using biochar, J. Environ. Chem. Eng. 6 (2018) 2335–2343. <https://doi.org/10.1016/j.jece.2018.03.028>.
- [157] G. Arslan, I. Sargin, M. Kaya, Hexavalent chromium removal by magnetic particle-loaded micro-sized chitinous egg shells isolated from ephippia of water flea, Int. J. Biol. Macromol. 129 (2019) 23–30. <https://doi.org/10.1016/j.ijbiomac.2019.01.180>.
- [158] A. Ajmani, T. Shahnaz, S. Subbiah, S. Narayanasamy, Hexavalent chromium adsorption on virgin, biochar, and chemically modified carbons prepared from *Phanera vahlii* fruit biomass: equilibrium, kinetics and thermodynamics approach, Environ. Sci. Pollut. Res. 26 (2019) 32137–32150. <https://doi.org/10.1007/s11356-019-06335-z>.

APPENDICES

Appendix A: BSG Samples and Activated Carbon

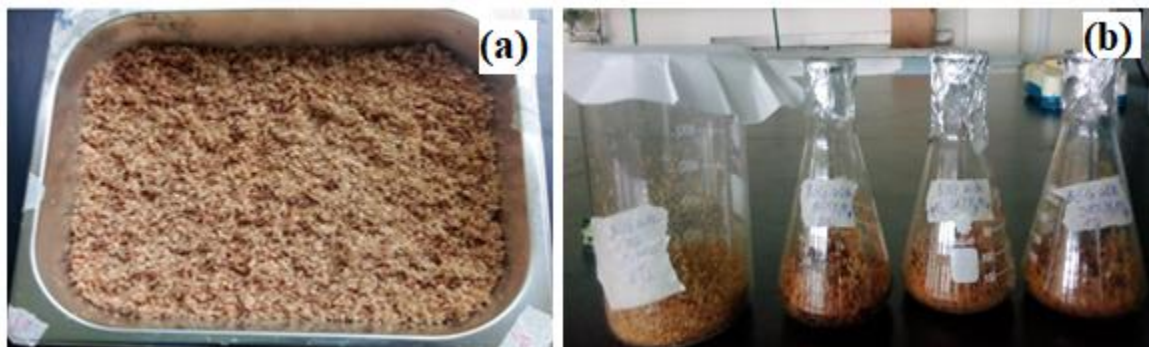


Figure 8A.1: BSG (a). before soaking; (b). after soaking

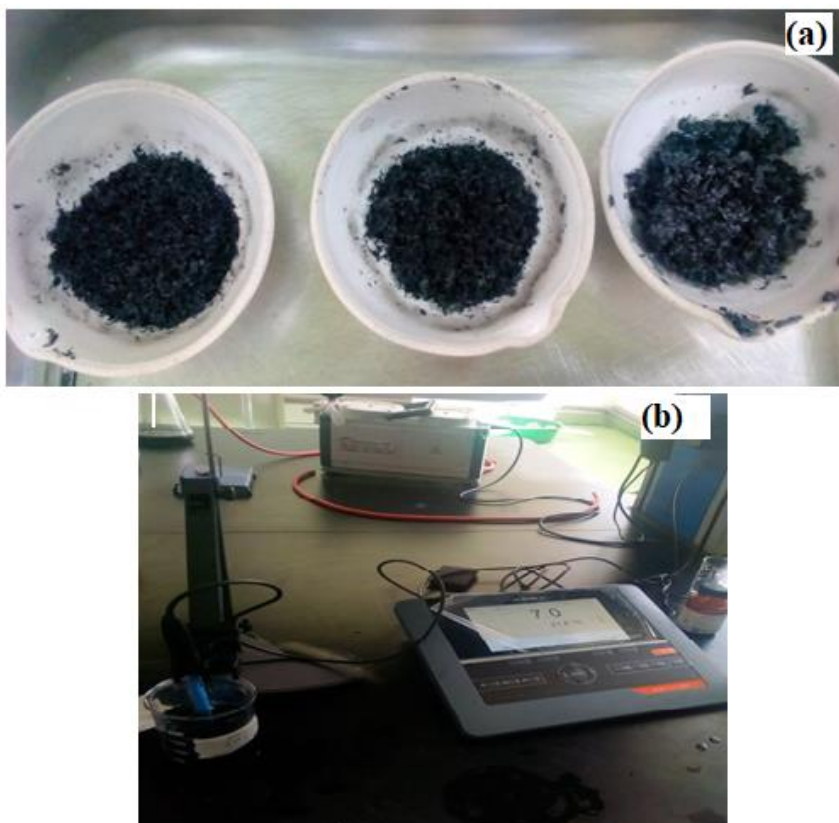


Figure 8A.2: Synthesized AC (a) and (b) Its neutralization at pH=7

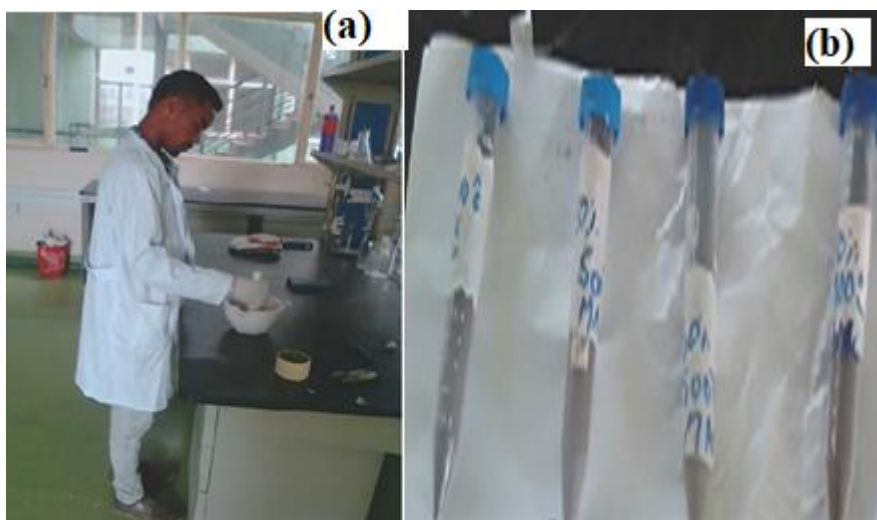


Figure 8A.3: Synthesized MAC; (a). Grinding and (b). Packing

Appendix B: UV-Vis Analysis

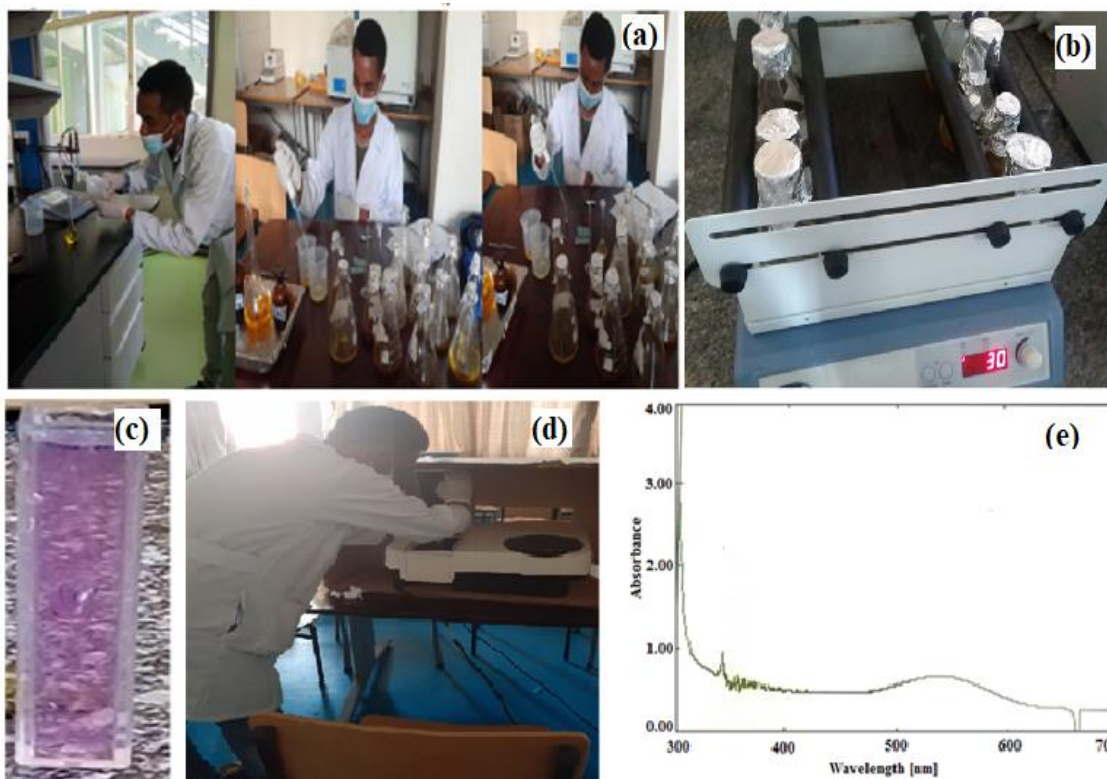


Figure 8B: UV-Visible analysis of Cr (VI); (a). Solution preparation; (b). Orbital shaking; (c). quartz cuvette; (d). UV-Vis measuring; (e). λ_{max} determination

Appendix 8C: BET Analysis

Horiba Instruments, Inc.
SA-9600 Series Surface Area Analyzer

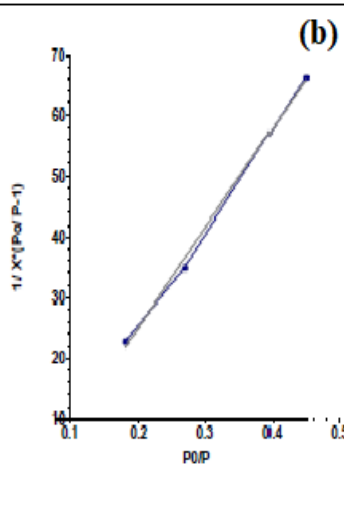
Analysis Report
Aug/02/2020

Customer : Belay G. _
Description : Magnetic Activated Carbon
Filename : Belay

Operator ID : SARA, CHED, AASTU
Analysis Date : Aug/02/2020
Analysis Time : 13:39:31

Condition Settings

Room Temp : 25.0 (°C) Atm. Pres : 700.0 (mm)
Gas Used : Nitrogen Gas Conc : 0.500

Channel: 1 (a)		(b)	
Sample Name	MAC		
Tube Number	1		
Tare Weight	10.0870 (gm)		
Sample Weight	10.1320 (gm)		
Degas Temp.	200 (°C)		
Degas Time	45 (min)		
Surface Area (M ² /gm)	495.461		
Slope	163.804		
Intercept	-7.721		
V _m	0.006		
BET Const	-20.215		
Pearson Coef	0.998		
X[1] - 0.449	66.309		
X[2] - 0.269	34.795		
X[3] - 0.179	22.737		

Appendix 8C.1: BET surface area value of; (a). MAC and (b). adsorption desorption graph of MAC

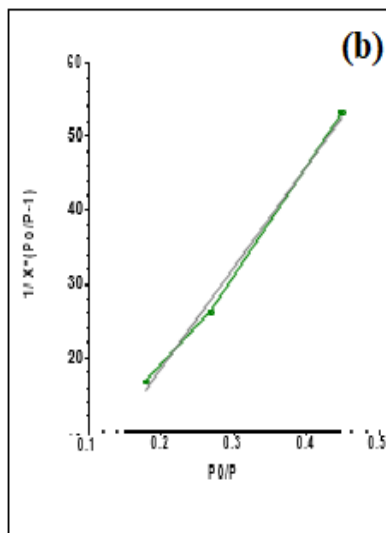
Customer : Belay G.
Description : A C
Filename : Belay,sa2

Operator ID : SARA, CHED, AASTU
Analysis Date : Aug/05/2020
Analysis Time : 10:36:59

Condition Settings

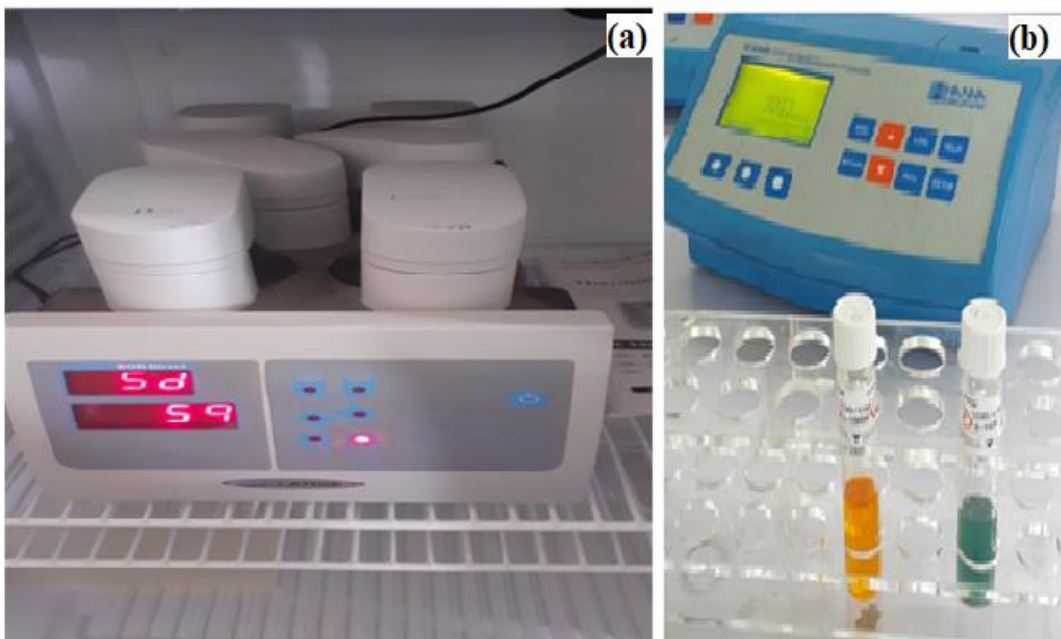
Room Temp : 23.0 (°C) Atm. Pres : 700.0 (mm)
Gas Used : Nitrogen Gas Conc : 0.500, 0.002, 0.002 %

	Channel: 2	(a)
Sample Name	3,2	
Tube Number	2	
Tare Weight	10. (gm)	
Sample Weight	10. (gm)	
Degas Temp.	200 (°C)	
Degas Time	45 (min)	
Surface Area (M ² /gm)	694.210	
Slope	137.503	
Intercept	-8.966	
V _m	0.008	
BET Const	-14.337	
Pearson Coef	0.997	
X[1] - 0.449	53.281	
X[2] - 0.269	26.415	
X[3] - 0.179	16.807	



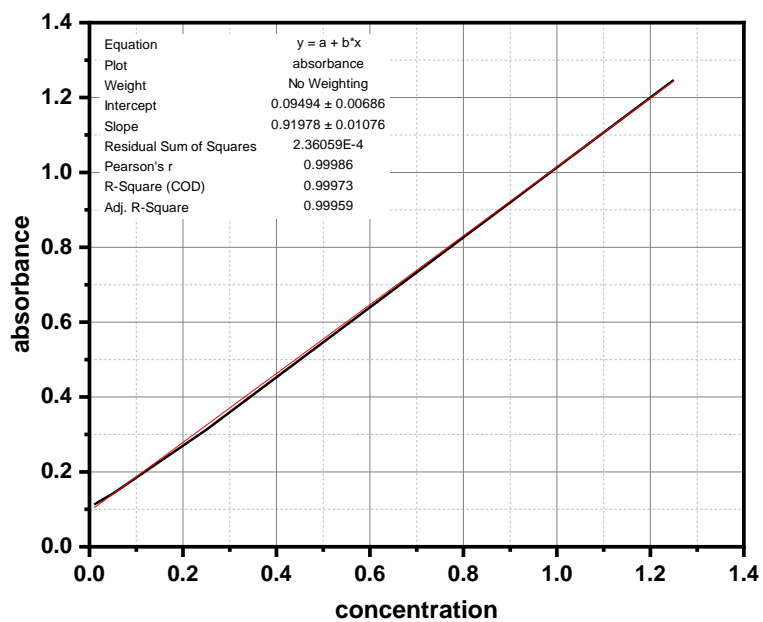
Appendix 8C.2: BET surface area value of; (a). AC and (b). adsorption desorption graph of AC

Appendix 8D: BOD and COD Analysis



Appendix 8D.1: Analysis the value of Awash Tannery effluent

Appendix 8E: Real Wastewater Analysis



Appendix 8E.1: Calibration Curve of Real Wastewater

Appendix 8F: Recycling of MAC Adsorbent



Appendix 8G: surface response value of Cr (VI)

Appendix 8F.1: Recycling of MAC Adsorbent from Simulated Wastewater

Source	Sum of Squares	df	Mean Square	F-value	p-value	
Model	6429.03	14	459.22	48.40	< 0.0001	significant
A-dosage	953.69	1	953.69	100.51	< 0.0001	
B-contact time	1640.93	1	1640.93	172.94	< 0.0001	
C-pH	1043.20	1	1043.20	109.94	< 0.0001	
D-initial con	314.58	1	314.58	33.15	< 0.0001	
AB	432.74	1	432.74	45.61	< 0.0001	
AC	18.81	1	18.81	1.98	0.1795	
AD	125.38	1	125.38	13.21	0.0024	
BC	116.69	1	116.69	12.30	0.0032	
BD	140.13	1	140.13	14.77	0.0016	
CD	46.27	1	46.27	4.88	0.0432	
A ²	227.59	1	227.59	23.99	0.0002	
B ²	956.58	1	956.58	100.82	< 0.0001	
C ²	605.06	1	605.06	63.77	< 0.0001	
D ²	400.62	1	400.62	42.22	< 0.0001	
Residual	142.33	15	9.49			
Lack of Fit	111.49	10	11.15	1.81	0.2664	not significant
Pure Error	30.84	5	6.17			
Cor Total	6571.35	29				

Appendix 8G:(b). CCD Experimental Design Matrix of the Four Factors and Corresponding Response of Cr (VI) Removal

	Factor 1	Factor 2	Factor 3	Factor 4	Response Cr ⁺⁶ removal	
Run	Dosage (g/l)	Contact time (min)	pH	Initial concentration (mg/l)	Experimental value %	Predicted value %
1	5	30	2	40	96.50	96.55
2	3	40	1	60	83.51	84.20
3	5	30	2	2	96.50	96.55
4	7	40	3	60	88.50	87.10
5	3	20	1	60	57.00	56.31
6	5	50	2	40	96.80	96.88
7	7	20	3	60	71.01	69.21
8	7	40	1	60	85.03	90.93
9	5	30	4	40	60.00	65.60
10	3	20	3	60	45.05	41.23
11	5	30	2	40	96.30	96.55
12	5	30	2	40	96.50	96.55
13	3	20	3	20	65.01	61.53
14	7	20	1	60	84.00	81.06
15	3	40	3	60	82.03	77.12
16	1	30	2	40	70.03	72.40
17	3	40	1	20	92.02	96.25
18	7	20	1	20	80.05	87.37
19	5	30	2	40	96.50	96.55
20	9	30	2	40	97.20	91.12
21	5	30	2	40	96.40	96.55
22	7	20	3	20	73.07	73.52
23	5	30	2	40	96.50	96.55
24	7	40	3	20	78.00	81.15
25	5	10	2	40	52.01	54.91
26	3	20	1	20	76.03	78.62
27	5	10	2	40	52.00	54.28
28	3	40	3	20	83.00	87.16
29	7	40	1	20	82.02	86.99
30	5	30	2	40	96.50	96.55